

**WIND RESOURCE ASSESSMENT ON THE
CAMPUS AREA OF İZMİR INSTITUTE OF
TECHNOLOGY: USE OF MULTI POINT DATA
SOURCES**

**A Thesis Submitted to
the Graduate School of Engineering and Sciences of
İzmir Institute of Technology
in Partial Fulfillment of the Requirements for the Degree of**

MASTER OF SCIENCE

in Mechanical Engineering

**by
Çağdaş ÜNVEREN**

**July 2010
İZMİR**

We approve the thesis of **Çağdaş ÜNVEREN**

Prof.Dr. Barış ÖZERDEM
Supervisor

Assist.Prof.Dr. Koray ÜLGEN
Committee Member

Assist.Prof.Dr. Tahsin BAŞARAN
Committee Member

13 July 2010

Prof.Dr. Metin TANOĞLU
Head of the Department of
Mechanical Engineering

Assoc.Prof.Dr. Talat YALÇIN
Dean of the Graduate School of
Engineering and Sciences

ACKNOWLEDGEMENTS

The author would like to express his sincerely gratitude to his supervisor, Prof.Dr.Bariş ÖZERDEM for his guidance and support.

The author is thankful to Şule ERKOÇ from GL Garrad Hassan for her assistance throughout this study.

The author is also grateful to Bariş KARABUDAK and Mahir TOSUN for their valuable assistance.

Especially, the author would like to express his sincere gratitude to his family for their support and encouragement.

ABSTRACT

WIND RESOURCE ASSESSMENT ON THE CAMPUS AREA OF IZMIR INSTITUTE OF TECHNOLOGY: USE OF MULTI POINT DATA SOURCES

Wind data which belong to the three different points on Izmir Institute of Technology campus area but has different time intervals have been used to evaluate the wind power potential on this area which has a complex terrain. The results showed that, this region has significant wind power potential and it is suitable for building a wind farm that has capacity factor over 42%. Mean wind speeds at station which has higher priority with 70 meters of height have been found 8.17 m/s at 50 m height and 8.63 m/s at 80 m height. The prevailing wind direction has also been found as north direction. WAsP and GH WindFarmer software have been used to evaluate the wind statistics and maximize the energy yield by taking into account of noise and visual constraints. Wind turbines which have 2500 kW nominal power have been microsited at the most efficient locations on the wind energy density map. Eighteen turbines with a total capacity of 45 MW were located on the selected sites. The estimated annual net energy productions of the wind turbines have been calculated as 167 GWh/year.

ÖZET

İZMİR YÜKSEK TEKNOLOJİ ENSTİTÜSÜ KAMPÜS ALANI RÜZGAR KAYNAĞININ DEĞERLENDİRİLMESİ: ÇOKLU NOKTA VERİ KAYNAĞI KULLANIMI

Bu çalışma kapsamında, kompleks arazi yapısına sahip İzmir Yüksek Teknoloji Enstitüsü kampüs alanının, üç farklı noktasındaki dört ölçüm istasyonundan alınan farklı zaman aralıklarına sahip rüzgar verisi, bu bölgedeki rüzgar potansiyelinin belirlenmesi için kullanılmıştır. Sonuçlar göstermiştir ki, bölge önemli ölçüde rüzgar enerjisi potansiyeline sahiptir ve kapasite faktörü %42'den büyük olan bir rüzgar tarlası kurulmasına uygundur. Çalışmada kullanılan ve diğer ölçüm istasyonlarına göre yüksek öncelik verilen 70 metre yüksekliğe sahip ölçüm istasyonundan alınan verilere göre, bölgedeki ortalama rüzgar hızları, 50 metre için 8.17 m/s ve 80 metre için 8.63 m/s olup, hakim rüzgar yönünün kuzey olduğu belirlenmiştir. Rüzgar istatistiklerinin ve gürültü, gölgeleme gibi çevresel etkilerin göz önüne alınması ile hesaplanan maksimum enerji getirisinin değerlendirilmesinde ise WAsP ve GH WindFarmer yazılımları kullanılmıştır. 2500 kW nominal güce sahip rüzgar türbinlerinin mikrokonuşlandırılması, rüzgar enerji yoğunluğu haritasındaki en uygun bölgeler saptanarak yapılmıştır. Varsayımsal olarak yerleştirilen ve kurulu gücü 45 MW olan bu 18 türbinden, 167 GWh/yıl enerji üretilebileceği belirlenmiştir.

TABLE OF CONTENTS

LIST OF FIGURES.....	x
LIST OF TABLES.....	xiii
LIST OF SYMBOLS AND ABBREVIATIONS.....	xiv
CHAPTER 1. INTRODUCTION	16
CHAPTER 2. WIND ENERGY AND METEOROLOGY	27
2.1. GLOBAL WINDS	27
2.2. LOCAL WINDS	30
2.2.1. Land and sea breezes	30
2.2.2. Mountain and Valleys winds.....	31
2.3. WIND VELOCITY PROFILES.....	31
2.3.1. Atmospheric Boundary Layer	32
2.3.2. Wind Velocity Gradient.....	32
2.3.3. Turbulence.....	36
2.3.4. Acceleration effect.....	37
2.4. WIND STATISTICS AND FORMULAS	38
2.4.1. Statistical models for wind data analysis.....	39
2.4.1.1. Normal Distribution	40
2.4.1.2. Weibull distribution	40
2.4.1.3. Rayleigh distribution.....	41
2.4.2. Wind Power Formula.....	42
2.4.2.1. Momentum theory.....	44
2.4.2.2. Power coefficient	45
2.4.2.3. The Betz limit	46
2.5. WIND ATLAS.....	46
CHAPTER 3. MEASUREMENT OF WIND.....	52
3.1. MEASUREMENT TECHNIQUES OF WIND.....	52

3.2. MEASUREMENT DEVICES.....	54
3.2.1 Anemometers	54
3.2.1.1. Cup anemometers	55
3.2.1.2. Propeller anemometer	56
3.2.1.3. Plate anemometers	57
3.2.1.4. Pressure tube anemometers	58
3.2.1.5. Hot-wire Anemometers.....	59
3.2.1.6. Sonic anemometers.....	60
3.2.1.6. Laser Doppler anemometers.....	61
3.2.2. Wind Vane	62
3.2.3. Air Temperature and Pressure Measurement.....	63
3.2.4. Humidity Sensor.....	63
3.3. WIND MASTS	64
CHAPTER 4. THE MATERIALS AND METHODS	65
4.1. FIELD INSPECTION.....	65
4.2. SOFTWARE FOR ANALYSIS.....	65
4.2.1. WAsP	65
4.2.2. GH WindFarmer	66
4.2.2.1. MCP+ Module	68
4.2.2.2. Energy Calculation.....	69
4.2.2.3. Program Inputs.....	69
4.2.2.4. Association Method	70
4.2.2.5. Methodology of the Energy Calculation.....	71
4.2.2.6. Direction Correction	71
4.3. ANALYSIS OF RAW DATA	72
4.3.1. Data Inspection.....	73
4.3.1.1. Viewing Data.....	73
4.3.1.2. Cleaning Data	74
4.3.2. Data Analysis	75
4.3.2.1. Frequency Distribution Table.....	75
4.3.2.2. Turbulence Intensity	76
4.3.2.3. Wind Rose	77

4.3.2.4. MCP Procedure.....	78
4.3.2.5. Removing Seasonal Bias in Tab Files.....	82
4.4. DIGITAL MAP PROCESSING.....	82
4.4.1. Editing & Digitizing Topographical Maps	83
4.4.2. Creation of Roughness Map.....	84
4.4.3. Creation of Obstacle Map	87
4.5. WIND RESOURCE ANALYSIS	90
4.5.1. Configuring Resource Grid.....	90
4.6. ANALYSIS OF ENVIRONMENTAL EFFECT.....	92
4.6.1. Shadow Flicker Effect	92
4.6.1.1. Program inputs.....	93
4.6.2. Noise Level Calculation.....	94
4.6.2.1. Accuracy of the Method.....	95

CHAPTER 5. CASE STUDY: IZMIR INSTITUTE OF TECHNOLOGY CAMPUS

AREA	96
5.1. INSPECTION OF CAMPUS AREA.....	96
5.1.1. Orography	97
5.1.2. Roughness	98
5.1.3. Obstacles	99
5.2. MEASUREMENT DEVICES & MASTS	99
5.2.1. Measurement Devices.....	102
5.2.1.1. Anemometers.....	102
5.2.1.2. Wind Vanes	103
5.2.1.3. Thermometers & Humidity Sensors	104
5.2.1.4. Barometers.....	106
5.3. ASSESSMENT OF WIND POTENTIAL	106
5.3.1. Digital Maps.....	107
5.3.1.1. Topographical Map.....	108
5.3.1.2. Roughness Map	109
5.3.1.3. Obstacle Map.....	109
5.3.2. Wind Climate	110
5.3.2.1. Frequency Distribution.....	110

5.3.2.2. Wind Rose	110
5.3.2.3. Turbulence Intensity	111
5.3.3. Wind Resource Map	112
5.4. ENVIRONMENTAL EFFECT OF POTENTIAL SITE	113
5.4.1. Shadow Flicker Effect	114
5.4.2. Noise Levels	114
 CHAPTER 6. CONCLUSIONS	 115
 REFERENCES.....	 116
 APPENDIX A. WIND SPEED AND WIND ENERGY DENSITY MAPS OF IZTECH CAMPUS AREA.....	 120

LIST OF FIGURES

<u>Figure</u>	<u>Page</u>
Figure 1.1. European Union energy mix change (from 2000 to 2009).....	19
Figure 1.2. World wind map with resolution of 5km at 80 m height.....	19
Figure 1.3. Gross generation & net consumption of electricity of Turkey.....	24
Figure 1.4. Total electricity generation (GWh) according to main fuel types in 2008...24	
Figure 1.5. Total installed capacity (MW) according to main fuel types in 2008.....	25
Figure 2.1. Three cell model for atmospheric circulation.....	27
Figure 2.2. Wind direction affected by the Coriolis force.....	28
Figure 2.3. (a) Yearly and (b) daily variations of the mean wind speed for three different wind climates. (c) Frequency distributions of the wind speed at the same three locations.....	29
Figure 2.4. Lake - sea breeze and atmospheric depth.....	31
Figure 2.5. Decrease in wind speed as influenced by varieties of terrain roughness.....	33
Figure 2.6. Wind velocity gradient by altitude.....	33
Figure 2.7. Definition of “flat countryside” in the environment of a wind turbine.....	34
Figure 2.8. Roughness lengths and roughness classes for various surface characteristics.....	35
Figure 2.9. Turbulence created by an obstruction.....	36
Figure 2.10. The acceleration effect over ridges.....	38
Figure 2.11. The energy extracting stream-tube of a wind turbine.....	42
Figure 2.12. An energy extracting actuator disc and stream-tube.....	43
Figure 2.13. The wind resource maps of the European Wind Atlas.....	48
Figure 2.14. The wind atlas methodology used for the European Wind Atlas.....	49
Figure 2.15. Wind speed map of Turkey at 70 meters.....	51
Figure 3.1. Griggs-Putnam index of deformity.....	52
Figure 3.2. Classification of wind speed according to the Beaufort scale.....	53
Figure 3.3. Cup anemometer.....	55
Figure 3.4. Propeller anemometer.....	56
Figure 3.5. Illustration of pressure plate anemometer.....	57
Figure 3.6. Principle of pressure tube anemometer.....	58
Figure 3.7. Hot-wire anemometer.....	59

Figure 3.8. Sonic anemometer.....	60
Figure 3.9. Laser Doppler anemometer.....	61
Figure 3.10. Wind vane.....	62
Figure 3.11. Temperature sensor.....	63
Figure 4.1. Interface of WindFarmer software.....	67
Figure 4.2. Interface of MCP+ module of WindFarmer.....	68
Figure 4.3. Typical row data series.....	72
Figure 4.4. Interface of data inspection process.....	74
Figure 4.5. Cleaning process of malfunction data.....	75
Figure 4.6. Frequency distribution table.....	76
Figure 4.7. Wind rose.....	77
Figure 4.8. Illustration of methodology of MCP process.....	79
Figure 4.9. Least Squares method.....	80
Figure 4.10. PCA method.....	81
Figure 4.11. Overlay of digital map on to background map.....	83
Figure 4.12. Roughness class 0.....	85
Figure 4.13. Roughness class 1.....	85
Figure 4.14. Roughness class 2.....	86
Figure 4.15. Roughness class 3.....	86
Figure 4.16. The reduction of wind speed due to shelter.....	87
Figure 4.17. Defining process of obstacle.....	89
Figure 4.18. Interface of grid configuring process of WAsP.....	92
Figure 4.19. Example of shadow flicker illustration in GH WindFarmer.....	94
Figure 4.20. Example of noise levels illustration in GH WindFarmer.....	95
Figure 5.1. View of Iztech campus area.....	96
Figure 5.2. 3D View of orographic features of Iztech campus area.....	97
Figure 5.3. 70 Meters of height lattice tower on the campus area of Iztech.....	100
Figure 5.4. 30 Meters of height tubular mast on the campus area of Iztech.....	101
Figure 5.5. Digital topographical map overlaid on background map.....	107
Figure 5.6. Digital roughness map overlaid on background map.....	108
Figure 5.7. Observed frequency distribution and wind rose of 70 m tower.....	109
Figure 5.8. Mean wind speed map of Iztech campus area.....	111
Figure 5.9. Wind power density map of Iztech campus area.....	112

Figure 5.10. Shadow flicker effect of potential wind farm.....	113
Figure 5.11. Noise levels of potential wind farm.....	114

LIST OF TABLES

<u>Table</u>	<u>Page</u>
Table 1.1. Wind energy situation of countries.....	20
Table 3.1. Griggs-Putnam index of deformity in terms of m/s.....	53
Table 4.1. Porosity table.....	88
Table 5.1. Specifications of Ornytion 107A type anemometer.....	102
Table 5.2. Specifications of Ammonit Classic type anemometer.....	102
Table 5.3. Specifications of NRG type anemometer.....	103
Table 5.4. Specifications of Ornytion 207 Type Wind Vane.....	103
Table 5.5. Specifications of Ammonit Classic Type Wind Vane.....	103
Table 5.6. Specifications of NRG Type Wind Vane.....	104
Table 5.7. Specifications of EOL 307 series temperature sensor.....	104
Table 5.8. Specifications of Ammonit “xPC” series temperature sensor.....	104
Table 5.9. Specifications of Ammonit “xPC” series humidity sensor.....	105
Table 5.10. Specifications of NRG brand temperature sensor.....	105
Table 5.11. Specifications of NRG brand humidity sensor.....	105
Table 5.12. Specifications of Ammonit PTB 100A model air pressure transducer sensor.....	106
Table 5.13. Specifications of NRG brand barometric pressure sensor.....	106

LIST OF SYMBOLS AND ABBREVIATIONS

A	cross-sectional area
α	Inflow factor
c	Weibull scale factor
C_p	Power coefficient
e_w	Partial pressure of water vapor
e_w^*	Saturated vapor pressure of water
F	Force
f_i	Frequency of the corresponding interval
$f(V)$	The probability density function
$F(V)$	The cumulative distribution function
Φ	Relative humidity
ha	Hectare
hc	Maximum level difference
I	Measure of the overall level of turbulence
k	Weibull shape factor
μ	Mean of the normal distribution
n	Number of wind data
p	Pressure
ρ	Air density
R^2	Linear correlation coefficient
σ	Standard deviation of wind speed variations
σ^2	Variance
V_m	Mean wind speed
V	Wind velocity
U	Flow velocity
Z	Height (m)
Z_0	Roughness height
Z_R	Desired height
a.g.l	Above ground level
ABL	Atmospheric Boundary Layer

ED50	European Datum 1950
EWEA	European Wind Energy Association
GCM	General Command of Mapping
GIS	Geographical Information System
GMT	Greenwich Mean Time
ISO	International Organization for Standardization
ITCZ	Intertropical Convergence Zone
MCP	Measure-Correlate-Predict
OECD	Organization for Economic Cooperation and Development
OWC	Observed Wind Climate
PCA	Principal Components Analysis
RSF	Discrete Resource File
REPA	Rüzgar Enerjisi Potansiyeli Atlası
SI	The International System of Units
SIS	State Institute of Statistics
SRTM	Shuttle Radar Topography Mission
TAB	Table files
TEIAS	Turkish Electricity Transmission Company
UTM	Universal Transverse Mercator
WAsP	Wind Atlas Analysis and Application Program
WGS84	World Geodetic System 1984
WRG	Wind Resource Grid
WWEA	World Wind Energy Association

CHAPTER 1

INTRODUCTION

Today, it is commonly accepted that the earth's fossil energy resources are very limited. In the next few decades, the global oil, gas and coal price will rise continuously while the production rates show declining tendency, if new reserves of these resources could not be discovered. However, fossil fuel power plants load the atmosphere with greenhouse gases and particulates; they are responsible for 50 to 60% greenhouse gases released into the atmosphere, resulting in global warming and climate change. It's commonly agreed that, at least 10% our energy supply should come from renewable sources to reduce the emission levels. For a carbon free world, The Kyoto Protocol is signed by 186 countries that includes Turkey, and considered as a positive step. It targets an average reduction of emission levels of greenhouse gases of 5.2% from 1990 levels by the year 2012 [1, 2].

The earth receives around $1.7 \cdot 10^{14}$ kW of power from the sun in the form of solar radiation and it is the major source of wind and the other renewable energies [1]. Unequal warming of the land masses closer to equator and near the poles causes differences in pressure. Warm air rises and circulates in the atmosphere to sink back to the surface in cooler areas. Wind is these large masses of air moving on over the earth's surface. The resulting large-scale motion of the air is strongly influenced by coriolis forces due to the earth's rotation. This influence generates a large-scale atmospheric circulation pattern. We called these global winds as prevailing winds.

The non-uniformity of the earth's surface, with its pattern of land masses and oceans, provides that this global circulation pattern is disturbed by smaller-scale variations on continental scales. Topographical features such as mountains and valleys can distort the direction and speed of prevailing winds. These small-scale variations are local winds and caused by two mechanisms such as temperature difference between lands and seas in day/night period and altitude difference between mountains and lowlands [3].

Human efforts to harness wind for energy date back to the ancient times, when he used sails to propel ships and boats. They have been used predominantly for grinding

grains and for pumping water. There is disagreement on the origin of the concept of using wind for mechanical power. Some believe that the concept originated in ancient Babylonia. Others argue that the birth place of wind mills is India. The earliest documented design of wind mill dates back to 200 B.C. The Persians used wind mills for grinding grains during this period. Those were vertical axis machines having sails made with bundles of reeds or wood. By the 13th century, grain grinding mills were popular in most of Europe. In contrast with the vertical axis Persian design, European mills had horizontal axis. Especially, the Dutch windmills which appeared in different variants were erected in large numbers in the 17th and 18th century in Europe. This is followed by the water pumping wind mill, which is still considered as one of the most successful application of wind power. The so-called American multi bladed wind turbine appeared in the wind energy history by the mid-1800 [1, 3].

The first modern wind turbine, specifically designed for electricity generation, was constructed in the USA and Denmark in 1890. They generated 12 kW DC and supplied electricity to the rural areas. However, for much of the 20th century there was little interest in using wind energy other than for battery charging for remote dwellings and these low-power systems were quickly replaced once access to the electricity grid became available. One notable exception was the 1,250 kW Smith-Putnam wind turbine constructed in the USA in 1941. This remarkable machine had a steel rotor 53 m in diameter, full-span pitch control and flapping blades to reduce loads [1, 3].

In the later years, cheaper and more reliable electricity, generated from fossil fuel based plants became available. Several nuclear power projects were also embarked on, believing that it would be the ultimate source for the future energy needs. Thus, the interest in wind energy declined gradually, especially by 1970. The oil crisis in 1973 forced the scientists, engineers and policy makers to thought on the fossil fuel dependence. Research and development on wind energy are seen intensified in the later years. The so-called 'Danish' wind turbine concept emerged of a three-bladed, stall-regulated rotor and a fixed-speed, induction machine drive train. This deceptively simple architecture has proved to be remarkably successful and has now been implemented on turbines as large as 126 m in diameter and at ratings of 7.5 MW [1, 3].

After years of facing significant economic and technical challenges, renewable energy is making great strides forward. Today, it is being increasingly recognized worldwide as a viable means to reduce the threat of global climate change, encourage

development, and create jobs. At the same time, improvements in cost, reliability, and grid integration have addressed many of the historical concerns associated with a greater reliance on renewable energy resources. Today, much of the growth in the renewables sector has been driven by the rapidly expanding wind energy industry and wind energy has emerged as one of the more viable utility-scale renewable energy solutions. As wind turbine technology continues to advance and the installed base of wind turbines grows, the cost of wind-generated electricity is becoming competitive with other energy options. Main factor in the growing is acceptance of this technology. Today's wind technology has grown not only in size, but also has become increasingly advanced and highly reliable [4, 5].

The benefits of wind energy are obvious: It does not generate air or water emissions, it does not produce hazardous waste, it does not consume natural resources such as coal, oil, gas, or water, nor does it cause environmental damage through resource extraction and transportation. On the other hand, an investigation of the environmental impacts of wind energy production reveals a few hazards. Locating the wind turbines in or near the flyways of migrating birds and wildlife refuges may result in birds flying into the supporting towers and rotating blades. Bat fatalities are another serious concern. Also, the rotating magnets in the turbine electrical generator produce a low level of electromagnetic disturbance that can affect television and radio signals within 2–3 km of large installations. The noise caused by rotating blades is another unavoidable side effect of wind turbine operation [4, 5].

In respect of reference case of International Energy Outlook 2009, world marketed energy consumption is projected to rise by 44% from 2006 to 2030. Total energy demand in the OECD (Organization for Economic Cooperation and Development) countries increases by 15%, compared with an increase of 73% in the non-OECD countries. World net electricity generation increases by 77% in the reference case, from 18,000 TWh in 2006 to 23,200 TWh in 2015 and 31,800 TWh in 2030. According to this reference case, total net generation in the non-OECD countries increases by an average of 3.5% per year, compared with an average of 1.2% per year in the OECD nations. From 2006 to 2030, world renewable energy use for electricity generation which also includes hydroelectric power grows by an average of 2.9% per year, and the renewable share of world electricity generation increases from 19% in 2006 to 21% in 2030. Much of the growth is in hydroelectric power and wind power. Of

the 3,300 TWh of new renewable generation added over the projection period, 1,800 TWh is ascribed to hydroelectric power and 1,100 TWh to wind power. By the end of the year 2009, all wind turbines installed globally contribute 340 TWh to the worldwide electricity supply which represents 2 % of the global electricity demand [6].

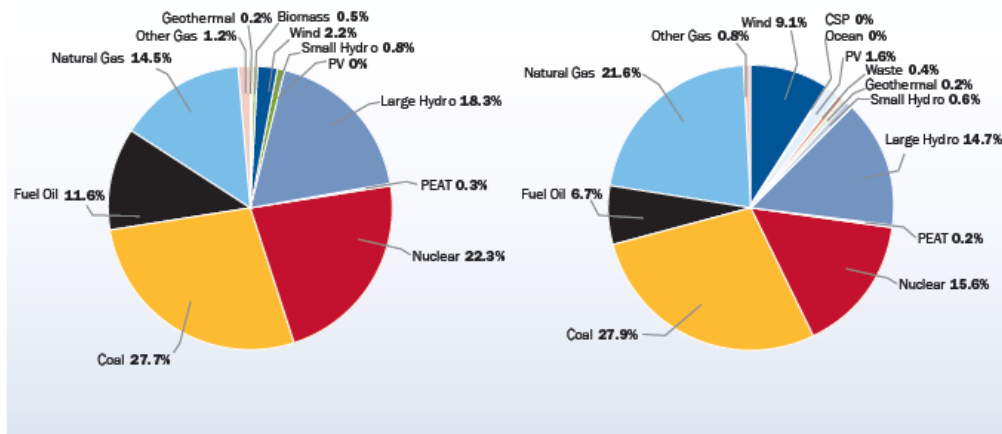


Figure 1.1. European Union energy mix change (from 2000 to 2009)
(Source: Wilkes [7], 2009)

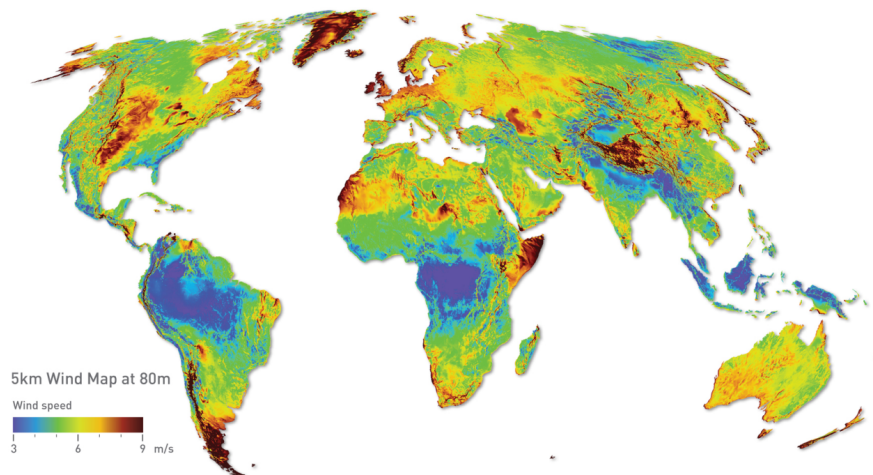


Figure 1.2. World wind map with resolution of 5km at 80m height
(Source: 3TIER [8], 2010)

Many studies have been completed to estimate the wind potential in different parts of the world. One of the these studies, the researchers collected wind speed measurements from approximately 7,500 surface stations and another 500 balloon-launch stations to determine global wind speeds at 80 meters above the ground surface (Figure 1.2), which is the hub height of modern wind turbines, and their estimate of the globe's wind power is 72 TW [9].

Since the Wind Force 12 report, which was published by European Wind Energy Association (EWEA) and Greenpeace, wind power has maintained its status as the world's fastest-growing energy source, the annual growth rate that is the relation between the new installed wind power capacity and the installed capacity of the previous year, continued to increase since the year 2004, and reaching 31.7 % in 2009. One of the highest growth rates of the year 2009 with more than 100 % could be found in Turkey by 132 % [6] (Table 1.1.).

The year 2009 brought new records for wind energy usage around the world; the wind capacity worldwide reached 159,213 MW with the addition of 38,312 MW of new generating capacity.

Turkey is one of the rapidly growing electricity generation and natural gas markets in the world. Reason for this, Turkey is growing fast, both in population and economical sense, with 1.5% population growth rate and 4.5% mean economical growth rate in long term.

Table 1.1. Wind energy situation of countries
(Source: WWEA [6], 2009)

Position 2009	Country / Region	Total capacity end 2009 [MW]	Added capacity 2009 [MW]	Growth rate 2009 [%]	Position 2008	Total capacity end 2008 [MW]
1	USA	35,159.00	9,922.00	39.3	1	25,237.00
2	China	26,010.00	13,800.00	113	4	12,210.00
3	Germany	25,777.00	1,880.00	7.9	2	23,897.00
4	Spain	19,149.00	2,460.00	14.7	3	16,689.00
5	India	10,925.00	1,338.00	14	5	9,587.00

(cont. on next page)

Table 1.1. (Cont.).

6	Italy	4,850.00	1,114.00	29.8	6	3,736.00
7	France	4,521.00	1,117.00	32.8	7	3,404.00
8	United Kingdom	4,092.00	897	28.1	8	3,195.00
9	Portugal	3,535.00	673	23.5	10	2,862.00
10	Denmark	3,497.00	334	10.6	9	3,163.00
11	Canada	3,319.00	950	40.1	11	2,369.00
12	The Netherlands	2,240.00	5	0.2	12	2,235.00
13	Japan	2,056.00	176	9.4	13	1,880.00
14	Australia	1,877.00	383	25.6	14	1,494.00
15	Sweden	1,579.00	512	48	16	1,066.90
16	Ireland	1,260.00	233	22.7	15	1,027.00
17	Greece	1,109.00	119	12	18	989.7
18	Austria	995	0	0	17	994.9
19	Turkey	796.5	463.1	138.9	25	333.4
20	Poland	666	194	41.1	19	472
21	Brazil	600	261.5	77.3	24	338.5
22	Belgium	555	171	44.6	22	383.6
23	New Zealand	497	172	52.9	26	325.3
24	Chinese Taipeh	436	78	21.8	23	358.2
25	Norway	431	2	0.5	20	429
26	Egypt	430	40	10.3	21	390
27	Mexico	402	317	372.9	34	85
28	Korea (South)	364.4	86.4	31.1	27	278
29	Morocco	253	129	104	32	124
30	Bulgaria	214.2	56.7	36	28	157.5
31	Hungary	201	74	58.3	31	127
32	Czech Republic	191	41	27.3	29	150
33	Finland	147	4	2.8	30	143
34	Estonia	142.3	64	81.8	36	78.3
35	Costa Rica	123	49.5	66.9	37	74

(cont. on next page)

Table 1.1. (Cont.).

36	Lithuania	91	37	68	38	54.4
37	Ukraine	90	0	0	33	90
38	Iran	82	0	0	35	82
39	Chile	78	58	288.6	47	20.1
40	Nicaragua	40	40	New	new	0
41	Luxembourg	35.3	0	0	39	35.3
42	Philippines	33	8	31.8	42	25.2
43	Argentina	29.8	0	0	41	29.8
44	Jamaica	29.7	9	43.5	44	20.7
45	Latvia	28.5	1.6	5.9	40	26.9
46	Croatia	27.8	9.6	52.9	50	18.2
47	Netherlands Antilles	24.3	12	97.6	54	12.3
48	South Africa	21.8	0	0	43	21.8
49	Guadeloupe	20.5	0	0	45	20.5
50	Uruguay	20.5	0	0	46	20.5
51	Colombia	20	0	0	49	19.5
52	Tunisia	20	0	0	48	20
53	Switzerland	17.6	4	29	52	13.8
54	Russia	16.5	0	0	51	16.5
55	Romania	14	7	100	56	7
56	Guyana	13.5	0	0	53	13.5
57	Vietnam	8.8	7.5	600	66	1.3
58	Cuba	7.2	0	0	55	7.2
59	Israel	6	0	0	57	6
60	Slovakia	6	0	0	58	6
61	Pakistan	6	0	0	58	6
62	Faroe Islands	4.1	0	0	60	4.1
63	Cape Verde	2.8	0	0	62	2.8
64	Ecuador	2.5	0	0	61	4

(cont. on next page)

Table 1.1. (Cont.).

65	Mongolia	2.4	0	0	63	2.4
66	Belarus	1.9	0.9	77.3	68	1.1
67	Nigeria	2.2	0	0	64	2.2
68	Antarctica	1.6	1	165	73	0.6
69	Jordan	1.5	0	0	65	1.5
70	Indonesia	1.4	0.2	16.7	67	1.2
71	Martinique	1.1	0	0	68	1.1
72	Falkland Islands	1	0	0	70	1
73	Eritrea	0.8	0	0	71	0.8
74	Peru	0.7	0	0	72	0.7
75	Kazakhstan	0.5	0	0	74	0.5
75	Namibia	0.5	0	0	74	0.5
75	Syria	0.5	0.1	22.5	76	0.4
78	Dominican Republic	0.2	0	0	77	0.2
79	Dominica	0.2	0	0	77	0.2
80	North Korea	0.2	0	0	77	0.2
81	Algeria	0.1	0	0	80	0.1
82	Bolivia	0.01	0	0	81	0.01

All data included in this table has been obtained from World Wind Energy Association (WWEA) reports.

In respect of State Institute of Statistics (SIS), population of Turkey is 72,561,312 and growing by the mean rate of 1% and expected to grow to 83.5 million in 2025.

In 2008, 789.4 GWh energy was imported, while the total net consumption was 161,947.6 GWh and the total gross generation was 198,418 GWh. The energy consumption of Turkey increased every year with 7.4% mean rate of last 20 years period (Figure 1.3.).

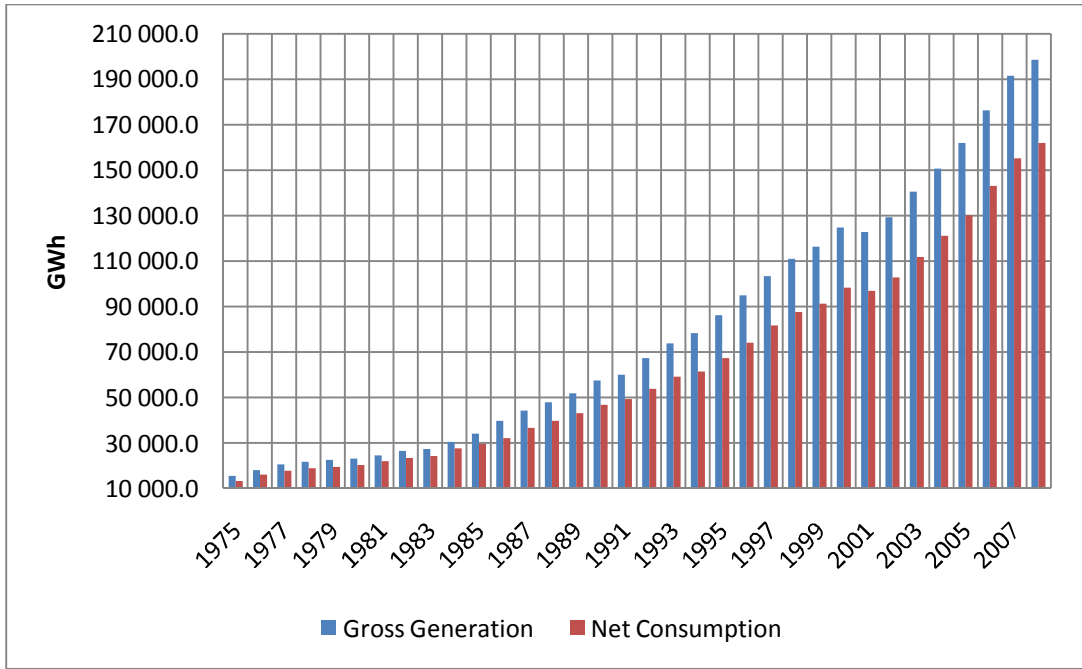


Figure 1.3. Gross generation & net consumption of electricity of Turkey

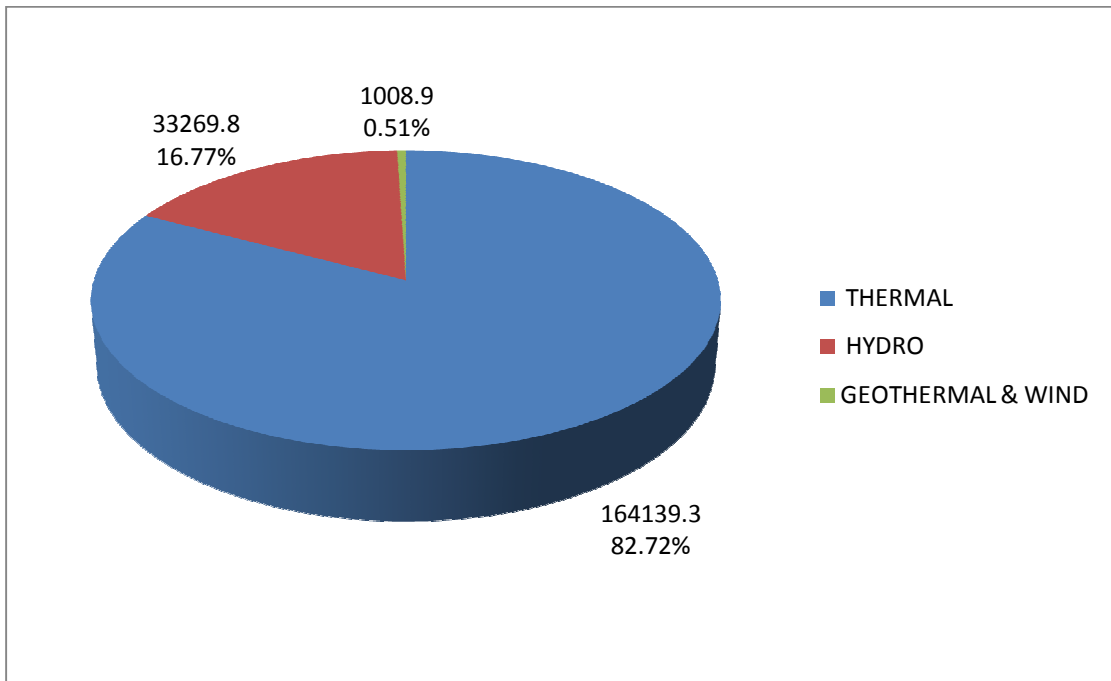


Figure 1.4. Total electricity generation (GWh) according to main fuel types in 2008

In 2008, the total installed capacity of the power plants reached 41,817.2 MW, and the gross generation was 198,418 GWh. According to 10 years capacity projection

report of Turkish Electricity Transmission Company (TEIAS), electricity demand of Turkey will be 335,815 GWh at 2018 according to “low demand scenario” with 6.5% mean rate of growth in demand.

According to SIS, the electric generation increased 3.6 percent in 2008 and the consumption rate increased 4.4. 82.72% of the generation is supplied by the thermal plants and 16.77% by hydroelectric plants (Figure 1.4.). Sum of both geothermal and wind energy are 0.51%. 47 % of the thermal plants use natural gas and this percentage will increase to 57% in respect of the capacity projections of TEIAS.

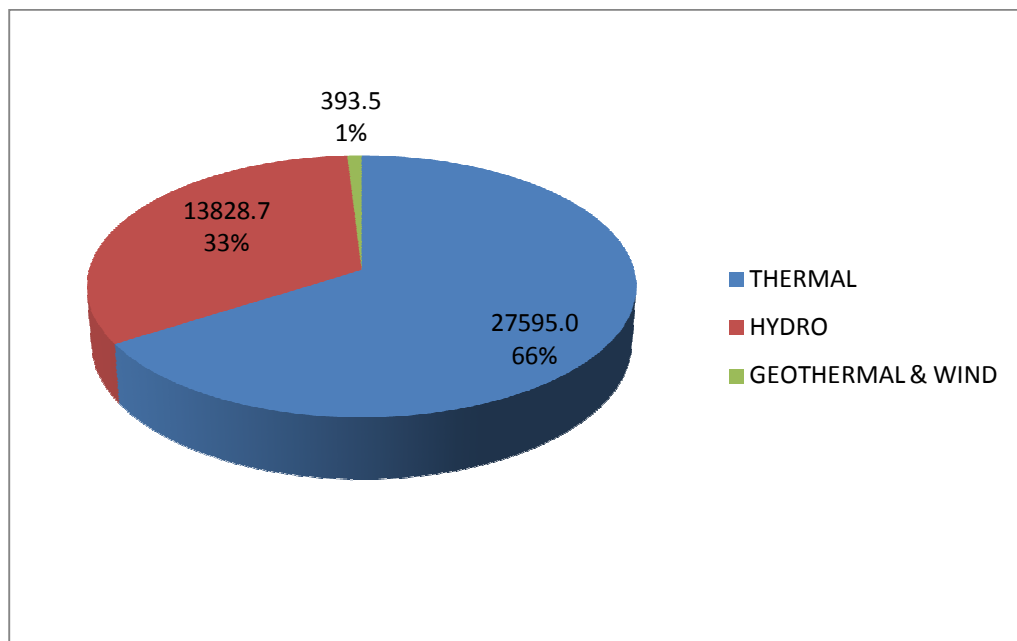


Figure 1.5. Total installed capacity (MW) according to main fuel types in 2008

In order to meet this growing demand in electricity, Turkish government expect that at least 14,565 MW of new generation capacity will be needed by 2018, according to “low demand scenario” of TEIAS. This growth can be met with an average of 1,500 MW of new generation capacity every year till 2018.

There are many studies to estimate the wind potential that calculated by using statistical methods, numerical methods or both of these methods in different parts of the World and Turkey.

Some of those studies have been performed about wind resource assessment in World, especially in our neighborhoods, by Fyrippis [10], in Naxos Island, Greece in 2009; Vogiatzis [11], in North Aegean, Greece in 2003; Keyhani [12], in Tehran, Iran in

2009; Al-Mohamad [13], in Syria, 2002; Ouammi [14], in Italy in 2010; Migoya [15], in Madrid region in 2006; de Araujo Lima [16], in Triunfo-Pernambuco, Brazil in 2009.

Some studies that have been performed about wind potential assessment in Turkey, by Ucar [17], in Uludag-Bursa, in 2009; Sahin [18], in Belen-Hatay, in 2009; Ozgur [19], in Kutahya, in 2009; Oner [20], in Bababurnu, in 2009; Genc [21], in Kayseri, in 2009; Bilgili [22], in southern and southwestern region of Turkey, in 2009; Eskin [23], in Gokceada Island, in 2008; Ozerdem [24], in the campus of Izmir Institute of Technology, in 2005; Turksoy [25], in Bozcaada, in 1995. In this thesis, wind resource assessment on the campus area of Izmir Institute of Technology is studied by using of multi point data sources for more accurate results on complex terrain.

CHAPTER 2

WIND ENERGY AND METEOROLOGY

2.1. Global Winds

The earth receives power from the sun in the form of solar radiation and wind energy is simply an indirect form of solar energy. 1-2% of the total solar radiation that absorbed by surface is converted to wind energy [1]. Conversion process occurs by that way; solar radiation heats the atmospheric air and then the amount of this heating will be more at the equator due to nearly vertical sun lights. Air around the poles becomes less warm, as the angle at which the radiation reaches the surface is nearly horizontal. Increasing temperature decreases the density of air. Hence, lighter air near the equator rises up into the atmosphere to a certain height and then advects. This causes a pressure difference between poles and equator, and attracts the cooler air from near the poles to the equator.

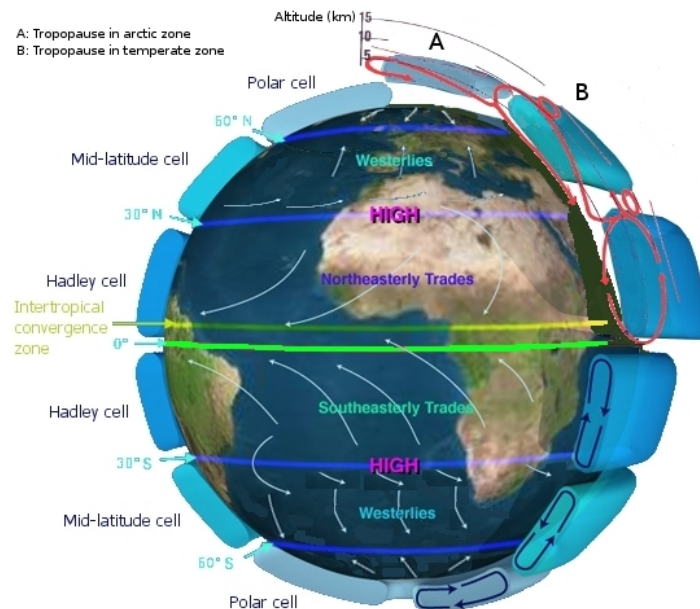


Figure 2.1. Three cell model for atmospheric circulation (Source: Wikipedia [26], 2009)

Therefore, the wind is generated due to the pressure difference resulting from the non-uniform heating of earth's surface by the sun; we called this motion of air as the wind. The wind described above, which is driven by the temperature difference, is called the geostrophic wind, or more commonly the global wind. Global winds, which are not affected by the earth surface, are found at higher heights.

The rotation of earth contributes to another phenomenon near its surface called the Coriolis effect, named after the famous mathematician Gustave Gaspard Coriolis [1]. Because of the Coriolis effect, the direct motion of air mass from the high pressure region to the low pressure region is deviated as shown in Figure 2.2.

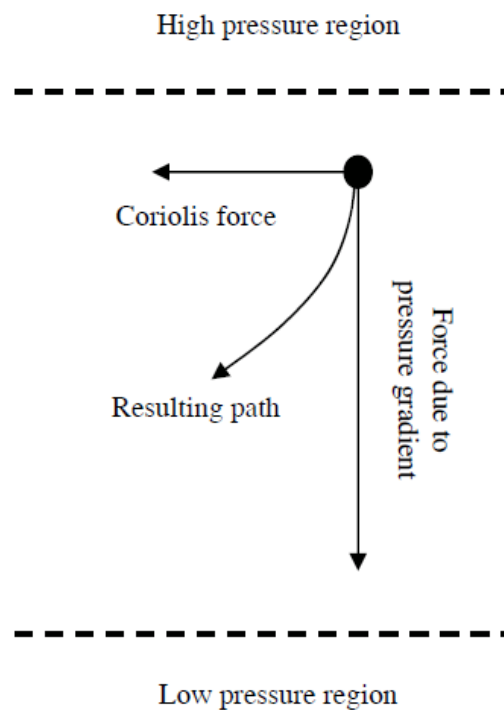


Figure 2.2. Wind direction affected by the Coriolis force
(Source: Mathew [1], 2007)

The air advects nearly parallel to the isobars under the influence of Coriolis forces. Therefore, wind tends to rotate clockwise in the northern hemisphere where as in the southern hemisphere the motion is in the anti-clockwise direction [1].

The wind belts divide the planet to organize into three cells: the Hadley cell, the Ferrel cell, and the Polar cell [1]. The huge majority of the vertical movement occurs in

the Hadley cell. Opposite relative pressures in the upper troposphere equilibrate low and high pressures on earth's surface.

George Hadley sets an explanation for the trade winds matches with observations very well. It is a closed circulation loop that begins at the equator with warm and moist air rose to great height in equatorial low pressure areas (the Intertropical Convergence Zone, ITCZ) to the tropopause and carried pole ward. At about 30°N/S latitude, it descends in a high pressure area. Some of the descending air travels equatorially along the surface closes the loop of the Hadley cell and creates the Trade Winds.

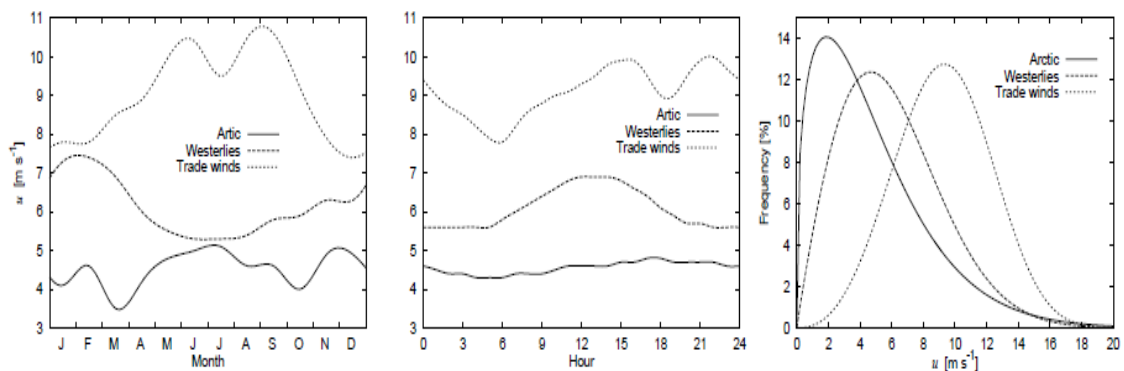


Figure 2.3. (a) Yearly and (b) daily variations of the mean wind speed for three different wind climates. (c) Frequency distributions of the wind speed at the same three locations. (Source: Petersen [27], 1997)

The Polar cell is also a simple system. In spite of the cool and dry air relative to equatorial air, air masses at the 60th parallel are still sufficiently warm and moist to have convection and cause a thermal loop. Air loops inside the troposphere; limited vertically by the tropopause at approximately 8 km. Warm air rises at lower latitudes and moves poleward through the upper troposphere at both the north and south poles. When the air arrives at the polar areas, it cools substantially, and comes down as a cold, dry high pressure area, moving away from the pole along the surface but twisting westward as a result of the Coriolis effect to produce the Polar easterlies. The Hadley cell and the Polar cell are similar in that case; they are thermally direct and their thermal characteristics override the effects of weather in their field.

The Ferrel cell, theorized by William Ferrel (1817-1891), is a secondary circulation feature. It behaves much as an atmospheric ball bearing between the Hadley

cell and the Polar cell, and comes about as a result of the Eddy circulations (the high and low pressure areas) of the mid-latitudes. Therefore, it is sometimes known as the "zone of mixing."

2.2. Local Winds

Nearly 100 m above the ground, the wind pattern is further influenced by several local factors. In this region, variation in velocity and direction of wind is an important issue. The nonuniformity of land masses and oceans insures that this global circulation pattern is affected by smaller-scale variations on continental scales. These variations interact in a highly complex form and are the source of the unpredictability of the weather in particular locations. Obviously though, fundamental tendencies stay which contribute to clear climatic variations between regions. These differences are tempered by more local topographical and thermal effects.

2.2.1. Land and Sea Breezes

In the daytime, land surface gets heated more quickly than the sea surface. As a result, the air above the land rises and forms a low pressure region. This region attracts cool air to the land from the sea. This is called the sea breeze.

In the night time, the process gets reversed due to faster cooling on land. Hence, wind blows from the land to the sea and this is called the land breeze.

Lands those near the seas are often windy due of unequal heating between land and sea. While the sea is warmer than the land, a local circulation develops in which surface air flows from the land to the sea, with warm air rising over the sea and cool air sinking over the land. The pattern reverses when the land is warmer. The land will heat up and cool down more quickly than the sea surface, and so this process tends to reverse over a 24 h cycle.

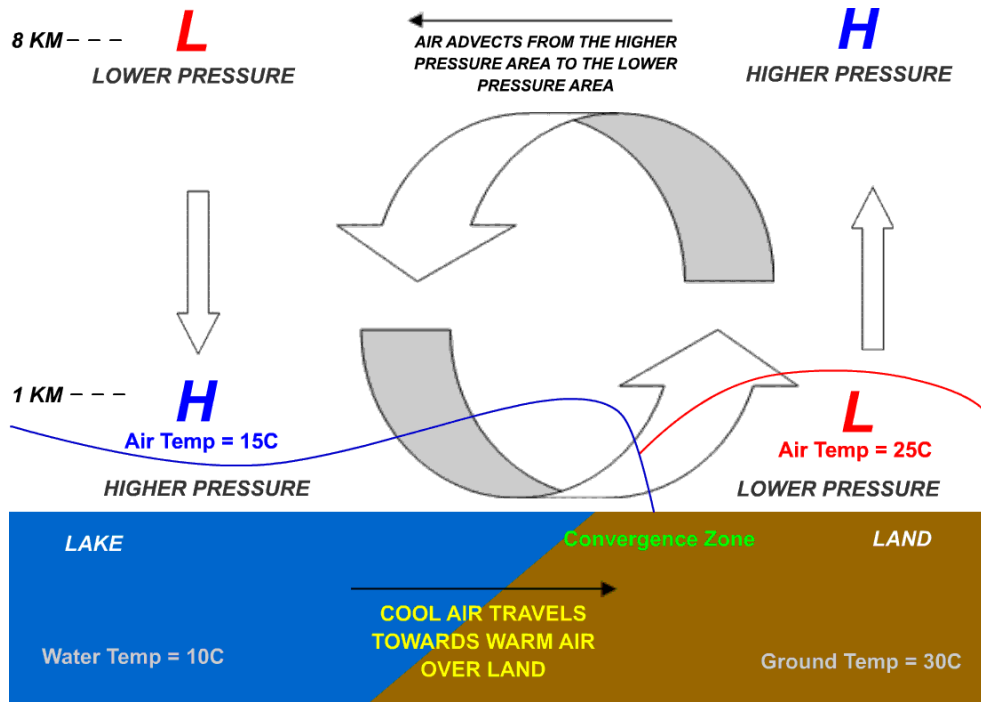


Figure 2.4. Lake - sea breeze and atmospheric depth
 (Source: Weather [28], 2006)

2.2.2. Mountain and Valleys Winds

Hills and mountains affect wind speed in local regions. This is partially a result of altitude due to the earth's boundary layer means that wind speed generally increases with altitude, and tops of hill and mountain may cause into the higher wind-speed layers.

The air masses over the surface get heated and rise up along the slopes on the day time. This is replaced by the cool air, leading to the valley winds. During the night, the flow is from the mountain to the valley which is known as the mountain wind.

2.3. Wind Velocity Profiles

In common usage, wind gradient, more specifically, wind velocity or alternatively shear wind, is the vertical gradient of the mean horizontal wind speed in the lower atmosphere. It is the rate of increase of wind strength with unit increase in

height above ground level. In metric units, it is often measured in units of meters per second of speed, per kilometer of height (m/s/km).

2.3.1. Atmospheric Boundary Layer

The atmospheric boundary layer (ABL), also known as the planetary boundary layer (PBL), is the lowest region of the atmosphere and its behavior is directly influenced by the Earth's surface. In this layer, physical quantities such as flow velocity, temperature, moisture etc., show rapid fluctuations and vertical mixing is strong. In the ABL the wind is affected by surface drag and turns across the isobars. Also, the bottom 10% of the ABL is called the surface layer.

Sutton (1953) separated the boundary layer into two regions:

1. A surface layer region 50-100 m deep of approximately constant (in the vertical) shearing stress, where the flow is insensitive to the earth's rotation and the wind structure is determined primarily by surface friction and the vertical gradient of temperature ,
2. A region above that layer extending to a height of 500-1000 m, where the shearing stress is variable and the wind structure is influenced by surface friction, temperature gradient, and the earth's rotation.

The two-layer concept roughly parallels that of the inner and outer regions in laboratory shear flows, although the true extent of the similarity in the scaling laws in each of those regions to laboratory flow was not known at that time. Above these two layers is the free atmosphere, where the flow is in near-geostrophic balance and no longer influenced by surface friction [29].

2.3.2. Wind Velocity Gradient

Wind gradient, more specifically wind velocity gradient, or alternatively shear wind, is the vertical gradient of the mean horizontal wind speed in the lower atmosphere. It is the rate of increase of wind speed with unit increase in height with altitude.

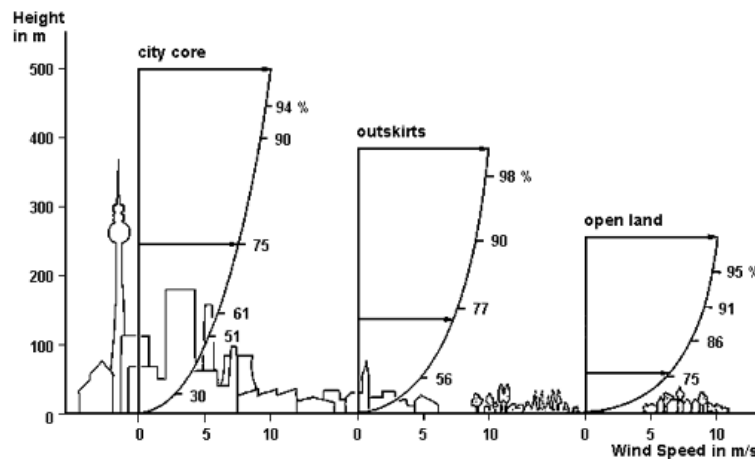


Figure 2.5. Decrease in wind speed as influenced by varieties of terrain roughness (Source: Baumbach [30], 1991)

Generally, result of the aerodynamic drag, there is a wind gradient in the wind flow just a few hundred meters over the Earth's surface. Wind speed increases with increasing altitude, starting from zero due to the no-slip condition. Flow near the surface meets obstacles that reduce the wind speed. The reduction in speed near the surface is a function of surface roughness, so wind velocity profiles are different for different terrain types. Rough, irregular surface and human-made obstacles on the ground reduces wind velocity.

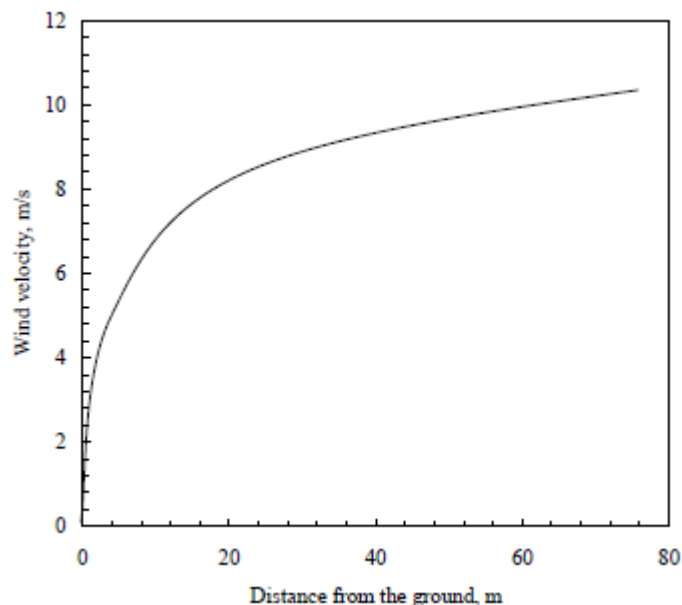


Figure 2.6. Wind velocity gradient by altitude (Source: Mathew [1], 2007)

When the temperature profile is adiabatic, the wind velocity should vary logarithmically with height. Measurements over open terrain in 1961 showed good agreement with the logarithmic fit up to 100 m or so, with near constant average wind speed up through 1000 m [31].

When considering global wind resource maps and fundamental laws, it must not be forgotten that at any location, the prevailing wind regime will display local peculiarities. It is better to know when the local terrain can be acceptable to be “obstacle-free”.

According to Frost, the terrain in the surroundings of a wind turbine can be considered “flat” if:

- differences in elevation do not exceed 60 m within a radius of 11.5 km,
- the ratio of the maximum level difference (hc) to the horizontal distance between these two marked points is less than 0.032 for a distance of 4 km upwind and 0.8 km downwind, and the height of the rotor relative to the lowest point within a distance of 4 km upwind is at least three times greater than the largest existing level difference hc . (Figure 2.7.)

Naturally, the existence of level differences can also be used in a positive sense. Wind speeds on mountain ridges with an especially advantageous shape (slopes of 1:3 to 1:4) can increase to double the value prevailing far away from the ridge [32].

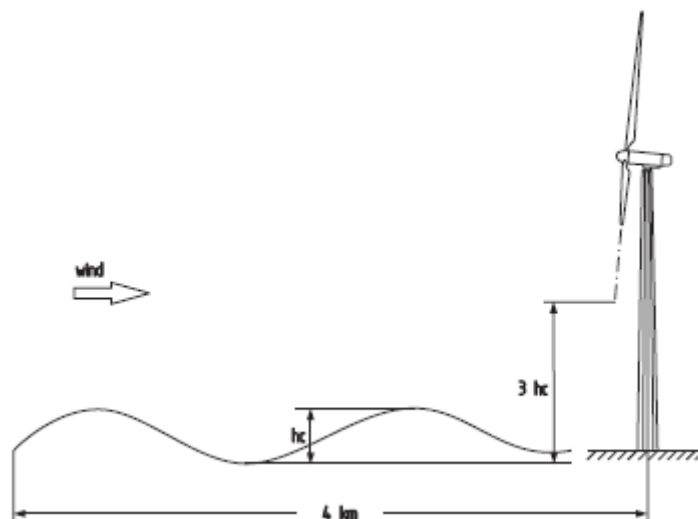


Figure 2.7. Definition of “flat countryside” in the environment of a wind turbine
(Source: Hau [32], 2006)

The rate at which the speed increases with altitude depends on the roughness of the terrain. Presence of plantations, forests, and bushes slows down the wind substantially. Flat and smooth terrains do not have much effect on the wind speed. The surface roughness of a terrain is usually represented by the roughness class or roughness height. The roughness height of a surface may be close to zero (surface of the sea) or even as high as 2 (town centers). Some typical values are 0.005 for flat and smooth terrains, 0.025-0.1 for open grass lands, 0.2 to 0.3 for row crops, 0.5 to 1 for orchards and bushes and 1 to 2 for forests, town centers etc. [1].

z_0 [m]	Types of terrain surfaces	Roughness class
1.00	City Forest	3
0.50	Suburbs	
0.30	Built-up terrain	
0.20	Many trees and/or bushes	2
0.10	Agricultural terrain with a closed appearance	
0.05	Agricultural terrain with an open appearance	1
0.03	Agricultural terrain with very few buildings, trees, etc. Airports with buildings and trees	
0.01	Airports, runway Meadow	0
$5 \cdot 10^{-3}$	Bare earth (smooth)	
10^{-3}	Snow surfaces (smooth growth)	
$3 \cdot 10^{-4}$	Sand surfaces (smooth)	
10^{-4}	Water surfaces (lakes, fjords and the sea)	

Figure 2.8. Roughness lengths and roughness classes for various surface characteristics (Source: Hau [32], 2006)

In wind energy calculations, we are related with the velocity available at the rotor height. The data logged at any heights can be extrapolated to other heights on the basis of the roughness height of the terrain.

Because of the boundary layer effect, wind velocity increases with the height in a logarithmic pattern. If the wind data is available at a height Z and the roughness height is Z_0 , then the velocity at a height Z_R is given by Equation (2.1)

$$V(Z_R) = V(Z) \frac{\ln\left(\frac{Z_R}{Z_0}\right)}{\ln\left(\frac{Z}{Z_0}\right)} \quad (2.1)$$

where $V(Z_R)$ and $V(Z)$ are the velocities at heights Z_R and Z respectively.

2.3.3. Turbulence

The speed and direction of wind change rapidly while it passes through rough surfaces and obstacles like constructions, trees and rocks. This is cause of the turbulence generated in the flow and the presence of turbulence reduces the power available in the stream.

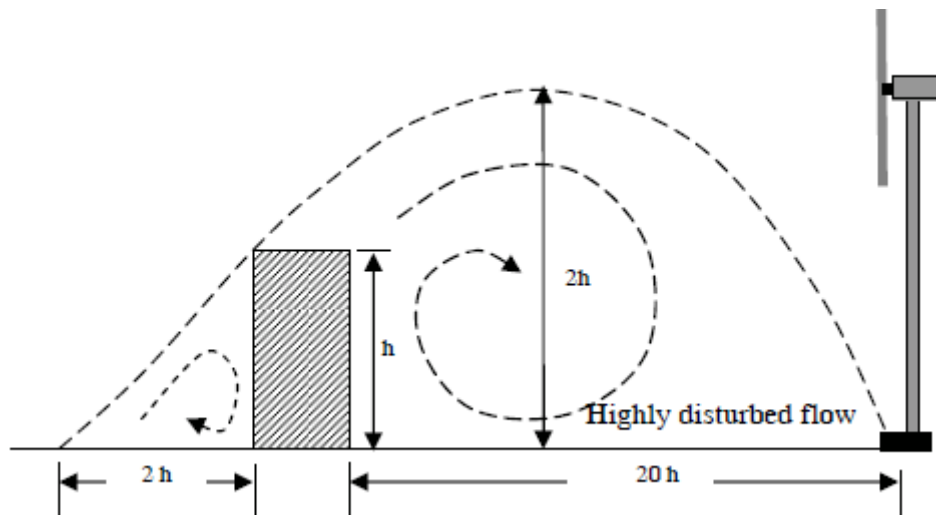


Figure 2.9. Turbulence created by an obstruction
(Source: Mathew [1], 2007)

Intensity of the turbulence depends on the size and shape of the obstacle. The turbulent zone can extend up to 2 times the height of the obstacle in the upwind side and 10 to 20 times in the downwind side. Its influence in the vertical direction may be high to 2 to 3 times the obstacle height [1].

Turbulence is obviously a complex process, and one which cannot be represented simply in terms of deterministic equations. Obviously it follows certain physical laws, such as the conservation of mass, momentum and energy. However, in order to describe turbulence using these laws it is necessary to take account of temperature, pressure, density, humidity and the motion of the air itself in three dimensions. It is then possible to formulate a set of differential equations describing the process.

The turbulence intensity I is a measure of the overall level of turbulence. It is defined as

$$I = \frac{\sigma}{V_m} \quad (2.2)$$

where σ is the standard deviation of wind speed variations about the mean wind speed V_m . Turbulent wind speed fluctuations can be taken to be approximately Gaussian, meaning that the speed variations are normally distributed, with standard deviation σ , about the mean wind speed V_m . The turbulence intensity clearly depends on the roughness of the ground surface and the altitude. However, it also depends on topographical features such as hills or mountains. It also depends on the thermal behavior of the atmosphere [3].

2.3.4. Acceleration Effect

A smooth ridge, as shown in Figure 2.11, speeds up the wind stream passing over it. The acceleration is caused by the squeezing of wind layers over the mount as shown in the figure. The degree of acceleration depends on the shape of the ridge. This effect can be fully used for energy generation, if the slope of the ridge is between 6° and 16° . Slopes greater than 27° and less than 3° are not favorable [1]. Some other crucial factor is the orientation of the ridge. The speedup effect is high when the prevailing

wind is perpendicular and low when it is parallel to the ridge line. Likewise, if the ridge has a concave side confronting the wind, the effect is more desirable [1].

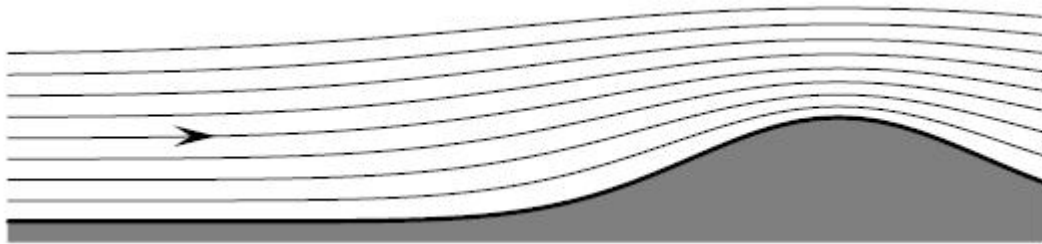


Figure 2.10. The acceleration effect over ridges
(Source: Petersen [27], 1997)

Triangular formed ridges offer better acceleration followed by the smooth and round geometry. Flat topped ridges may present the problem of turbulence, especially in the lower region.

Mountain passes are some other geographical feature causing speedup of wind. While the flow passes through the notches in the mountain barriers, due the venturi effect, the wind velocity is increased. The higher acceleration is occurred by the smoother the surface.

2.4. Wind Statistics and Formulas

One of the most important data in the wind available at a location is its mean velocity. In simple terms, the mean velocity (V_m) is given by

$$V_m = \frac{1}{n} \sum_{i=1}^n V_i \quad (2.3)$$

where V is the wind velocity and n is the number of wind data. However, for wind power calculations, averaging the velocity using Equation (2.3) is often misleading. Thus, the velocity should be considered for its power capacity while calculating the average.

Therefore, the mean wind velocity is given by

$$V_m = \left(\frac{1}{n} \sum_{i=1}^n V_i^3 \right)^{1/3} \quad (2.4)$$

Distribution of wind velocity is also a critical factor in wind resource assessment, other than the average strength of wind over a period. The standard deviation (σ) is one measure for the variability of velocities in a given set of wind data. Standard deviation gives us the deviation of each speed from the mean value. Hence

$$\sigma = \sqrt{\frac{\sum_{i=1}^n (V_i - V_m)^2}{n}} \quad (2.5)$$

Lower values of σ point the equal distribution of the data set. For an easy understanding on wind variability, the data are grouped and presented in the form of frequency distribution. This shows us the information on the number of hours for which the velocity is inside a specific range. If the velocity is presented in the form of frequency distribution, the mean and standard deviation are given by

$$V_m = \left(\frac{\sum_{i=1}^n f_i V_i^3}{\sum_{i=1}^n f_i} \right)^{1/3} \quad (2.6)$$

$$\sigma = \sqrt{\frac{\sum_{i=1}^n f_i (V_i - V_m)^2}{\sum_{i=1}^n f_i}} \quad (2.7)$$

Here f_i is the frequency and V is the mid value of the corresponding interval. Generally, the average wind velocity is higher than the most frequent wind velocity, if we exclude the trade winds which are relatively steady.

2.4.1. Statistical Models for Wind Data Analysis

It is logical to represent the wind velocity distributions by standard statistical functions. Several probability functions were matched with the field data to identify suitable statistical distributions for representing wind regimes. Weibull and Rayleigh distributions can be used to describe the wind variations in a regime with an acceptable accuracy.

2.4.1.1. Normal Distribution

The normal distribution, also known as Gaussian distribution, is a continuous probability distribution that often gives a good description of data around the mean. The graph of the related probability density function is convex, with a top at the mean, and is known as the Gaussian function or bell curve.

The normal distribution is generally used to describe any variable that tends to gather around the mean.

$$f(x) = \frac{1}{\sqrt{2\pi\sigma^2}} e^{-\frac{(x-\mu)^2}{2\sigma^2}} = \frac{1}{\sigma} \phi\left(\frac{x-\mu}{\sigma}\right) \quad (2.8)$$

The parameter μ is the mean, the median and the mode of the normal distribution at the same time. The parameter σ^2 is called the variance; as for any real-valued random variable, it describes the distribution of concentration around its mean. σ is called the standard deviation and is the width of the density function.

For a standard normal distribution, $\mu = 0$ and $\sigma^2 = 1$. The last part of the equation above shows that any other normal distribution can be thought of another type of the standard normal distribution that has been stretched horizontally by a factor σ and then translated rightward by a distance μ . Therefore, μ defines the position of the bell curve's central peak, and σ defines the "width" of the bell curve.

2.4.1.2. Weibull Distribution

In Weibull distribution, the variations in wind velocity are characterized by the two functions;

1. The probability density function and
2. The cumulative distribution function.[1]

The probability density function $f(V)$ points the divide of time (or probability) for which the wind is at a given velocity V . It is given by

$$f(V) = \frac{k}{c} \left(\frac{V}{c}\right)^{k-1} e^{-\left(\frac{V}{c}\right)^k} \quad (2.9)$$

Here, k is the Weibull shape factor and c is scale factor. The cumulative distribution function of the velocity V gives us the fraction of time (or probability) that the wind velocity is equal or lower than V . Hence the cumulative distribution $F(V)$ is

$$F(V) = 1 - e^{-\left(\frac{V}{c}\right)^k} \quad (2.10)$$

2.4.1.3. Rayleigh Distribution

The reliability of Weibull distribution in wind regime analysis depends on the accuracy in estimating k and c . Collected data over shorter time intervals are essential for the precise calculation of k and c . The data that we have may be in the form of the mean wind velocity over a given time period. Under such situations, a simplified case of the Weibull model can be derived, assuming $k=2$. This is known as the Rayleigh distribution. The probability density function $f(V)$ of the Rayleigh distribution, by taking $k = 2$, we get

$$f(V) = \frac{\pi}{2} \frac{V}{V_m^2} e^{-\left[\frac{\pi}{4} \left(\frac{V}{V_m}\right)^2\right]} \quad (2.11)$$

and likewise, the cumulative distribution is given by

$$F(V) = 1 - e^{-\left[\frac{\pi}{4} \left(\frac{V}{V_m}\right)^2\right]} \quad (2.12)$$

Therefore, we can calculate the probability density and cumulative distribution functions of wind by using its mean velocity. The validity of Rayleigh distribution in wind energy assessment has been based by comparing the Rayleigh generated wind pattern with long term field data.

2.4.2. Wind Power Formula

A wind turbine is a device for extracting kinetic energy from the wind. The wind must slow down due to removing some of its kinetic energy, but only that mass of air which passes through the rotor disc is affected. Assuming that the affected air mass stays separate from the air which does not pass through the rotor disc and does not slow down a boundary surface can be drawn containing the affected air mass and this boundary can be extended upstream as well as downstream forming a long stream-tube of circular cross section. No air flows across the boundary and so the mass flow rate of the air flowing along the stream-tube will be the same for all stream-wise positions along the stream-tube. Because the air within the stream-tube slows down, but does not become compressed, the cross-sectional area of the stream-tube must expand to accommodate the slower moving air [3] (Figure 2.11).

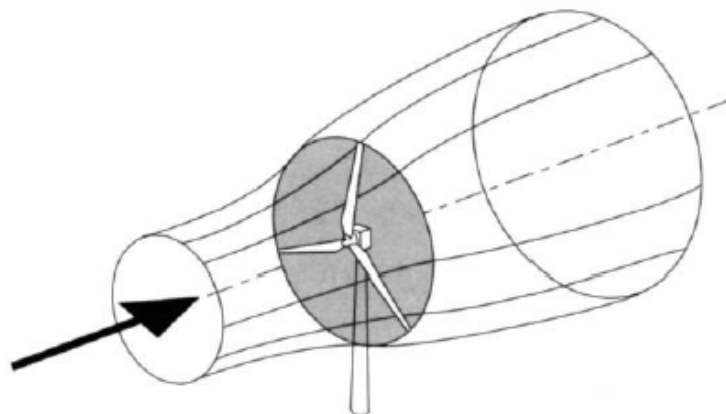


Figure 2.11. The energy extracting stream-tube of a wind turbine
(Source: Burton [3], 2001)

Since the air passes through the rotor disc, there is a drop in static pressure due to design, thus, the leaving air is below the atmospheric pressure level. Then, the air continues downstream with reduced speed and static pressure, also this region of the flow is called the wake. Finally, far downstream, the static pressure in the wake must return to the atmospheric level for equilibrium to be reached.

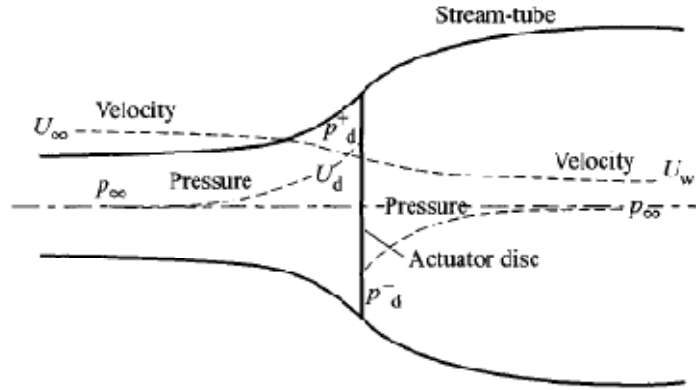


Figure 2.12. An energy extracting actuator disc and stream-tube
(Source: Burton [3], 2001)

The raise in static pressure is at the expense of the kinetic energy and then causes a further slowing down of the wind. Thus, between the far upstream and far wake conditions, no change in static pressure exists but there is a reduction in kinetic energy.

The expansion of the stream-tube is because the mass flow rate must be the same everywhere. The mass of air which passes through a given cross section of the stream-tube in a unit length of time is $\rho \cdot A \cdot U$, where ρ is the air density, A is the cross-sectional area and U is the flow velocity. The mass flow rate must be the same everywhere along the stream tube and so,

$$\rho A_{\infty} U_{\infty} = \rho A_d U_d = \rho A_w U_w \quad (2.13)$$

The symbol ∞ refers to conditions far upstream, d refers to conditions at the disc and w refers to conditions in the far wake. It is common to consider that the actuator disc causes a velocity variation which must be superimposed on the free-stream velocity. The stream-wise component of this induced flow at the disc is given by $-\alpha U_{\infty}$, where α is called the axial flow induction factor, or the inflow factor. At the disc, therefore, the net stream-wise velocity is

$$U_d = U_{\infty} (1 - \alpha) \quad (2.14)$$

2.4.2.1. Momentum Theory

The air that passes through the disc undergoes an overall change in velocity, $U_\infty - U_w$ and a rate of change of momentum equal to the overall change of velocity times the mass flow rate:

$$\text{Rate of change of momentum} = (U_\infty - U_w)\rho A_d U_d \quad (2.15)$$

The force causing this change of momentum comes entirely from the pressure difference across the actuator disc because the stream-tube is otherwise completely surrounded by air at atmospheric pressure, which gives zero net force.

Therefore,

$$(p_d^+ - p_d^-)A_d = (U_\infty - U_w)\rho A_d U_\infty (1 - \alpha) \quad (2.16)$$

To obtain the pressure difference ($p_d^+ - p_d^-$), Bernoulli's equation is applied separately to the upstream and downstream sections of the stream-tube; separate equations are necessary because the total energy is different upstream and downstream. Bernoulli's equation states that, under steady conditions, the total energy in the flow, comprising kinetic energy, static pressure energy and gravitational potential energy, remains constant provided no work is done on or by the fluid. Thus, for a unit volume of air,

$$\frac{1}{2}\rho U^2 + p + \rho gh = \text{constant} \quad (2.17)$$

Upstream, therefore, we have

$$\frac{1}{2}\rho_\infty U_\infty^2 + \rho_\infty gh_\infty = \frac{1}{2}\rho_d U_d^2 + p_d^+ + \rho_d gh_d \quad (2.18)$$

Assuming the flow to be incompressible ($\rho_\infty = \rho_d$) and horizontal ($h_\infty = h_d$) then,

$$\frac{1}{2}\rho U_\infty^2 + p_\infty = \frac{1}{2}\rho U_d^2 + p_d^+ \quad (2.19)$$

Similarly, downstream,

$$\frac{1}{2}\rho U_w^2 + p_\infty = \frac{1}{2}\rho U_d^2 + p_d^- \quad (2.20)$$

Subtracting these equations we obtain

$$(p_d^+ - p_d^-) = \frac{1}{2}\rho_\infty(U_\infty^2 - U_w^2) \quad (2.21)$$

Equation (2.16) then gives

$$\frac{1}{2}\rho(U_\infty^2 - U_w^2)A_d = (U_\infty - U_w)\rho A_d U_\infty(1 - \alpha) \quad (2.22)$$

and so

$$U_w = (1 - 2\alpha)U_\infty \quad (2.23)$$

That is, half the axial speed loss in the stream-tube takes place upstream of the actuator disc and half downstream [3].

2.4.2.2. Power Coefficient

The force on the air becomes, from Equation (2.16)

$$F = (p_d^+ - p_d^-)A_d = 2\rho A_d U_\infty^2(1 - \alpha) \quad (2.24)$$

As this force is concentrated at the actuator disc the rate of work done by the force is FU_d and hence the power extraction from the air is given by

$$Power = FU_d = 2\rho A_d U_\infty^3(1 - \alpha)^2 \quad (2.25)$$

A power coefficient is then defined as,

$$C_p = \frac{\text{Power}}{\frac{1}{2}\rho U_\infty^3 A_d} \quad (2.26)$$

where the denominator represents the power available in the air, in the absence of the actuator disc [3]. Therefore,

$$C_p = 4\alpha(1 - \alpha)^2 \quad (2.27)$$

2.4.2.3. The Betz Limit

The maximum value of C_p occurs when,

$$\frac{dC_p}{d\alpha} = 4(1 - \alpha)(1 - 3\alpha) = 0 \quad (2.28)$$

which gives a value of $\alpha = 1/3$

Hence,

$$C_{p_{max}} = \frac{16}{27} = 0.593 \quad (2.29)$$

The maximum achievable value of the power coefficient is known as the Betz limit [33] after Albert Betz the German aerodynamicist and, up to now, no wind turbine has been designed which is able of exceeding this limit.

2.5. Wind Atlas

In the past, wind data were measured and assessed nearly exclusively from a meteorological viewpoint. The earlier meteorological data do not provide much detailed information about the increase in wind speed with altitude or the local wind conditions of a specific terrain. It is only in the past two decades that wide wind measurements have been accomplished with consideration of the special aspects concerning to the use of wind turbines. Meanwhile, full-coverage wind data are available in the countries in which wind energy usage is widespread.

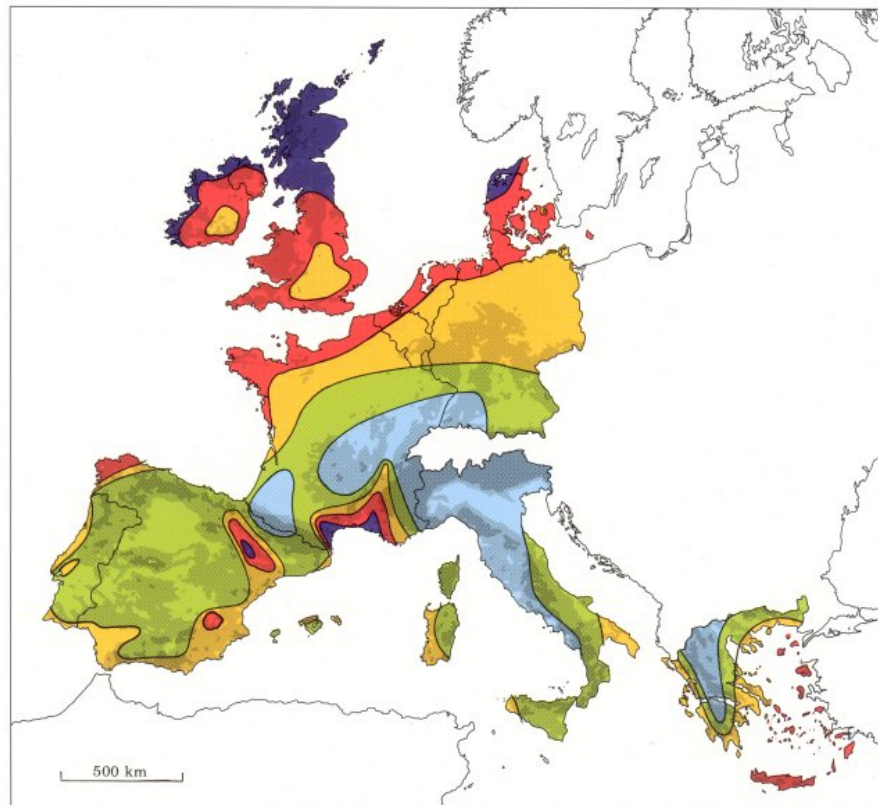
A reliable database is provided mainly by the long-term evaluation of the energy supply from existing wind turbines. However, the determination of the wind conditions at the intended site of the wind turbines remains an important task that cannot be solved by means of the available large-scale wind maps alone. Supplying reliable wind data must be the first step in any planning for the utilization of wind turbines. But it is impossible to carry out new, long-term measurements in every case; thus, critical theoretical verification of existing data is of special importance.

The value of verbal data provided by the local population and of natural indicators should not be ignored. As an example, trees growing at an angle are a reliable indicator of high mean wind speeds. Knowledge of the characteristics of the wind and of some of the laws governing its behavior with respect to its usage is essential for a successfully planning of wind energy projects.

One of the most important characteristic of the wind resource is its variability. The wind is highly variable, both geographically and temporally. This property of wind is amplified because of the cubic relationship of the wind speed to available energy. On a large scale, the global variability describes the fact that there are many different climatic regions in the world. Even inside the one climatic region, there is a lot of variation on a smaller scale influenced by the physical geography, the distribution and size of land and sea, the topography and vegetation on land. Above the open seas, the wind velocities are highest, whereas they rapidly decrease above the land surfaces.

The map from the European Wind Atlas (Figure 2.13) shows an overview of the regional wind status in Europe. It is clearly seen that the dominance of regions with high wind speeds along the northern European coasts. Nevertheless, there are also some regions with high mean wind velocities in the Mediterranean area, for example in Spain, in Southern France and on the Greek Isles [32].

The wind resource maps of the European Wind Atlas show the mean annual wind speed at 50 m height, divided into five zones. In addition, the data for five roughness classes from “open sea” to “protected terrain” are specified. In addition to this, the wind atlas specifies the mean specific annual energy content in Watts per square meter rotor swept area.



Wind resources ¹ at 50 metres above ground level for five different topographic conditions									
Sheltered terrain ²		Open plain ³		At a sea coast ⁴		Open sea ⁵		Hills and ridges ⁶	
$m s^{-1}$	Wm^{-2}	$m s^{-1}$	Wm^{-2}	$m s^{-1}$	Wm^{-2}	$m s^{-1}$	Wm^{-2}	$m s^{-1}$	Wm^{-2}
> 6.0	> 250	> 7.5	> 500	> 8.5	> 700	> 9.0	> 800	> 11.5	> 1800
5.0-6.0	150-250	6.5-7.5	300-500	7.0-8.5	400-700	8.0-9.0	600-800	10.0-11.5	1200-1800
4.5-5.0	100-150	5.5-6.5	200-300	6.0-7.0	250-400	7.0-8.0	400-600	8.5-10.0	700-1200
3.5-4.5	50-100	4.5-5.5	100-200	5.0-6.0	150-250	5.5-7.0	200-400	7.0- 8.5	400- 700
< 3.5	< 50	< 4.5	< 100	< 5.0	< 150	< 5.5	< 200	< 7.0	< 400

Figure 2.13. The wind resource maps of the European Wind Atlas (Source: Risø DTU, 1989)

The European Wind Atlas consists of two parts: the first part describes wind conditions in Europe and the second part contains a mathematical method by means of which the wind conditions and the energy yield of one or more wind turbines can be predicted at a particular site from these data.

The first part is based on about 220 measuring stations. These measurement data include the local coordinates of the measuring station, the measuring height, roughness rose, i.e. the information on environmental roughness in directional sectors and the frequencies of wind speed and wind direction specified in the sectors. In addition, the database contains the daily variation and variation within a year in wind speed. By aid of this information, the Weibull parameters c and k have been calculated for each directional sector. From these raw data, the so-called “*regional wind climatology*” is determined by using the *geostrophic law of friction* which is a fundamental theoretical

approach to describing the wind conditions in the boundary layer of the earth's atmosphere. The forces resulting from the pressure gradients in the atmosphere are brought into equilibrium with the frictional forces of the earth's surface, removing local influences like:

- Orography,
- Environmental roughness,
- Obstacles,

from the local raw data of the measuring stations and calculating the Weibull parameters (c and k) for “regionally” valid wind data. These data then apply to “flat and even” terrain and “no shading by obstacles” and are computed for four different roughness classes [32]

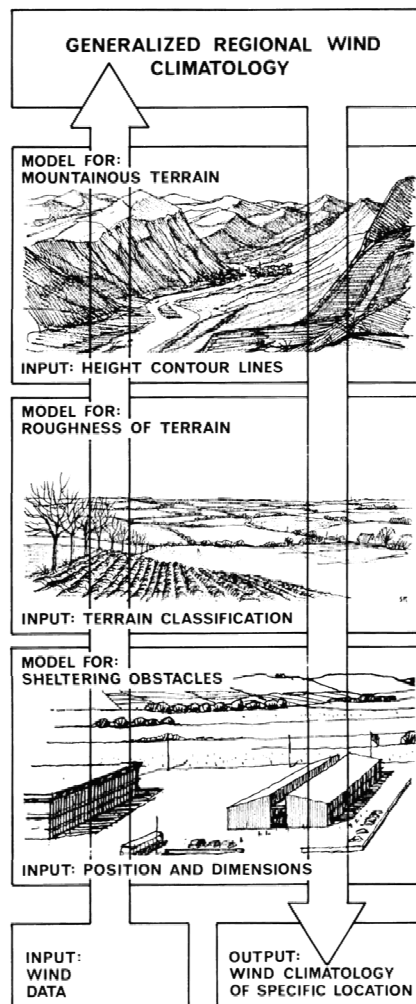


Figure 2.14. The wind atlas methodology used for the European Wind Atlas (Source: Petersen [27], 1997)

In the second part, the sites were classified in accordance with the criteria of orography, surface roughness and obstacles. For this aim, the landscape is divided into five different landscape types and four surface roughness classes are defined.

The second part of the wind atlas, the “Wind Atlas Analysis and Application Program” (WAsP) contains descriptions on how the wind data for an actual possible site for a wind turbine can be found from the regional data. In this method, the calculation of regional data from the basic local raw data of the measuring stations is reversed and the same physical and mathematical models are used.

The insight of wind energy usage into the inland parts with their much more complex topographical conditions in comparison with the open and flat coastal regions has made it clear that a more exact determination of the wind data is necessary. The widely used method of the European Wind Atlas shows distinct weaknesses at inland sites. These are essentially attributable to two reasons:

- The influence of the terrain relief (orography) on the local wind field is reproduced only insufficiently.
- The logarithmic height formula for the increase in wind speed with height, used in the WAsP method loses its validity outside the Prandtl layer.

Against this background, numeric simulation models are increasingly used which do provide more accurate results. The basic concept of these simulation calculations is based on a digital three-dimensional model of the orography including surface features. The result is a three-dimensional wind field which reproduces the influence of the shape of the terrain with its surface characteristics and manages without extrapolating to a greater height the wind speed of measuring stations close to the ground [32].

Also there is a study that has been performed in 2007 for wind potential atlas of Turkey. Similar methodology had been used in this study and it is called as REPA (Wind Energy Potential Atlas) of Turkey. By aid of this atlas;

- Average wind speeds at height of 30, 50, 70 and 100 meters in daily, monthly, seasonally and yearly time period,
- Wind power density at height of 50 and 100 meters in monthly, seasonally and yearly time period,
- Yearly capacity factor at 50 meters,
- Yearly wind classes at 50 meters,

- Monthly temperature values at 2 and 50 meters,
 - Monthly pressure values at sea level and 50 meters,
- could be learnt in resolution of 200 m x 200 m throughout of Turkey.

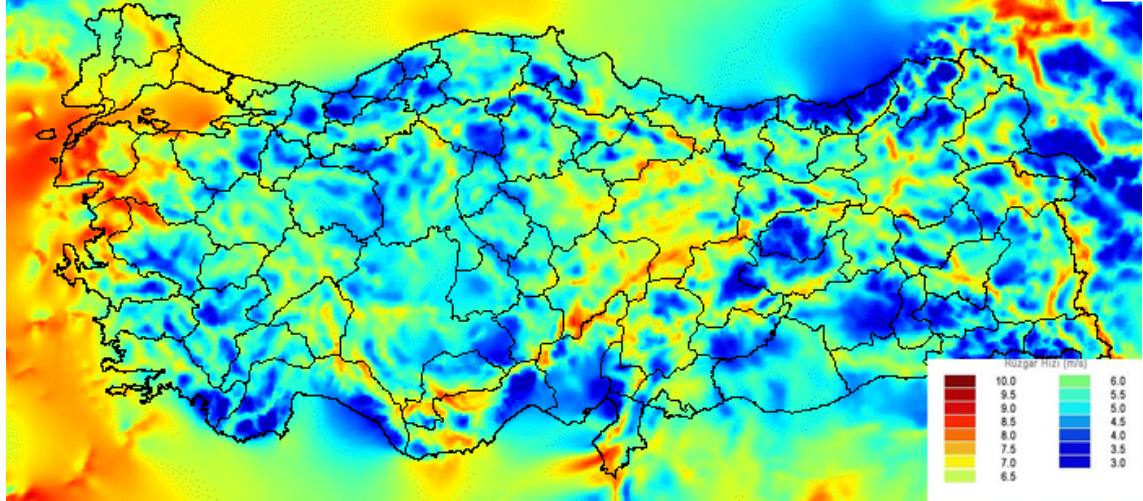


Figure 2.15. Wind speed map of Turkey at 70 meters
(Source: EİE, 2009)

Also some thematic maps that contain data of topography, rivers and lakes, residential areas, forests, motorways and railways, environmental areas in special protection, ways of migrating birds, harbors and airports, energy transmission lines, transformer stations and power plants were integrated into REPA by aid of GIS (Geographical Information System) to identify suitable areas for building wind farms.

CHAPTER 3

MEASUREMENT OF WIND

Planner or user of a wind turbine is often faced with having no information on the wind regime at the intended location. There are basically only two choices for providing wind data. The European Wind Atlas can be used as an option or measurements will be taken at the site. Both methods should be used in parallel whenever possible so that the results can be compared.

3.1. Measurement Techniques of Wind

Measuring the wind on site is the most reliable method and the energy yield of a wind turbine can only be predicted with statistically validated values of mean wind speed, wind speed distribution and the vertical wind profile. Statistically reliable values require long-term measurements.

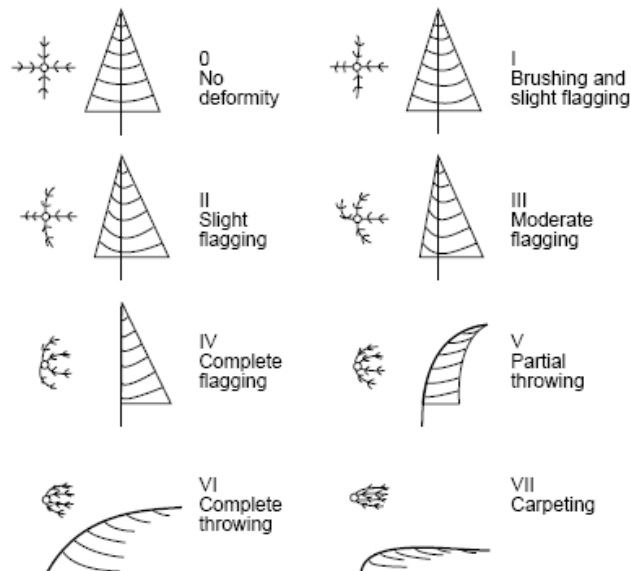


Figure 3.1. Griggs-Putnam index of deformity

(Source: Gipe [34], 2004)

Table 3.1. Griggs-Putnam index of deformity in terms of m/s

Index	I	II	III	IV	V	VI	VII
Speed m/s	3-4	4-5	5-6	6-7	7-8	8-9	10+

Generally, specification of a reliable value for the long-term mean annual wind speed requires the mean value taken over at least ten years. On the other hand, the areas showed in the wind maps are generally very large that the data are not transferable to specific local points, particularly not in complex terrain. Wind measurement over one year, gives the possibility of comparing these values with the long-term data measured within the same period of time at the closest station at which the long-term mean value is measured. Additionally, if the wind speed is plotted over time, indications as to the turbulence intensity can be derived from the wind variations.

Wind speed m/s from to		Wind force acc. to Beaufort	Wind force notation	Visible effects inland
0.0	0.2	0	Calm	Smoke rises vertically
0.3	1.5	1	Light air	Smoke indicates wind, wind vanes do not
1.6	3.3	2	Light breeze	Wind perceptible on face, wind vanes move
3.4	5.4	3	Gentle breeze	Leaves and thin branches move, wind extends pennants
5.5	7.9	4	Moderate breeze	Thin branches move, dust and paper are raised
8.0	10.7	5	Fresh breeze	Small trees begin to sway, white caps form on lakes
10.8	13.8	6	Strong breeze	Thick branches move, telegraph lines whistle
13.9	17.1	7	Moderate gale	Whole trees move, difficult to walk
17.2	20.7	8	Fresh gale	Wind breaks branches off trees
20.8	24.4	9	Strong gale	Minor damage to houses (roof tiles)
24.5	28.4	10	Whole gale	Trees are uprooted
28.5	32.6	11	Storm	Significant damage to houses (very rare inland)
32.7	56	12 - 17	Hurricane	storm damage Widespread devastation

Figure 3.2. Classification of wind speed according to the Beaufort scale
(Source: Hau [32], 2006)

Usable data can only be obtained by means of measurements over a certain period and recording of the measured values. This requires a stationary measuring system on a mast with a logging device for the measured data. The sensors of a wind measuring system suitably consist of a combination of an anemometer and wind vane or, nowadays, of an ultrasonic sensor which has no moving parts [32].

The sensors are mounted on top of or on side arms of a mast or a tower. The mast height depends on the necessities of the project. If just the data are compared in the wind maps are proposed, then the standard measuring height of 10 m is enough.

The wind speed is showed in meters per second in the SI system of units. The Beaufort scale, which uses more graphical way, of “wind forces” is widely used in many areas.

3.2. Measurement Devices

A precise knowledge of the wind characteristics at the prospective sites is essential for the successful planning and implementation of wind energy projects. The basic information required for such an analysis is the speed and direction of the prevailing wind at different time scales. Ecological factors may often be helpful in identifying a candidate site for wind power project. Wind data from the nearby meteorological stations can give us a better understanding on the wind spectra available at the site. However, for a precise analysis, the wind velocity and direction at the specific site has to be measured with the help of accurate and reliable instruments.

3.2.1. Anemometers

An anemometer is an instrument used in a weather station for measuring the wind speed. Anemos, that is comes from the Greek word, means wind. The first known description of an anemometer was given by Leon Battista Alberti in around 1450 [35].

There are different types of anemometers. Based on the working principle, they can be classified as:

1. Rotational anemometers (cup anemometers and propeller anemometers)

2. Pressure type anemometers (pressure tube anemometers, pressure plate anemometers and sphere anemometers)
3. Thermoelectric anemometers (hot wire anemometers and hot plate anemometers)
4. Phase shift anemometers (ultra sonic anemometers and laser Doppler anemometers) [1].

3.2.1.1. Cup Anemometers

In wind energy measurements, the cup anemometer is used most commonly. It consists of three or four cups attached by equal angle to a centrally rotating vertical axis through spokes (Figure 3.3.).



Figure 3.3. Cup anemometer
(Source: Ammonit [36], 2009)

The cups can be hemispherical or conical in shape and made with light weight material. This type of anemometer is basically a drag device. When kept in the flow, the wind applies drag force on the cups. The intensity of rotation is directly proportional to the velocity of incoming wind.

Although these anemometers can keep going on in variety of hard conditions of environment, they have some limitations. It accelerates quickly with the wind but

retards slowly as wind ceases. Due to this slow response, cup anemometers do not give reliable measurement in wind gusts. Also, as the drag force is proportional to the density, any changes in the air density will affect the accuracy of metered velocity.

Nevertheless of these limitations, cup anemometers are widely used for measuring wind velocity in meteorological as well as wind energy applications.

3.2.1.2. Propeller Anemometer

A propeller type anemometer, also known as aero-vane, consists of a four blade helicoid propeller. The blades are made with light weight materials like aluminum or carbon fiber thermoplastic. These devices work predominantly on lift force. [1]



Figure 3.4. Propeller anemometer
(Source: Young [37], 2009)

Through with air flow parallel to propellers axis, the propeller blades experiences a lift force, which turns the propeller at a speed proportional to the wind velocity.

An aero-vane combines a propeller and a tail on the same axis to get accurate and precise wind velocity and direction measurements from the same device.

3.2.1.3. Plate Anemometers

The first anemometer of any kind is the pressure plate anemometer. It was invented by Leon Battista Alberti as early as in 1450 and then further refined by Robert Hooke (1664) and Rojer Pickering (1744). It basically consists of a swinging plate held at the end of a horizontal arm. This is attached to a vertical shaft around which the arm can rotate freely (Figure 3.5.). A wind vane directs the plate always perpendicular to the wind flow. This pressure makes the plate to swing inward. The pressure of the wind on its face is balanced by a spring. The compression of the spring determines the actual force which the wind is exerting on the plate.

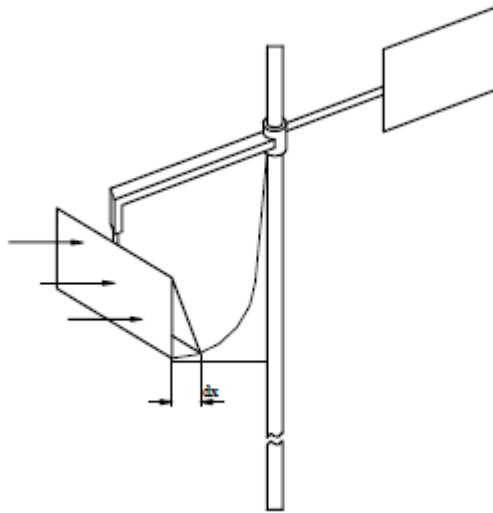


Figure 3.5. Illustration of pressure plate anemometer
(Source: Mathew [1], 2007)

Pressure plate anemometers are suited for measuring gusty winds and do not respond to light winds, are inaccurate for high wind readings, and are slow at responding to variable winds. Plate anemometers have been used to trigger high wind alarms on bridges.

3.2.1.4. Pressure Tube Anemometers

The pressure tube anemometer is another type of anemometer which uses the wind pressure to measure the speed. This works on the principle that, the wind flow passing through the tube creates pressure whereas the flow across a tube results in suction.

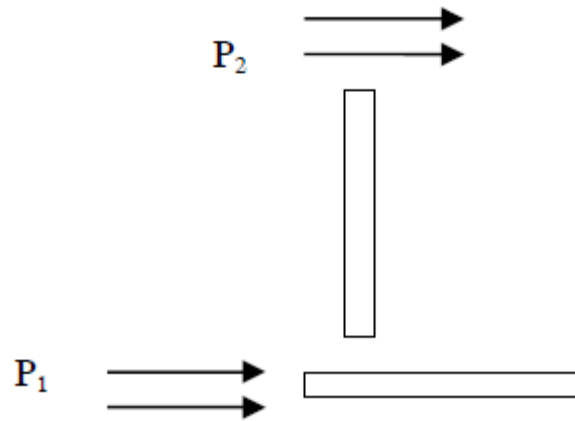


Figure 3.6. Principle of pressure tube anemometer
(Source: Mathew [1], 2007)

Consider two tubes as shown in the Figure 3.6. The pressure in the tube parallel to the wind is the sum of atmospheric pressure and the wind pressure.

Thus,

$$P_1 = P_A + C_1 \frac{1}{2} \rho_a V^2 \quad (3.1)$$

Similarly in the tube perpendicular to the wind, the pressure is

$$P_2 = P_A - C_2 \frac{1}{2} \rho_a V^2 \quad (3.2)$$

where P_A is the atmospheric pressure and C_1 and C_2 are coefficients. Subtracting P_2 from P_1 and solving for V , we get

$$V = \left[\frac{2(P_1 - P_2)}{\rho_a(C_1 + C_2)} \right]^{0.5} \quad (3.3)$$

Thus, by measuring the difference in pressure inside the two tubes, the wind velocity can be estimated. Values of C_1 and C_2 come with the device. The pressure is measured using standard manometers or pressure transducers. One of the most important advantages of pressure tube anemometer is that it does not have any moving parts. Otherwise, this anemometer has limited application in the open field measurements due to dust, moisture and insects can affect its accuracy [1].

3.2.1.5. Hot-wire Anemometers

The Hot-Wire anemometer is the most well known thermal anemometer, and measures a fluid velocity by noticing the heat convected away by the fluid. The core of the anemometer is an exposed hot wire either heated up by a constant current or held at a constant temperature. In both case, the heat lost to fluid convection is a function of the fluid velocity.

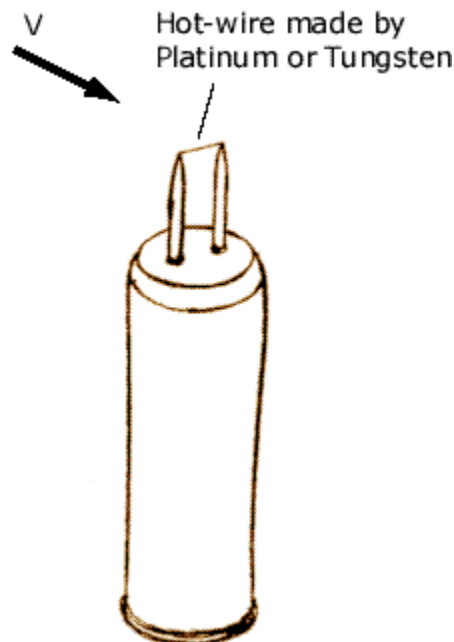


Figure 3.7. Hot-wire anemometer
(Source: eFunda [38], 2009)

By measuring the change in wire temperature under constant current or the current required to maintain a constant wire temperature, the heat lost can be obtained. The heat lost can then be converted into a fluid velocity in accordance with convective theory.

Hot-wire anemometers, as extremely fragile, have extremely high frequency-response and fine spatial result compared to other measurement methods, and as such are almost universally employed for the detailed study of turbulent flows, or any flow in which rapid velocity fluctuations are of interest [39].

3.2.1.6. Sonic Anemometers

Sonic anemometers measure the wind velocity by sensing the changes in the speed of sound in air. It has three arms, mounted perpendicular to each other, as shown in Figure 3.8 Transducers fitted at the tips of each arm emit acoustic signals which travel up and down through the air. Speed of sound in moving air is different from that through still air.



Figure 3.8. Sonic anemometer
(Source: Met One Instruments [40], 2009)

They are reliable and accurate for measuring wind velocity in the range of 0 to 65 m/s. However, they are costlier than the other types of anemometers. Two-dimensional (wind speed and wind direction) sonic anemometers are used in applications such as weather stations, ship navigation, wind turbines, aviation and weather buoys.

3.2.1.6. Laser Doppler Anemometers

A portable lidar system has been developed for monitoring the evolution of the atmospheric boundary layer (ABL) using aerosols as the tracers of atmospheric motion. This lidar system uses last technology with a high repetition rate, low pulse energy laser, and photon-counting detection [41].

Particulates flowing along with air molecules near where the beam exits reflect, or backscatter, the light back into a detector, where it is measured relative to the original laser beam. When the particles are in great motion, they produce a Doppler shift for measuring wind speed in the laser light, which is used to calculate the speed of the particles, and therefore the air around the anemometer [42].



Figure 3.9. Laser Doppler anemometer
(Source: Natural Power [43], 2009)

3.2.2. Wind Vane

Direction of wind is an important factor in the locating of a wind energy conversion system. It is important to avoid any obstacles to the wind flow from side that If we receive the major percentage of energy available in the wind from a specific direction. In earlier day's anemometers, wind vanes were used to identify the wind direction.

Data of the velocity and direction of wind can be presented in the wind roses in a combined form. The wind rose is a graph that shows the distribution of wind in different directions. The chart is divided into 8, 12 or 16 equally spaced sectors representing different directions. Three kinds of information can be showed in a wind rose.

1. The percentage of time for which we receive wind from a particular direction. This can show us the direction from which we get most of our wind.
2. The product of this percentage and the average wind velocity in this direction. This tells us the average strength of the wind spectra.
3. The product of time percentage and cube of the wind velocity. This helps us in identifying the energy available from different directions [1].



Figure 3.10. Wind vane
(Source: Kintech Engineering [44], 2009)

3.2.3. Air Temperature and Pressure Measurement

The energy in the wind for a given wind velocity depends on the air density. The air temperature and pressure should be measured to be able to adjust for changes in air density.



Figure 3.11. Temperature sensor
(Source: Kintech Engineering [45], 2009)

At high temperatures it is recommended that relative humidity also be measured, and corrected for.

The standard requires that the measured power is corrected by multiplying it by the ratio of the standard air density and the test air density, calculated from the temperature and pressure, but only when the average air density lies outside the standard value, plus or minus 0.05 kg/m³ [3].

3.2.4. Humidity Sensor

Relative humidity(Φ) is defined as the ratio of the partial pressure of water vapor (e_w) in the mixture to the saturated vapor pressure of water (e_w^*) at a certain temperature and commonly showed as a percentage and is calculated by using the following equation:

$$\Phi = \frac{e_w}{e_w^*} \times 100\% \quad (3.4)$$

The calculation of the air humidity does not directly affect a wind site assessment, but knowing this parameter helps evaluating the potential danger of ice build-up at the measuring location.

3.3. Wind Masts

There are two basic tower types for sensor mounting: tubular and lattice. Tilt-up, telescoping, and fixed versions are available for both types. Also, these types may be either guyed or self-supporting. Tubular, tilt-up guyed types are suggested for their ease of installation (the tower can be assembled and sensors mounted and serviced at ground level), minimal ground preparation, and relative low cost. Otherwise, major advantage of the lattice towers is easy to climb tower and reach sensors in case of any problem without grounding the tower [46].

Towers should:

- Have an erected height sufficient to attain the highest measurement level
- Be able to withstand wind and ice loading extremes expected for the location
- Be structurally stable to minimize wind-induced vibration
- Have guy wires secured with the proper anchor type, which must match the site's soil conditions
- Be equipped with lightning protection measures including lightning rod, cable, and grounding rod
- Be secured against vandalism and unauthorized tower climbing
- Have all ground-level components clearly marked to avoid collision hazards
- Be protected against corrosion from environmental effects, including those found in marine environments
- Be protected from cattle or other grazing animals

CHAPTER 4

THE MATERIALS AND METHODS

4.1. Field Inspection

Visits should be guided to main goal of verifying site conditions. Items of importance include:

- Available land area
- Location of obstructions
- Roughness inspection near the mast
- Accessibility into the site
- Trees deformed by continuous strong winds (flagged trees)

A topographic map of the area should be used to note the presence or absence of the site characteristics. A Global Positioning System (GPS) receiver should be used to record the location coordinates (latitude, longitude, elevation) of the sites. A video or still camera record is useful for future reference and presentation purposes [46].

4.2. Software for Analysis

Two different software were used for wind potential evaluation and some features of these software that are used in this thesis were stated below.

4.2.1. WAsP

“Wind Atlas Analysis and Application Program” (WAsP) is a PC-program for the vertical and horizontal extrapolation of wind climate statistics. It contains several models to describe the wind flow over different terrains and close to sheltering obstacles. Conceptually, WAsP consists of five main calculation blocks:

1. Analysis of raw data: This option enables an analysis of any time-series of wind measurements to provide a statistical summary of the observed, site-specific

wind climate. This part is implemented in separate software tools: the Observed Wind Climate (OWC) Wizard and the WAsP Climate Analyst.

2. Generation of wind atlas data: Analyzed wind data can be converted into a regional wind climate or wind atlas data set. In a wind atlas data set the wind observations have been 'cleaned' with respect to site-specific conditions. The wind atlas data sets are site-independent and the wind distributions have been reduced to some standard conditions.
3. Wind climate estimation: Using a wind atlas data set calculated by WAsP or one obtained from another source - e.g. the European Wind Atlas - the program can estimate the wind climate at any specific point by performing the inverse calculation as is used to generate a wind atlas. By introducing descriptions of the terrain around the predicted site, the models can predict the actual, expected wind climate at this site.
4. Estimation of wind power potential: The total energy content of the mean wind is calculated by WAsP. Furthermore, an estimate of the actual, annual mean energy production of a wind turbine can be obtained by providing WAsP with the power curve of the wind turbine in question.
5. Calculation of wind farm production: Given the thrust coefficient curve of the wind turbine and the wind farm layout, WAsP can finally estimate the wake losses for each turbine in a farm and thereby the net annual energy production of each wind turbine and of the entire farm, i.e. the gross production minus the wake losses.

4.2.2. GH WindFarmer

The GH WindFarmer software package allows the user to design a wind farm to achieve maximum energy production within the geometric and environmental constraints of the site. GH WindFarmer allows the user to efficiently design a wind farm to achieve maximum energy production within the geometric and environmental constraints of the site. Some of the core features:

- Wind data analysis and correlation via MCP+ module

- Advanced energy calculation options (e.g. use of the measured distribution, turbine specific air density, sector management, wake loss and turbulence adjustments)
- Automatic layout optimization to design a wind farm with minimal impact on the environment
- Advanced wind farm wake loss modeling (GH Eddy Viscosity Model)
- Energy, wind speed, noise and ground slope maps
- Site condition assessment
- Noise impact modeling according to current international standards
- Shadow flicker calculation
- Uncertainty analysis with exceedance levels for the net energy yield (P90, P75, etc.)

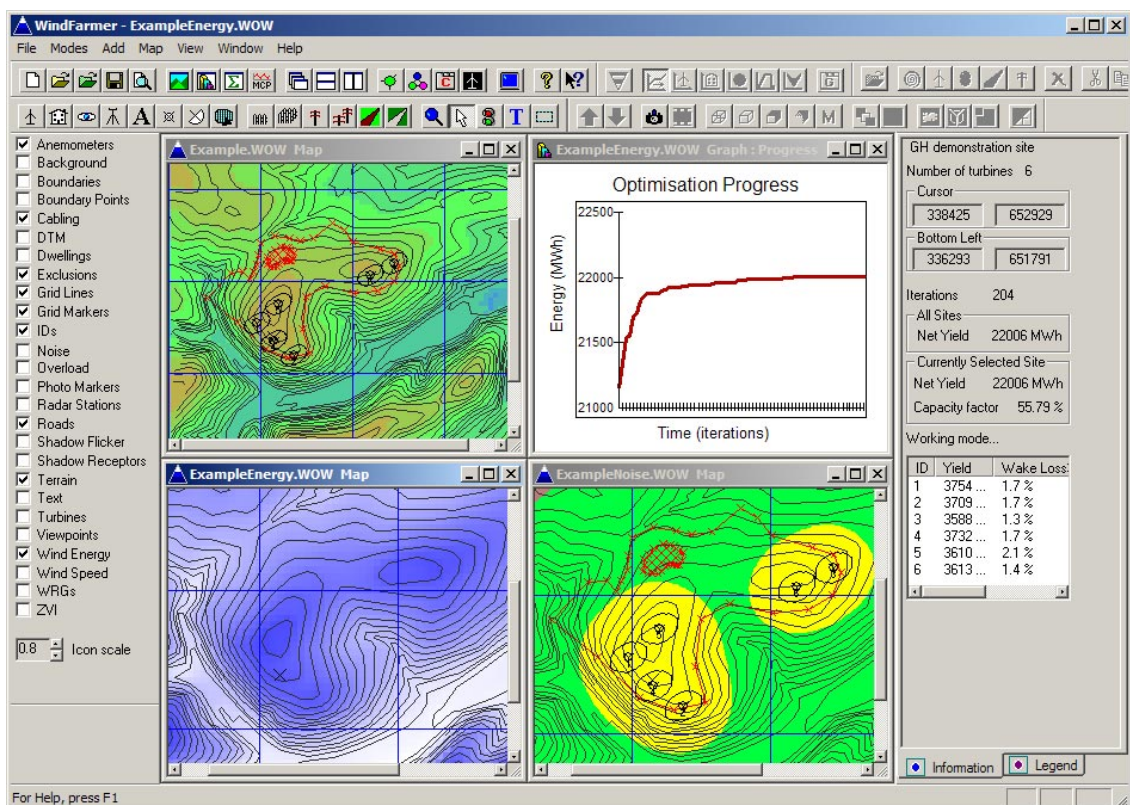


Figure 4.1. Interface of WindFarmer software
(Source: GL Garrad Hassan [47], 2009)

4.2.2.1. MCP+ Module

The MCP+ Module provides all the tools for the evaluation of measured wind data. Time-series of measured data can be imported cleaned, plotted, documented and then correlated to long term wind resource data. The user is able to process the measured raw data via MCP+ module.

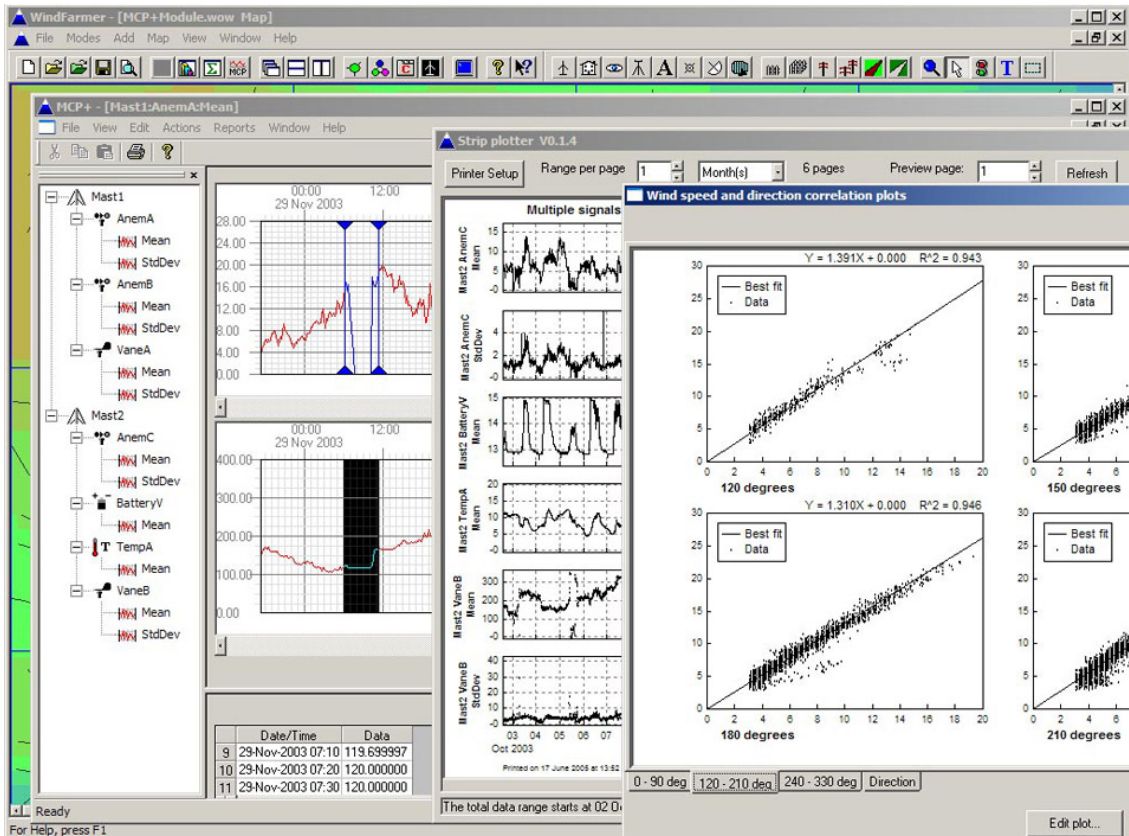


Figure 4.2. Interface of MCP+ module of WindFarmer
(Source: GL Garrad Hassan [48], 2009)

Some features of the MCP+ module:

- Load time series anemometry measurements from a range of data file formats
- Recalibrate the data
- Inspect and clean the data with an interactive plotter
- Print and export plots of time series data; export data listings and reports
- Create WAsP TAB format frequency distributions
- Present wind rose plots from time series or frequency distribution data

- Perform Measure Correlate Predict (MCP) analysis where concurrent reference station and site measurements are available
- Predict long term site data from the results of the MCP analysis. Output as frequency distribution or wind rose
- The resulting long term distributions are documented and output in WAsP compatible ASCII file format.

4.2.2.2. Energy Calculation

An energy calculation combines the incident wind speeds at each turbine with the power curve of the turbine to give the power output for the whole wind farm, applying the frequency distribution results in the expected energy yield.

The energy production of the wind farm is calculated using GH WindFarmer in conjunction with the WAsP or a wind flow model with compatible output the wind flow model is used to determine the ambient wind speeds at each turbine location. The output of a wind flow model consists of the directional Weibull c and k parameters which represent the wind speed probability distribution and a directional probability for every point on a grid.

GH WindFarmer enables you to use the probability distribution of the wind speed and direction measured at an on-site mast by associating this file with the predictions of the wind flow model. Through this association method, the measured data are scaled to the turbine locations using the predictions of the wind flow model.

A wake model is used to determine the changes to the incident wind speeds at each turbine within a wind farm due to the effects of other turbines. The accuracy of wake prediction has become increasingly important as larger wind farms are being developed and turbines are being placed closer together [49].

4.2.2.3. Program Inputs

The following inputs to the GH WindFarmer model are required to produce an estimate of the wind farm energy production:

- A WAsP wind resource grid (WRG) format file at the turbine hub height with extents covering all the intended turbine locations or a WAsP discrete resource (RSF) format file with wind speed results at individual turbine locations
- Turbine locations as grid co-ordinates
- Turbine performance data, which includes power, thrust and rotor speed characteristics
- Turbine dimensions, specifically hub height and diameter

The resource file is generated within WAsP and is a grid representation of the directional wind speed distribution at each point over the site [49].

4.2.2.4. Association Method

For the association method, it is recommended that the following optional input files are used in addition:

- A single point WAsP wind resource grid file for the reference mast at measurement height, and when using an RSF file; an additional single point WRG file at hub height at the mast location
- A joint wind speed and direction frequency distribution table for the reference mast location, in the format of the WAsP table files (TAB)

If these two files are not specified, GH WindFarmer will use the information from the WAsP wind resource grid file which is based on a fit a Weibull distribution to the measured data. For certain wind regimes, the Weibull distribution may not give a good representation of the wind climate at the site [49].

Using the association method allows the user to:

- Use the measured wind speed and directional distribution instead of a Weibull distribution
- Model the variation of the turbulence intensity over a wind farm
- Model the influence of the topography on turbine wakes
- Assess the flow models modification to the directional probability

4.2.2.5. Methodology of the Energy Calculation

Before performing an energy calculation, the program determines the topographic speed-ups over the site. Using the association method, this is the ratio of the wind speed at each grid point in the WAsP wind resource grid file to the wind speed at the reference location. The topographic speed-up is determined separately for each of the direction sectors in the wind resource grid file. The speed-up factors are then applied to the measured wind speed and direction frequency distribution table that is assumed to be representative for the site. This method avoids errors due to fitting a Weibull distribution to measured data.

The program considers each wind direction sector in turn and each wind speed bin individually. For each wind direction, the program determines the topographic speed-up of wind speed for the grid points nearest each turbine location. The speed-up factor is assumed constant for all wind speeds considered.

The wake effect of each turbine on the others is calculated for each wind speed step as the wake effect varies with wind speed. The first step in the process is to calculate the wind speed and turbulence intensity incident upon the turbine. If a turbine is in more than one wake, the overall wake effect is taken as the largest wind speed deficit, and other smaller wake effects are neglected. This methodology is based on the results of the assessment of measured data from a number of wind farms.

The wind speed incident on each turbine is therefore the combination of the topographic speed-up and the wake loss. The incident wind speed can then be used to determine the power output. A power look-up table is created where the power output of each turbine is stored for each reference wind direction and wind speed considered.

The energy output is calculated as the sum product of the reference wind speed and direction frequency distribution table and the power output look-up table.

4.2.2.6. Direction Correction

The direction of the wind flow is changed when passing over terrain. The modification is usually calculated by the wind flow model and represented in the wind resource file. GH WindFarmer allows optional use of this shift in direction. Directional correction factors are obtained with the same methodology as the non-directional speed-

up factors. By using this function, the energy results can be improved in areas where the measured distribution is no longer an adequate representation of the site conditions. Users are however advised to use this function with care as sparsely occupied directions sectors may lead to unrealistic results [49].

4.3. Analysis of Raw Data

Time-series of wind data or climatologically (statistical) summaries may be obtained from synoptic stations, from stations established for the collection of climatic data or from other sources. In the selection of wind data a number of goals should be aimed at which can be summarized as follows:

- Sufficient time period. At least one year, but preferably several (whole) years.
- Well exposed anemometer, far from buildings and other obstacles. This requirement is often the most difficult to satisfy.
- Accurate description of anemometric conditions and data of 10-min or hourly averages collected for e.g. each 3-hour period throughout the 24-hour day.

Date	Time	v1Ave	v1Max	v1Min	v1Sig	v2Ave	v2Max	v2Min	v2Sig	DirAve	DirMax	DirMin	DirSig	Hygro	Thermo	Baro
01.01.01	00:10	14,1	18,6	10,9	1,3	13,0	17,2	9,2	1,4	167	183	151	0	78	12,3	955,0
01.01.01	00:20	13,5	15,7	10,1	1,0	12,8	16,5	8,8	1,3	160	182	132	17	74	12,0	955,0
01.01.01	00:30	14,8	18,9	11,6	1,6	13,9	18,5	10,6	1,5	159	173	140	13	72	12,0	955,0
01.01.01	00:40	18,2	22,4	14,2	1,9	16,6	22,1	12,9	2,0	159	170	148	0	72	12,5	954,0
01.01.01	00:50	19,4	22,7	13,6	1,3	17,5	22,8	13,5	1,8	160	171	149	0	71	12,5	955,0
01.01.01	01:00	19,5	22,6	16,6	1,2	17,8	22,1	13,5	1,8	160	176	147	0	68	12,5	954,0
01.01.01	01:10	19,1	22,1	15,7	1,4	17,3	20,7	13,0	1,4	159	170	146	0	68	12,9	954,0
01.01.01	01:20	18,2	21,2	13,8	1,5	16,9	21,0	12,2	1,8	159	179	147	15	65	12,6	954,0
01.01.01	01:30	19,6	24,2	15,8	1,6	17,5	21,6	13,1	1,8	157	172	148	11	64	12,6	953,0
01.01.01	01:40	17,0	21,7	12,1	2,1	15,2	20,1	10,0	2,0	153	167	133	16	62	12,7	954,0
01.01.01	01:50	16,1	20,1	12,0	1,8	14,5	18,9	9,6	1,9	153	164	141	15	66	12,7	955,0
01.01.01	02:00	16,7	19,5	14,0	1,2	14,9	18,9	10,9	1,5	153	171	139	8	71	12,6	954,0
01.01.01	02:10	17,5	21,5	13,4	1,7	15,9	20,4	10,6	2,0	153	168	133	14	73	12,6	954,0
01.01.01	02:20	17,5	22,7	13,1	1,9	15,7	21,7	10,3	2,0	152	167	133	15	74	12,7	953,0
01.01.01	02:30	18,2	23,4	13,1	2,1	16,2	21,9	10,1	2,1	154	172	139	0	76	12,6	953,0
01.01.01	02:40	16,8	24,2	11,0	2,5	15,1	22,2	9,6	2,7	152	170	135	0	81	12,5	954,0
01.01.01	02:50	18,3	24,1	11,7	2,4	16,6	24,5	10,5	2,6	149	178	129	18	82	12,4	954,0
01.01.01	03:00	16,9	21,7	11,0	1,9	14,9	20,7	7,5	2,6	148	169	122	0	80	12,5	954,0
01.01.01	03:10	16,5	21,7	11,4	2,0	14,3	20,5	9,8	2,0	148	170	124	14	79	12,5	953,0
01.01.01	03:20	18,7	25,1	13,4	2,3	16,9	23,8	11,5	2,4	145	166	108	0	79	12,3	953,0
01.01.01	03:30	18,4	25,0	10,3	2,3	16,3	21,7	9,9	2,4	142	174	116	12	76	12,6	952,0
01.01.01	03:40	18,5	23,1	13,7	1,8	16,5	21,6	10,4	2,1	148	166	124	0	76	12,5	953,0
01.01.01	03:50	18,7	25,1	13,7	2,2	16,3	23,0	10,2	2,4	142	160	121	15	78	12,0	953,0
01.01.01	04:00	18,5	25,7	12,5	2,1	16,4	24,0	10,6	2,2	144	169	115	11	76	12,3	952,0
01.01.01	04:10	16,8	22,8	11,4	2,3	14,9	21,7	9,6	2,3	144	170	118	0	77	12,1	953,0
01.01.01	04:20	16,4	21,7	10,9	2,3	14,1	22,6	8,8	2,2	144	175	120	15	77	11,8	953,0
01.01.01	04:30	17,9	24,3	13,1	2,2	15,8	21,8	9,8	2,5	144	165	118	0	77	12,4	953,0
01.01.01	04:40	19,4	27,6	13,3	2,8	16,7	24,9	10,1	3,0	141	162	116	0	74	12,3	952,0
01.01.01	04:50	20,2	26,5	14,6	2,2	17,2	23,7	11,1	2,5	140	167	119	8	71	12,1	952,0
01.01.01	05:00	21,8	28,8	14,5	2,8	19,0	26,4	9,5	3,4	142	164	117	7	68	12,5	952,0
01.01.01	05:10	22,2	30,6	16,0	2,8	19,1	27,1	11,2	3,4	138	157	113	15	69	12,7	951,0
01.01.01	05:20	20,6	28,0	14,6	3,0	18,2	26,9	11,8	3,1	146	169	124	13	71	12,4	952,0
01.01.01	05:30	18,6	22,4	13,5	1,9	16,1	21,8	11,2	2,1	148	170	119	0	75	12,0	952,0
01.01.01	05:40	18,7	23,9	12,7	2,3	16,7	23,3	10,1	2,4	144	169	116	4	73	12,0	951,0
01.01.01	05:50	18,8	23,1	14,2	1,6	16,1	19,9	9,9	1,9	138	155	118	13	73	12,3	952,0
01.01.01	06:00	21,7	27,1	16,5	2,2	18,2	25,7	12,8	2,7	136	152	123	0	77	11,8	952,0
01.01.01	06:10	21,4	27,3	15,6	2,4	18,0	24,3	11,4	2,7	137	161	122	12	77	12,0	952,0
01.01.01	06:20	19,8	27,7	12,3	2,9	17,4	24,5	11,8	2,8	148	172	124	0	81	11,5	951,0
01.01.01	06:30	15,8	25,8	7,9	4,5	13,9	22,7	6,4	4,0	191	254	129	40	81	11,3	952,0
01.01.01	06:40	14,4	18,2	11,5	1,3	12,4	15,3	8,8	1,2	235	262	194	12	83	9,0	954,0
01.01.01	06:50	15,3	19,1	11,2	1,8	13,0	16,5	9,1	1,5	224	246	210	6	89	6,3	954,0
01.01.01	07:00	12,9	16,6	9,4	1,6	11,4	16,3	7,9	1,6	220	235	202	4	94	7,1	954,0
01.01.01	07:10	16,4	18,7	13,5	1,1	14,8	18,0	9,6	1,3	217	229	207	4	94	7,4	953,0
01.01.01	07:20	16,8	18,6	14,5	0,7	14,7	16,9	11,5	1,1	218	227	208	3	95	7,3	953,0
01.01.01	07:30	16,3	19,0	13,9	0,9	14,4	17,6	11,1	1,2	213	226	199	4	95	7,2	953,0
01.01.01	07:40	16,4	18,4	13,2	1,0	14,8	17,6	11,3	1,2	213	223	200	4	96	7,1	953,0
01.01.01	07:50	13,9	17,0	11,0	1,1	12,6	16,0	9,7	1,2	212	221	200	2	96	7,2	953,0
01.01.01	08:00	12,8	14,9	10,0	0,9	11,4	13,9	9,1	1,0	210	225	199	4	96	7,3	954,0
01.01.01	08:10	14,2	19,5	10,9	1,7	12,8	17,6	8,5	1,6	204	221	183	6	98	7,5	954,0
01.01.01	08:20	13,8	18,0	10,7	1,4	12,7	17,1	9,2	1,4	198	212	184	5	97	7,8	955,0
01.01.01	08:30	11,2	14,0	8,7	1,0	9,9	12,3	7,3	1,0	197	212	182	5	97	7,8	955,0
01.01.01	08:40	7,2	10,9	8,0	2,2	6,3	9,7	2,6	1,9	187	210	132	17	97	7,9	955,0
01.01.01	08:50	6,3	9,3	3,3	1,4	5,7	8,4	2,6	1,2	174	198	133	19	94	7,9	954,0

Figure 4.3. Typical row data series

Using raw data as the initial data source is generally preferable, since this allows detection of errors in the data which may be undetectable in data summaries.

4.3.1. Data Inspection

Data should be carefully inspected even though they are assumed to be quality-controlled by the supplying organization. The most important checks after receipt of the data are:

- Visual inspection of the time series of wind speed and direction
- Inspection of the frequency tables (histograms).
- By inspection, it is possible to detect data deficiencies such as:
 - Abnormally high wind speeds.
 - An abnormal number of observations in certain wind speed classes and/or wind direction sectors.
 - Certain patterns in the data caused by the transformation of data originally reported in Beaufort, knots, miles per hour etc. to meters per second. The transformation of data measured in e.g. 16 sectors to 12 sectors may also cause a pattern in the table.
 - Stations with a systematic lack of observations, e.g. no night-time observations.

The abnormally high wind speeds can be removed manually. Abnormal occurrences of wind speeds and directions should be checked against known climatology. In general, there is no simple procedure for filling in missing data.

4.3.1.1. Viewing Data

After converting the raw data to the meaningful signal, whole data can be viewed in both ways that each one has its own advantage:

- Concurrent viewing and editing (it allows to only two signals at the same time)
- Normal plotting (every signal can be viewed at the same time on the same page)

This process provides us to see and edit which data have to be excluded.

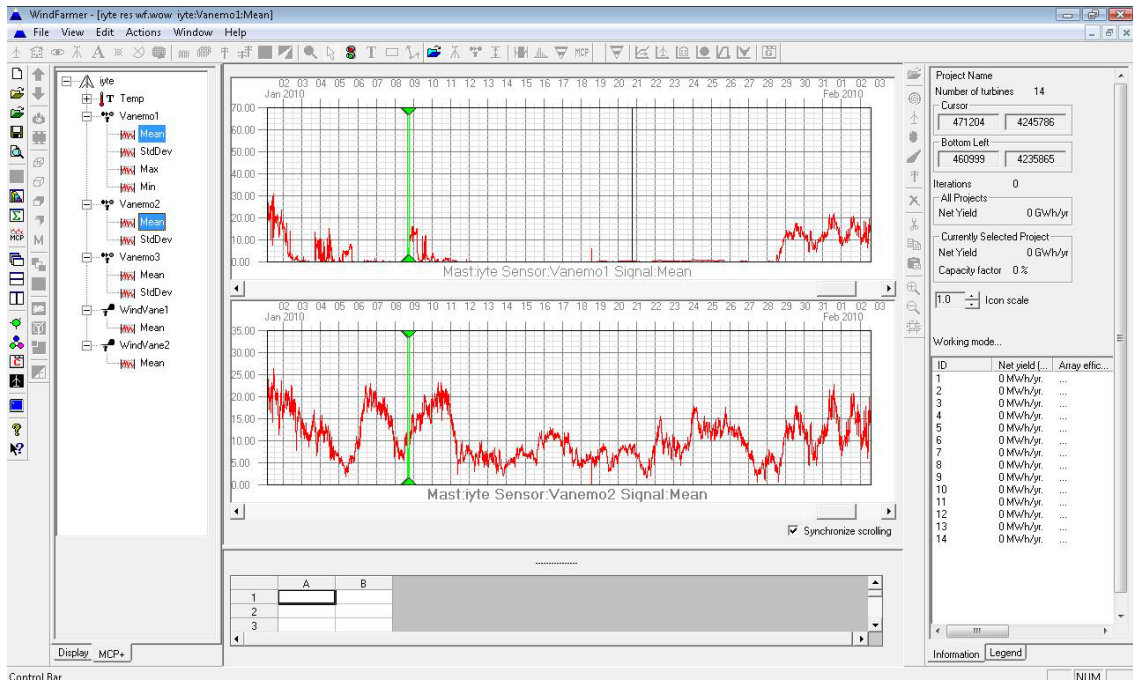


Figure 4.4. Interface of data inspection process

4.3.1.2. Cleaning Data

Cleaning inaccurate data from the set of data takes long time and requires attention. If the data shows the 0 (zero) value, it can be depended on either meteorological reason or any malfunction. Some reasons for inaccurate data:

- Effect of icing
- Low battery level
- Malfunction of measurement device
- Any damage on measurement device or mast

Zero values in data set are examined by plotting both wind speed data and other signals together. These zero value data must not included into calculations, otherwise the calculations may remain under the satisfactory level.

Inaccurate data can be excluded either manually in the raw data or by using MCP+ module. MCP+ module provides concurrent viewing, editing and cleaning of inaccurate data in the same window and it shortens the inspection time significantly.

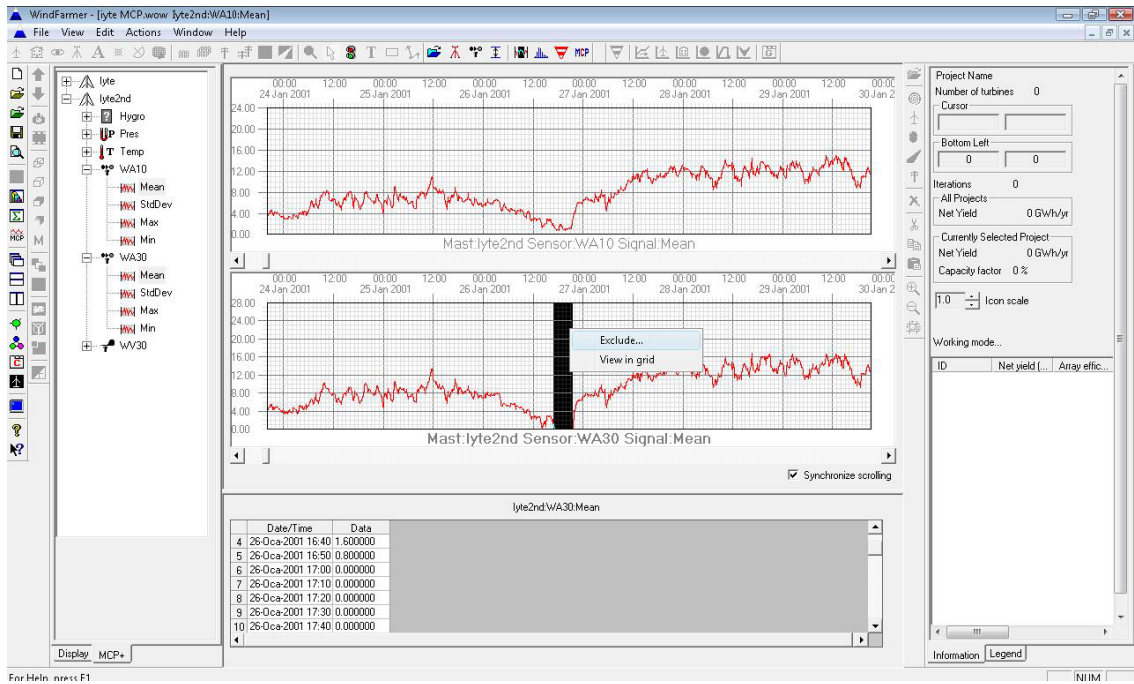


Figure 4.5. Cleaning process of malfunction data

4.3.2. Data Analysis

Having loaded the time series data for the wind speed and wind direction measurements, calibrated them and excluded those data which are known or suspected to be inaccurate, the user then has a choice of analysis procedures and outputs.

4.3.2.1. Frequency Distribution Table

The TAB file is a statistical analysis of the data, binning the data into columns according to the direction sectors and rows according to wind speed. An example is given below.

Direction probabilities are given at the top of each column, with the first direction centered on North. Within the columns, the data are normalized to sum to 100.

The wind speed bin labels are given in the first column, and are based on a 1 m/s step size. In line with WAsP requirements, these wind speed bin labels denote the value at the top of the bin range.

```

2001tab.tab 04.12.2009
0.00 0.00 30.00
12 1 0
36.011 10.655 1.951 1.654 1.564 8.905 12.485 5.693 4.108 3.538 5.811 7.623
0.5 14.3 31.1 157.8 158.6 109.4 33.3 31.1 36.1 44.4 74.2 53.1 41.9
1.5 15.8 62.1 181.5 96.6 167.8 46.1 36.6 88.2 141.7 164.5 53.1 52.4
2.5 41.8 62.1 175.4 151.7 197.1 48.7 39.3 130.3 144.5 148.3 74.6 86.9
3.5 80.2 84.6 204.7 89.6 138.7 46.1 45.7 122.2 113.9 116.2 68.8 91.4
4.5 84.0 55.7 52.7 89.7 138.6 51.3 41.1 106.2 119.5 100.1 80.7 106.3
5.5 74.5 76.1 40.9 96.5 80.3 82.0 88.7 84.2 163.9 100.0 121.8 89.8
6.5 71.9 58.9 29.2 75.9 29.2 92.3 111.5 110.2 102.7 64.6 98.2 92.8
7.5 67.8 65.3 93.5 103.5 29.2 99.9 106.0 80.1 100.0 51.6 123.7 77.8
8.5 69.1 73.9 23.4 68.9 29.2 79.4 86.9 50.1 27.8 64.5 74.6 58.4
9.5 85.9 65.4 17.5 48.3 0.0 60.2 96.0 60.1 16.7 54.8 84.4 62.9
10.5 88.5 51.4 5.8 6.9 29.2 69.2 87.7 48.1 19.4 35.4 60.9 65.8
11.5 70.1 42.8 11.7 6.9 14.7 28.2 64.0 12.0 2.8 12.9 37.3 67.3
12.5 69.4 56.7 5.8 6.9 14.7 41.0 58.5 20.0 0.0 6.5 17.7 46.4
13.5 53.6 51.5 0.0 0.0 7.3 25.6 35.6 14.0 0.0 0.0 11.8 37.4
14.5 38.4 32.1 0.0 0.0 7.3 43.6 21.9 14.0 0.0 3.2 11.8 18.0
15.5 24.1 23.7 0.0 0.0 0.0 25.7 21.0 12.0 2.8 0.0 13.7 3.0
16.5 22.9 26.9 0.0 0.0 0.0 20.5 11.0 0.0 0.0 0.0 5.9 0.0
17.5 10.2 15.1 0.0 0.0 0.0 23.1 4.6 4.0 0.0 0.0 5.9 1.5
18.5 7.3 5.4 0.0 0.0 0.0 25.7 4.6 2.0 0.0 0.0 2.0 0.0
19.5 4.4 12.9 0.0 0.0 7.3 23.2 2.7 4.0 0.0 0.0 0.0 0.0
20.5 1.6 9.7 0.0 0.0 0.0 12.9 2.7 2.0 0.0 0.0 0.0 0.0
21.5 1.3 6.5 0.0 0.0 0.0 6.4 1.8 0.0 0.0 0.0 0.0 0.0
22.5 0.9 4.3 0.0 0.0 0.0 6.4 0.9 0.0 0.0 3.2 0.0 0.0
23.5 0.6 11.8 0.0 0.0 0.0 1.3 0.0 0.0 0.0 0.0 0.0 0.0
24.5 0.9 5.4 0.0 0.0 0.0 5.2 0.0 0.0 0.0 0.0 0.0 0.0
25.5 0.0 5.4 0.0 0.0 0.0 2.6 0.0 0.0 0.0 0.0 0.0 0.0
26.5 0.3 2.1 0.0 0.0 0.0 0.0 0.0 0.0 0.0 0.0 0.0 0.0
27.5 0.0 1.1 0.0 0.0 0.0 0.0 0.0 0.0 0.0 0.0 0.0 0.0
28.5 0.0 0.0 0.0 0.0 0.0 0.0 0.0 0.0 0.0 0.0 0.0 0.0
29.5 0.0 0.0 0.0 0.0 0.0 0.0 0.0 0.0 0.0 0.0 0.0 0.0
30.5 0.0 0.0 0.0 0.0 0.0 0.0 0.0 0.0 0.0 0.0 0.0 0.0
31.5 0.0 0.0 0.0 0.0 0.0 0.0 0.0 0.0 0.0 0.0 0.0 0.0
32.5 0.0 0.0 0.0 0.0 0.0 0.0 0.0 0.0 0.0 0.0 0.0 0.0
33.5 0.0 0.0 0.0 0.0 0.0 0.0 0.0 0.0 0.0 0.0 0.0 0.0
34.5 0.0 0.0 0.0 0.0 0.0 0.0 0.0 0.0 0.0 0.0 0.0 0.0
35.5 0.0 0.0 0.0 0.0 0.0 0.0 0.0 0.0 0.0 0.0 0.0 0.0
36.5 0.0 0.0 0.0 0.0 0.0 0.0 0.0 0.0 0.0 0.0 0.0 0.0
37.5 0.0 0.0 0.0 0.0 0.0 0.0 0.0 0.0 0.0 0.0 0.0 0.0
38.5 0.0 0.0 0.0 0.0 0.0 0.0 0.0 0.0 0.0 0.0 0.0 0.0
39.5 0.0 0.0 0.0 0.0 0.0 0.0 0.0 0.0 0.0 0.0 0.0 0.0
40.5 0.0 0.0 0.0 0.0 0.0 0.0 0.0 0.0 0.0 0.0 0.0 0.0
41.5 0.0 0.0 0.0 0.0 0.0 0.0 0.0 0.0 0.0 0.0 0.0 0.0
42.5 0.0 0.0 0.0 0.0 0.0 0.0 0.0 0.0 0.0 0.0 0.0 0.0
43.5 0.0 0.0 0.0 0.0 0.0 0.0 0.0 0.0 0.0 0.0 0.0 0.0
44.5 0.0 0.0 0.0 0.0 0.0 0.0 0.0 0.0 0.0 0.0 0.0 0.0
45.5 0.0 0.0 0.0 0.0 0.0 0.0 0.0 0.0 0.0 0.0 0.0 0.0
46.5 0.0 0.0 0.0 0.0 0.0 0.0 0.0 0.0 0.0 0.0 0.0 0.0
47.5 0.0 0.0 0.0 0.0 0.0 0.0 0.0 0.0 0.0 0.0 0.0 0.0
48.5 0.0 0.0 0.0 0.0 0.0 0.0 0.0 0.0 0.0 0.0 0.0 0.0
49.5 0.0 0.0 0.0 0.0 0.0 0.0 0.0 0.0 0.0 0.0 0.0 0.0

```

Figure 4.6. Frequency distribution table

The first header line is a text line. The second header line of the TAB file lists the Latitude, Longitude and Mast Height, using the values entered for the mast during data loading: these parameters are used by the WASP wind flow program.

When creating the TAB file the user has a tick box option to remove seasonal bias. The TAB file is then created by giving equal weighting to each month, apart from a small adjustment for the differing numbers of days in individual months. In this way, bias is removed from time series which do not cover an integer number of complete years.

4.3.2.2. Turbulence Intensity

One of the crucial information that obtained by analysis is the turbulence intensity that is examined from wind data at the measurement point. High level of

turbulence intensity decreases the energy production rate, increases the forces act on the wind turbine and accelerates the effect of fatigue. In addition to this, service life of wind farms is reduced because of the turbulence. Turbulence intensity is calculated by the data of mean wind speed and standard deviation of wind speed. Standard deviation of the mean wind speed has to be in the limit of 0-3 m/s and standard deviation of wind direction has to be between the limits of 3° and 75°. Three cases are used for describing the turbulence intensity:

- Low level of turbulence intensity, between 0.0 and 0.10
- Medium level of turbulence intensity, between 0.10 and 0.25
- High level of turbulence intensity, greater than 0.25

Designer should avoid building a wind farm on areas that have high level of turbulence.

4.3.2.3. Wind Rose

A wind rose gives a very compact but information-loaded presentation of how wind speed and direction are generally distributed at a particular location.

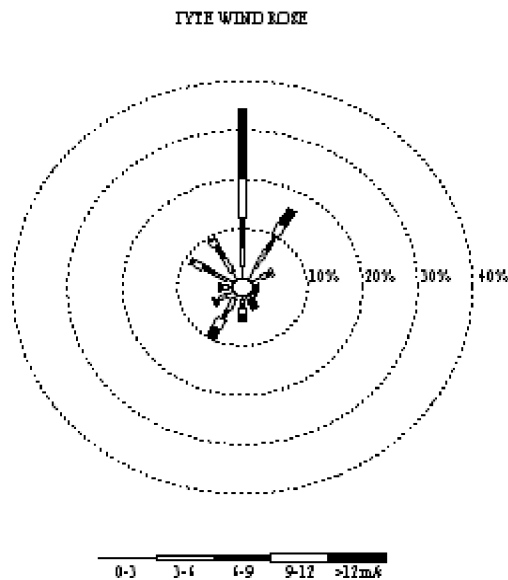


Figure 4.7. Wind rose

Presented in a circular format, the wind rose indicates the frequency of winds blowing from particular directions. The length of each spoke around the circle is related to the frequency of time that the wind blows from a particular direction. Each concentric circle represents a different frequency, starts from zero at the center to increasing frequencies at the outer circles.

The wind roses shown above contain extra information, in that each spoke is broken down into discrete frequency classes that present the percentage of time that winds blow from a particular direction and at certain speed ranges. Wind roses generally use 12 directions or 16 directions.

4.3.2.4. MCP Procedure

Measure-Correlate-Predict (MCP) methods are used to derive long-term representative wind speed and direction frequency distributions at planned wind farm sites from short-time measurements at the wind farm site and long-term measurements at a nearby reference station. In these processes, concurrent time series at both locations are compared and then relationships between the two are determined. These will comprise wind speed relationships and possibly direction shifts.

These relationships are then applied to the long-term reference measurement to obtain a long-term frequency distribution at the site. This derived long-term frequency distribution will be representative of the period of the reference measurements.

By carrying out MCP, a longer data series can be used to predict the energy output of your wind farm which in turn can reduce the uncertainty in the result, depending on the quality of the correlation.

In the MCP+ Module of GH WindFarmer, linear correlation methods are used to derive the relationships between reference and site wind speed measurements. It is assumed that for each direction sector the pairs of wind speed data can be fitted to a straight line that is characterized by its slope. This slope describes the speed-up between the two locations.

To calculate the slope, either a least squares method or a PCA method can be selected in GH WindFarmer. It is assumed that winds at the site and the reference station are being driven by the same meteorological systems. This implies that when it

is calm at the site, it is also calm at the reference station. Because of this assumption, the linear fit is forced through the origin with both fitting methods.

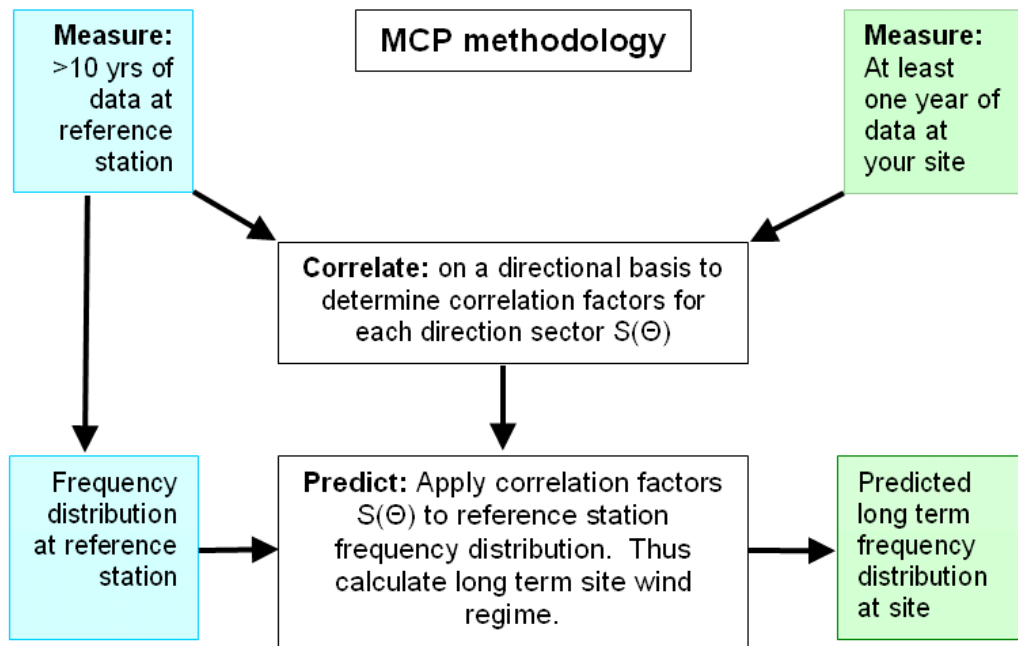


Figure 4.8. Illustration of methodology of MCP process
(Source: GL Garrad Hassan [49], 2009)

The general linear relationship between site and reference wind speed is therefore defined as

$$y = b \cdot x \quad (4.1)$$

where x is the wind speed at the reference station, b is the slope of the linear fit, also called speed-up, and y is the concurrent wind speed at the site.

The correlation coefficient indicates the strength and direction of a linear relationship between two random variables. It ranges from +1 to -1. A correlation coefficient of +1 means that there is a perfect positive linear relationship between variables (if the reference variable increases also the dependent variables increases). A correlation coefficient of -1 means that there is a perfect negative linear relationship between variables (if the reference variable increases also the dependent variables decreases). A correlation of 0 means there is no linear relationship between the two

variables. The directional and overall correlation coefficients are given in the speed-ups table in the correlation window R^2 .

The linear correlation coefficient is defined as

$$R^2 = \frac{\sum_i (x_i - \bar{x})(y_i - \bar{y})}{\sqrt{\sum_i (x_i - \bar{x})^2 \sum_i (y_i - \bar{y})^2}} \quad (4.2)$$

Least Squares Method: Assume at a specific time the measured wind speed is x_i at the reference station and y_i at the site. For a number n of such points, the least square method derives the linear fit that minimizes the sum of the squared distances in y from the fit, as illustrated in the figure below

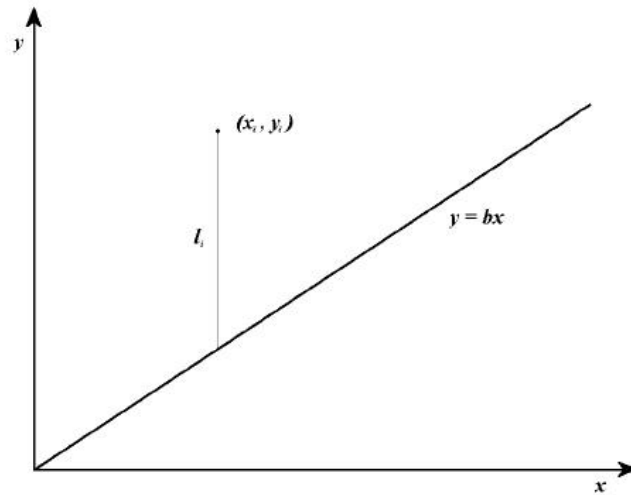


Figure 4.9. Least Squares method
(Source: GL Garrad Hassan [49], 2009)

This gives

$$\frac{\partial S}{\partial b} = \frac{\partial(\sum_i l_i^2)}{\partial b} = \frac{\partial(\sum_i (y_i - b \cdot x_i)^2)}{\partial b} = -2 \sum_i x_i (y_i - b \cdot x_i) = 0 \quad (4.3)$$

This leads to the estimation of the slope of the best fit of

$$b = \frac{\sum_i (x_i y_i)}{\sum_i (x_i)^2} \quad (4.4)$$

PCA (Principal Components Analysis) method: The PCA fitting method involves a mathematical procedure that transform a number of correlated variables into a smaller number of uncorrelated parameters called principle components. The approach is equivalent to a least-squares fit that minimizes the squared orthogonal (i.e. perpendicular) distance of the measured points from a linear function as illustrated. The perpendicular distance from the fit is

$$d_i = \frac{y_i - bx_i}{\sqrt{b^2 + 1}} \quad (4.5)$$

Minimizing the sum of the squared distance results in the estimation of the slope of the best fit being

$$b = -B + \sqrt{B^2 + 1} \quad (4.6)$$

,with

$$B = \frac{1}{2} \frac{\sum_i (x_i^2 - y_i^2)}{\sum_i (x_i y_i)} \quad (4.7)$$

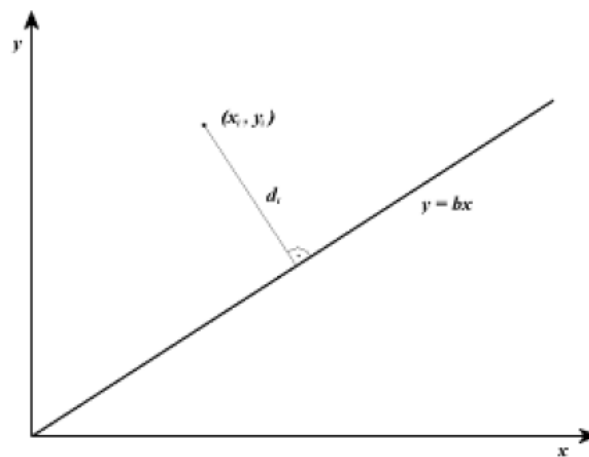


Figure 4.10. PCA method
(Source: GL Garrad Hassan [49], 2009)

4.3.2.5. Removing Seasonal Bias in Tab Files

When a *.tab file is created that is based on a time series which does not cover an integer number of complete years, or when there are data missing in the time series, the *.tab file will be biased according to seasonal variation of wind speed.

This bias can be removed using the option in GH WindFarmer. This can be applied when creating a *.tab file directly from a time series or when applying the MCP method to the short-term time series. This function is not available when a long-term reference *.tab file is used because *.tab files do not include seasonal information. In this case the user must use a long-term reference *.tab that is not seasonally biased.

In the first step, monthly seasonal wind speed and direction distributions are created using all data in the time series in a specific month, e.g. all data in a January. The annual *.tab file is then calculated by summing these monthly tables using weighting according to the number of days in each month.

To removal the seasonal bias the time series must contain data for all months. It should be noted that seasonal bias is not removed in wind roses and turbulence *.wti files.

4.4. Digital Map Processing

Estimation of the wind resource ranges from overall estimates of the mean energy content of the wind over a large area – called *regional assessment* – to the prediction of the average yearly energy production of a specific wind turbine at a specific location – called *siting*. The information necessary for siting generally needs to be much more detailed than in the case of regional assessment. However, both applications make use of the general concepts of topography analysis and regional wind climatology.

In order for WAsP to calculate the effects of topography on the wind at a given place ("the site") it is necessary to describe systematically the characteristics of the surroundings. The site may be a projected wind turbine site or a meteorological station or wind mast.

For a given situation, there are three main effects of topography on the wind: roughness, orographic and shelter effects. In nature these effects are not entirely

independent. The program takes this into account, but allows the user to specify the close-by sheltering obstacles, the roughness of the surrounding terrain, and the orography independently.

4.4.1. Editing & Digitizing Topographical Maps

1/25000 scale maps can be purchased or digitized in at least three different ways: using a digitizing tablet with a paper map, using the PC and mouse with a scanned map image, or transforming existing digital data to the WASP map format.

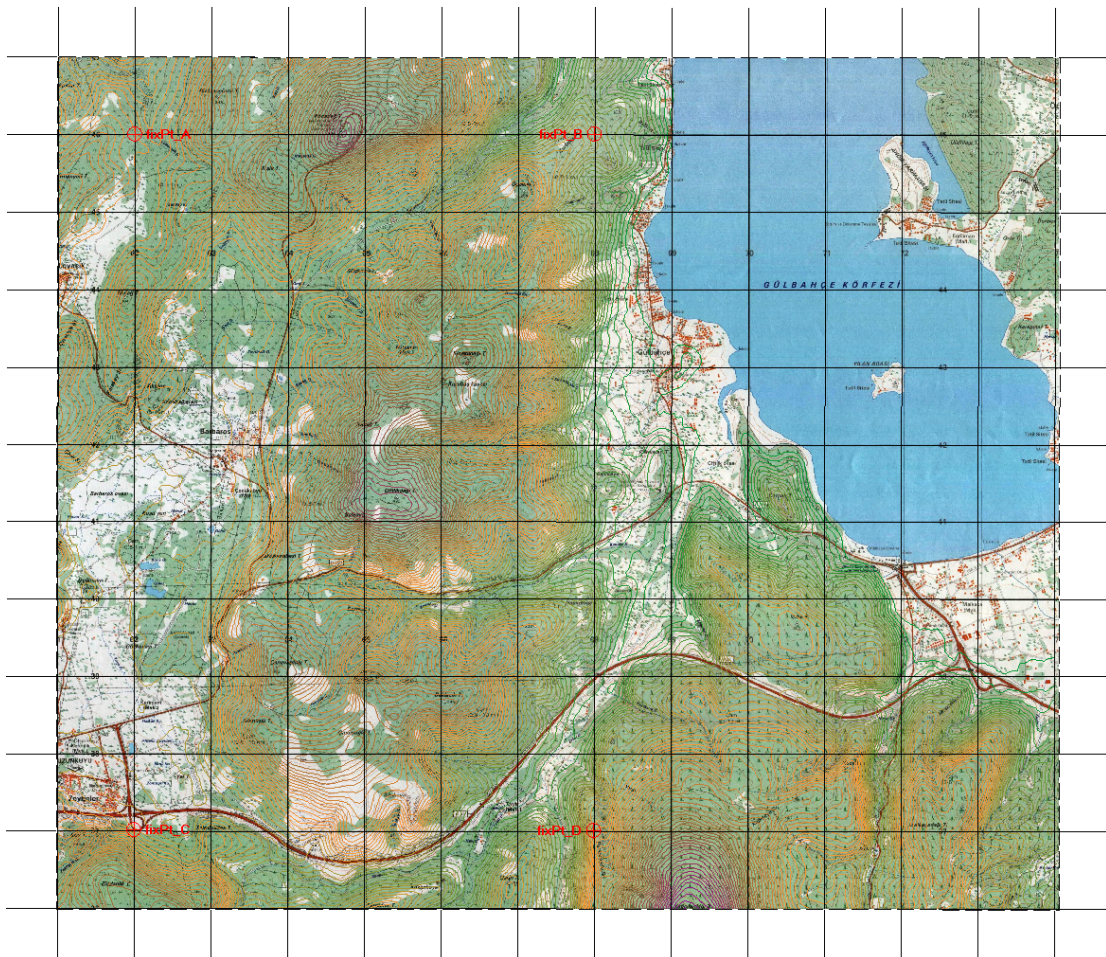


Figure 4.11. Overlay of digital map on to background map

When planning for the provision of the digital height contour map one should take the following points into consideration:

WAsP employs a zooming polar grid where resolution is very high close to the centre of the model (the site) and gets progressively lower towards the edge of the model.

The grid of the model is also zooming in the sense that the scale of the grid is adjusted so it contains the entire domain described in the digital map.

Special attention must be given to the site itself, especially if this is right on top of a hill or a ridge. Preferably, the 'closest' contour line should enclose the very site and in this way define the hilltop precisely. If this is not the case, one should supplement the map contours with a height contour just enclosing the site and with the same elevation as this.

An adequate height contour map should cover an area of at least 10 by 10 km, i.e. the map should extend to at least 5 km from any calculation site. The height contour interval should be less than about 20 m. The extreme elevation points in the terrain, hill tops and crests, should be specified as well.

4.4.2. Creation of Roughness Map

The collective effect of the terrain surface and obstacles, leading to an overall retardation of the wind near the ground, is referred to as the roughness of the terrain. However, not all the topographical elements contribute to the roughness. Vegetation and houses are examples of roughness elements, whereas long smooth hills, for example, are not, because they do not themselves cause an increase in the turbulence of the flow.

The roughness of a particular surface area is determined by the size and distribution of the roughness elements it contains; for land surfaces these are typically vegetation, built-up areas and the soil surface. In the European Wind Atlas, the different terrains have been divided into four types, each characterized by its roughness elements. Each terrain type may be referred to as a *roughness class*. A description and illustration of four such roughness classes is given in the figures below which furthermore give the relation between roughness length and roughness class, the former being the commonly used length scale to characterize the roughness of a terrain.

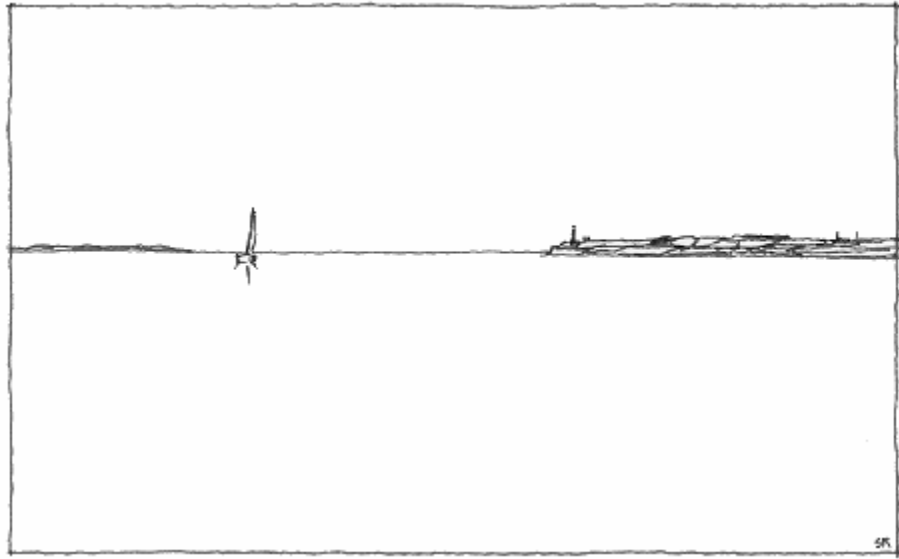


Figure 4.12. Roughness class 0
(Source: Mortensen [50], 2007)

Example of terrain corresponding to roughness class 0: water areas. This class comprises the sea, fjords, and lakes. The roughness length is $z_0 = 0.0002$ m. However, the roughness must be specified as 0.0 m in WASP.

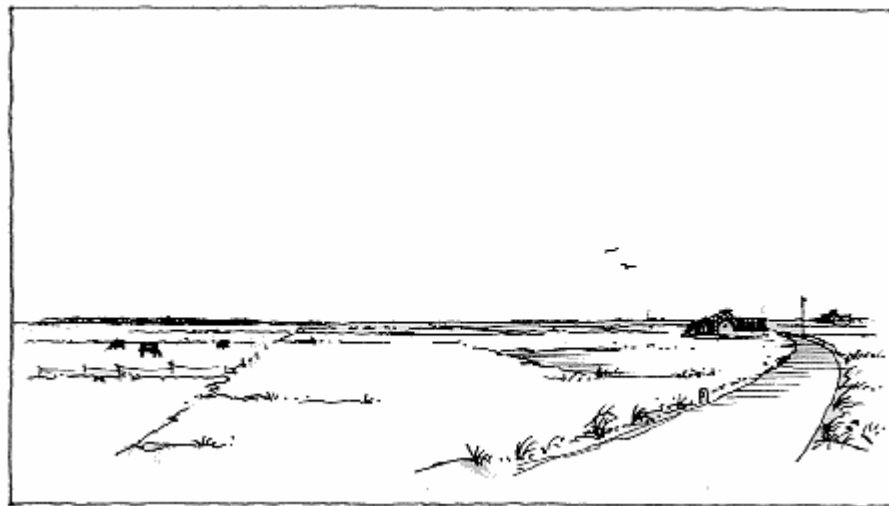


Figure 4.13. Roughness class 1
(Source: Mortensen [50], 2007)

Example of terrain corresponding to roughness class 1: open areas with few windbreaks. The terrain appears to be very open and is flat or gently undulating. Single farms and stands of trees and bushes can be found. The roughness length is $z_0 = 0.03$ m.



Figure 4.14. Roughness class 2
(Source: Mortensen [50], 2007)

Example of terrain corresponding to roughness class 2: farm land with windbreaks, the mean separation of which exceeds 1000 m, and some scattered built-up areas. The terrain is characterized by large open areas between the many windbreaks, giving the landscape an open appearance. The terrain may be flat or undulating. There are many trees and buildings. The roughness length is $z_0 = 0.10$ m.

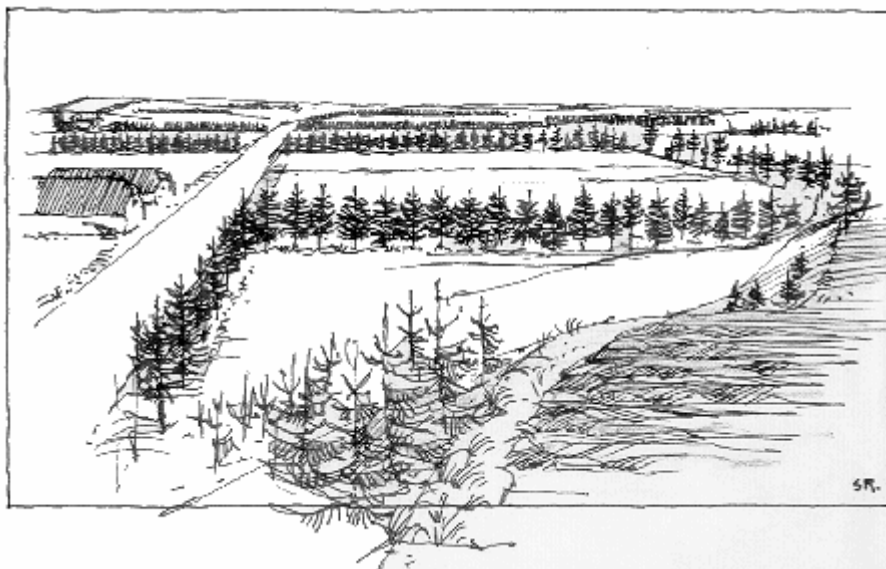


Figure 4.15. Roughness class 3
(Source: Mortensen [50], 2007)

Example of terrain corresponding to roughness class 3: urban districts, forests, and farm land with many windbreaks. The farm land is characterized by the many closely spaced windbreaks, the average separation being a few hundred meters. Forest and urban areas also belong to this class. The roughness length is $z_0 = 0.40$ m.

4.4.3. Creation of Obstacle Map

Close to an obstacle such as a building the wind is strongly influenced by the presence of the obstacle. The effect extends vertically to approximately three times the height of the obstacle, and downstream to 30 to 40 times the height. If the point of interest is inside this zone, it is necessary to take the sheltering effects into account, whereas if the point is outside the zone the building should be treated as a roughness element.

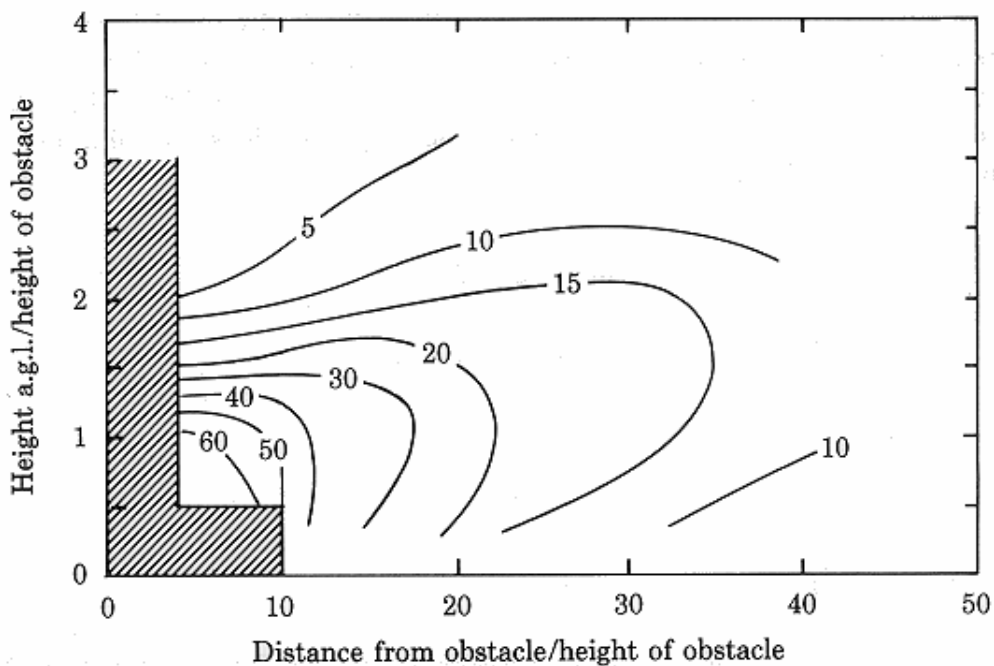


Figure 4.16. The reduction of wind speed due to shelter
(Source: Mortensen [50], 2007)

Shelter is defined as the relative decrease in wind speed caused by an obstacle in the terrain. Whether an obstacle provides shelter at the specific site depends upon:

- the distance from the obstacle to the site (x)
- the height of the obstacle (h)
- the height of the point of interest at the site (H)
- the length of the obstacle (L)
- the porosity of the obstacle (P)

The reduction of wind speed due to shelter from an infinitely long two-dimensional obstacle of zero porosity is shown below. The figure is based on the expressions given by Perera (1981).

The shelter decreases with diminishing length and increasing porosity of the obstacle. In the shaded area the sheltering is very dependent on the detailed geometry of the obstacle. In addition, wind speed is usually increased close to and above the obstacle - similar to the speed-up effects over hills.

Table 4.1. Porosity table
(Source: Mortensen [50], 2007)

Windbreak appearance	Porosity P
Solid (wall)	0
Very dense	< 0.35
Dense	0.35 - 0.50
Open	> 0.50

As a general rule, the porosity can be set equal to zero for buildings and ~ 0.5 for trees. A row of similar buildings with a separation between them of one third the length of a building will have a porosity of about 0.33. For windbreaks the characteristics listed in the table below may be applied. The porosity of trees changes with foliage, i.e. the time of year and like the roughness length, the porosity should be considered a climatologically parameter.

The porosity is the ratio, expressed in the table above as a fraction, of the area of the windbreaks 'pores', to its total area.

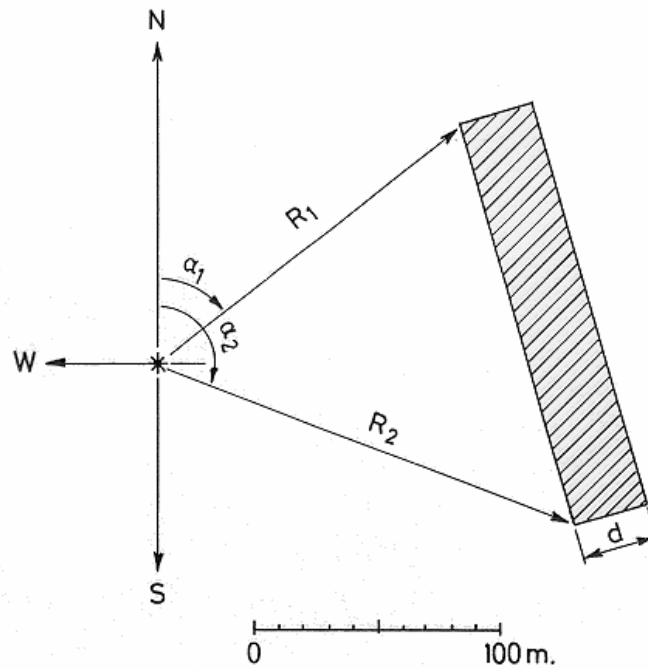


Figure 4.17. Defining process of obstacle
(Source: Mortensen [50], 2007)

Obstacles are thus specified relative to a specific site and are not linked directly to the topographic map.

a_1 angle from N to first corner [°]

R_1 radial distance to first corner [m]

a_2 angle from N to second corner [°]

R_2 radial distance to second corner [m]

h height of obstacle [m]

d depth of obstacle [m]

P estimated porosity (fraction 0-1)

Angles are measured from 0° (north) to 360° clockwise, corresponding to bearings taken with a compass. Distances are measured in meters.

Specifying obstacles: Obstacles are considered by WAsP as 'boxes' with a rectangular cross-section and footprint. Each obstacle must be specified by its position relative to the site, its dimensions and must be assigned porosity. The figure above defines the quantities that specify a single obstacle and that must be input to WAsP; the '*' marks the position of the site.

The figure 4.17 serves as a guideline when deciding whether to include obstacles in the terrain as sheltering obstacles or as roughness elements:

- If the point of interest (anemometer or wind turbine hub) is closer than about 50 obstacle heights to the obstacle and closer than about three obstacle heights to the ground, the object should probably be included as an obstacle. In this case the obstacle should not at the same time be considered as a roughness element.
- If the point of interest is further away than about 50 obstacle heights or higher than about three obstacle height, the object should most likely be included in the roughness description.

Since most anemometers are mounted at a standard height of 10 m above ground level (a.g.l) and often quite close to buildings, the shelter effect is potentially very serious in the analysis of wind data. On the other hand, a wind turbine with a hub height of 40-50 m a.g.l. and sited well away from buildings will rarely experience shelter effects at all.

4.5. Wind Resource Analysis

Wind resource analysis includes two parts that if all the works are excluded behind these step. WAsP software is used in this study for calculations. First step, resource grid resolution must be configured for calculations. Second step is the calculations and exporting the wind resource file for being able to use it in WindFarmer.

4.5.1. Configuring Resource Grid

The WRG file is a wind resource grid file as output by WAsP or other compatible wind flow software. When provided with data relating to the terrain, the surface roughness and the wind conditions for the site and its surroundings, WAsP can be utilized to predict the detailed wind regime at any point within or surrounding the wind farm site. A WRG file is simply a large array of such predictions structured into a grid format with a grid resolution defined by the user.

WRG files contain numerous fields of data for each point in the grid, including the x, y and z co-ordinates of each point (m), its energy density (W/m^2), overall Weibull

c and k parameters and Weibull c and k parameters for each of the direction sectors, along with P, the probability of occurrence, for each of these sectors. These sector-wise data describe a wind rose and wind-speed distribution at each point of the grid. It is from this information that GH WindFarmer is able to make predictions of the energy yield and wake losses for a wind farm.

There are a few simple rules that should be observed by users when creating WRG files in WAsP for use in GH WindFarmer.

GH WindFarmer calculates to an accuracy of 0.1m for the resolution of the grid. The WRG grid must cover the whole area that is available for turbine placement. The height above ground level at which the WRG is calculated must be within 0.5m of the hub-height of the wind turbine type to be analyzed. Separate WRGs must be created for each hub height to be used in the wind farm. A single point WRG at the mast position may additionally be required.

A grid resolution of 10 or 25m is commonly used for the WRG, although the grid size is a compromise between file size and accuracy. Making the grid resolution coarser can lead to interpolation errors in moderately varying terrain, but will decrease run times and storage requirements. It should be noted that the turbine positions are not limited to the grid points of the WRG in GH WindFarmer. A turbine derives its wind regime by interpolating between the four nearest WRG grid points.

A finer grid resolution reduces the impact of interpolation errors but can lead to very large WRG file sizes, which can be slow to load and run, and increased WAsP run-times. Where computer storage capacity and time permits, a 10m resolution is recommended. WRG files with a resolution of 10m have been shown to introduce negligible interpolation errors.

Multiple WRG files, calculated at different heights above ground level, may be loaded into GH WindFarmer at any one time, hence permitting the analysis of wind turbines with different hub-heights within a single layout. WRGs which have been initiated in WAsP from more than one mast can also be loaded into GH WindFarmer, hence allowing the more accurate analysis of large or complex wind farms. Where more than one WRG is being used, it is permissible for the areas covered by these files to overlap.

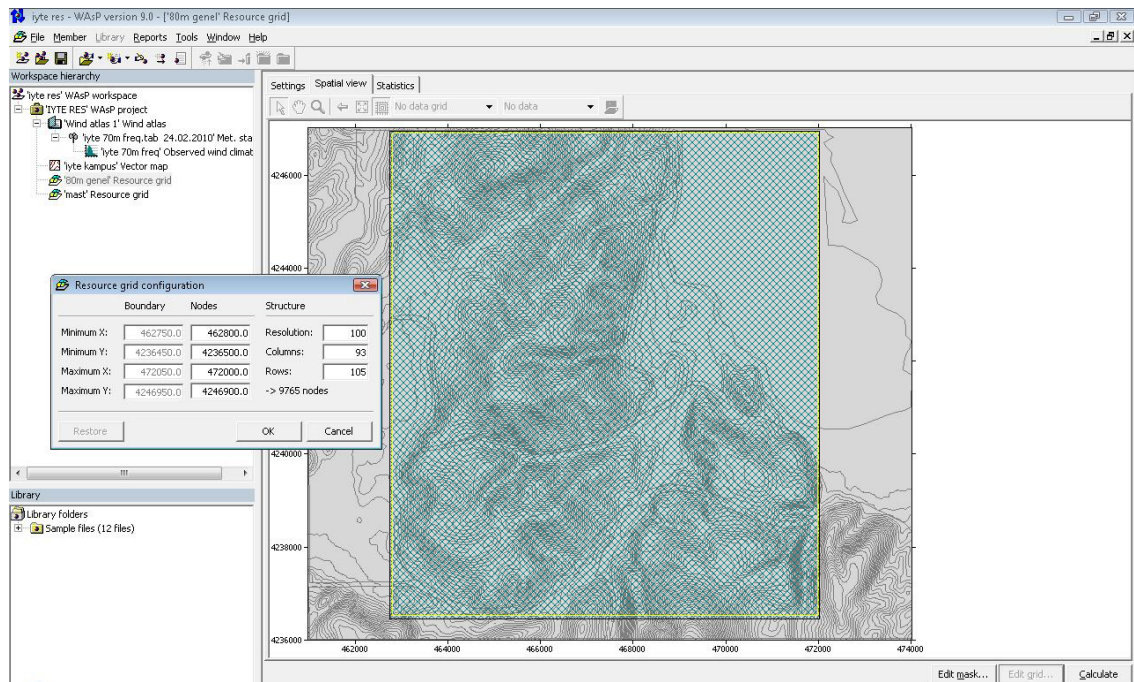


Figure 4.18. Interface of grid configuring process of WAsP

4.6. Analysis of Environmental Effect

Two cases will be considered for analysis of environmental effect in this thesis according to possible turbine locations on the campus area.

4.6.1. Shadow Flicker Effect

Shadow flicker caused by wind turbines is commonly defined as alternating changes in light intensity caused by rotating blades casting shadows on the ground and stationary objects, such as a window at a dwelling. No flicker shadow will be cast when the sun is obscured by clouds/fog or when the turbine is not rotating. Shadow flicker can occur in project area homes when the turbine is located near a home and is in a position where the blades interfere with very low angle sunlight. The most typical effect is the visibility of an intermittent light reduction in the rooms of the home facing the wind turbines and subject to the shadow flicker. Obstacles such as terrain, trees, or buildings between the wind turbine and a potential shadow flicker receptor significantly reduce or eliminate shadow flicker effects.

The shadow flicker module stimulates the path of the sun over the year and assesses at each time interval the possible shadow flicker at one or multiple receptor positions. The output of the module can be used to design a wind farm to fulfill planning requirements. The result of the module can also be used to reduce the shadow flicker annoyance at the receptors by providing the turbine controller or SCADA system with the time and date of shadow flicker occurrences so that the turbines can be switched off these times.

4.6.1.1. Program inputs

The following inputs to the GH WindFarmer model are required to produce an estimate of the wind farm shadow flicker effect:

- Latitude where the wind farm is located (γ)
- Longitude where the wind farm is located (λ)
- Zone longitude where the wind farm is located (λ zone)
- Minimum elevation angle of the sun
- Calculation time interval
- Maximum distance from turbine for calculation
- Resolution of calculation points
- Turbine and shadow receptor locations
- Turbine dimensions (hub height, rotor diameter, distance between rotor and turbine tower centre)

It is possible to use the following optional input data:

- Time zone

The zone longitude and the time zone are equivalent sets of information because for each hour deviation from the GMT there is 15 degree offset in the zone longitude.

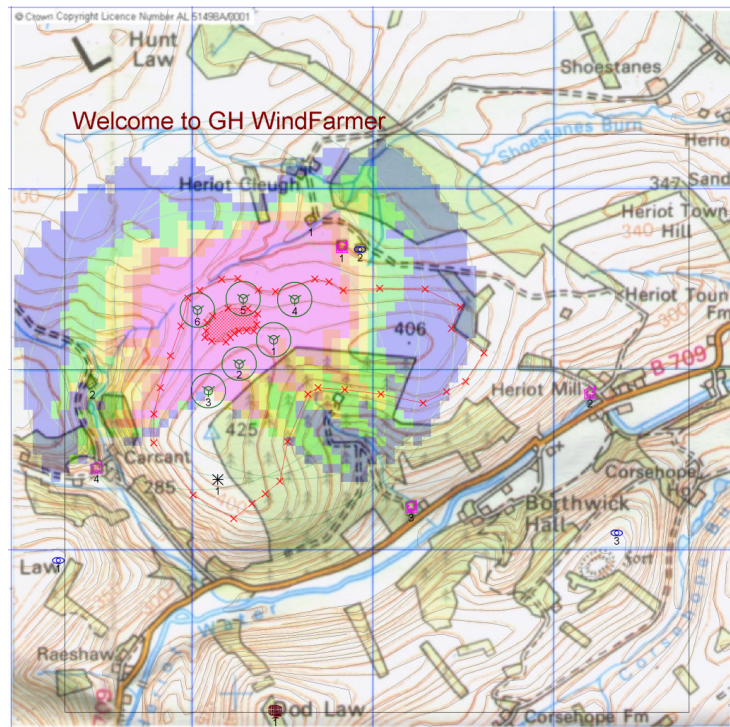


Figure 4.19. Example of shadow flicker illustration in GH WindFarmer
(Source: GL Garrad Hassan [49], 2009)

4.6.2. Noise Level Calculation

The noise functions in the base module allow the user to input the sound power levels for the turbines and calculate the noise distribution. The aim of the functions is to design wind farms within legal limits based on giving the information about sound power levels of the turbines. There are three noise models available within GH WindFarmer. All three are based on ISO 9613-2

- Simple noise model
- Complex (ISO9613) General
- Complex (ISO9613) Alternative

The Simple noise model calculates the attenuation for a single representative frequency and assumes hard ground surfaces. The model Complex (ISO9613) General considers noise attenuation for separate octave bands and includes the effect of ground attenuation as well as directional meteorological effects. The model Complex (ISO9613) Alternative does not assume frequency dependent ground attenuation [49].



Figure 4.20. Example of noise levels illustration in GH WindFarmer
 (Source: GL Garrad Hassan [49], 2009)

4.6.2.1. Accuracy of the Method

The propagation of sound and its attenuation depends on the meteorological and geographical conditions along the propagation path. The typical error associated with an assessment using the above method is +/- 3dB.

The ISO 9613-2 standard that is used in the noise propagation model is strictly only applicable when the terrain is almost flat or with a constant slope.

The application of this standard to wind turbine noise is, with large heights above ground and large propagation distances, outside the usual scope of the standard. Recommended value for the complex value is $G=0$ (hard ground) that is used for all surfaces, to account for possible differences in behavior of wind turbine noise as opposed to typical industrial noise.

CHAPTER 5

CASE STUDY: IZMIR INSTITUTE OF TECHNOLOGY CAMPUS AREA

5.1. Inspection of Campus Area

IZTECH campus area occupies 3500ha and it is located in Urla-Izmir, near Gülbahçe village. Same characteristics can be seen between the campus terrain which includes several hills and valleys, and terrain of Çeşme peninsula which is under effect of winds of North-South axis and very suitable area for the wind energy production according to REPA (Wind Energy Potential Atlas) of Turkey.



Figure 5.1. View of Iztech campus area
(Source: Izmir Institute of Technology [51], 2007)

It is a complex terrain covered with some scrub trees and bush, and Mediterranean flora is seen on the campus area which is under the effect of Mediterranean climate. IZTECH campus is tied to city center with both highway and motorway which allows fast and easy transportation.

The site has been chosen by taking into account the wind data, prevailing wind directions, the closeness to the obstacles, the orography.

5.1.1. Orography

Topography of the region is hilly, rocky and steep with 15% -25% incline. Position of hills on the campus area is nearly perpendicular to prevailing north-south wind axis. This type of terrain is an advantage for wind energy production due to orographic speed up effect. Highest point of the campus area with 473m is on the Ciftlik Mountain. First measurement station which is 70m lattice tower with 3 anemometer and 2 wind vane is located also near this point.

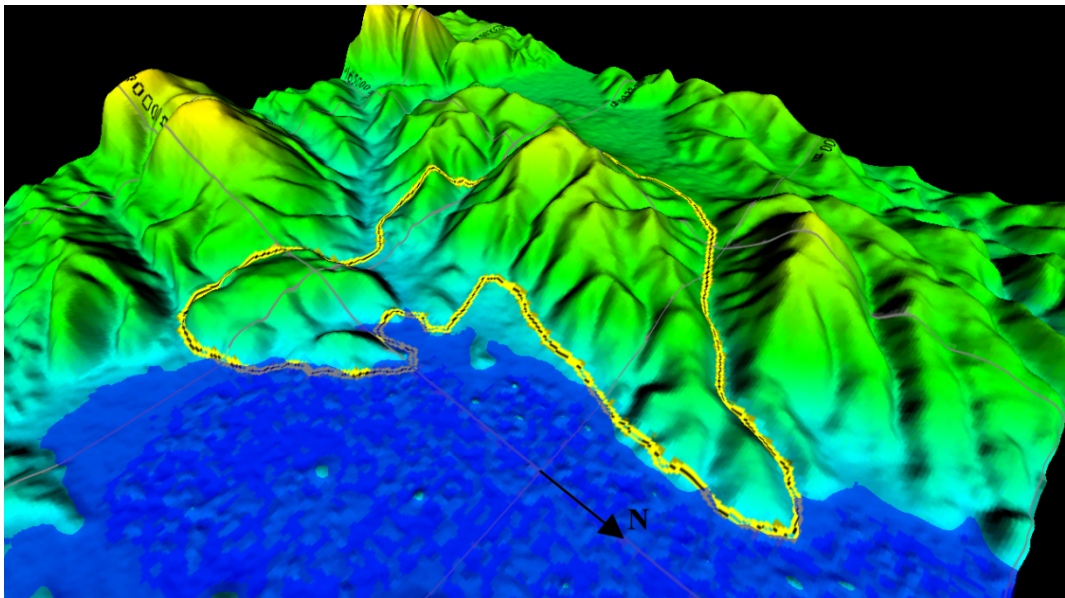


Figure 5.2. 3D view of orographic features of Iztech campus area

At the north direction of campus area, there is Kocadag Hill with 495m of height. There are Yagcilar Mountain and Ulastiran Mountain with 580m and 589m of height at the south direction. But between these two mountains, there is a valley along

the Sogut Creek and it allows to the wind which is blowing from south pass through. At the West, there is Barbaros village which is located on the Barbaros Lowland and some distance away from the lowland, there are hills lying down on the axis of north-south. These positions of hills block the wind to blow from this direction. At the East of the campus, there are Gulbahce Gulf and then the residential areas.

Because of the orographic features of the site:

At the first measurement station, 33% of average speed-up effect is observed from the direction of NW-N-NE and 34% of average speed-up effect is observed from the direction of SW-S for the 70m of height of measurement tower. But when the data of the 30m old mast which is located at the same point with the first station is observed, orographic speed-up effect is increased to averagely 44% for the north and 45% for the south directions. Reason of these speed-up increases is that the anemometer at 30m is more influenced than the anemometer at 70m due to the wind blowing along on the terrain.

At the second station (Barbaros, 30m of height), 34% of average speed-up effect is observed from the directions of NE-N-NW and 34.5% of average speed-up effect is observed from the direction of south for the 30m of height.

At the third station (Benzinlik, 30m of height), 11% of average speed-up effect is observed from the direction of NW, but winds coming from the prevailing north direction slows down instead of speed-up due to Çarpan Hill with 122m of height which is at the north of this measurement mast.

Any positive orographic turn effect due to the prevailing wind on the axis of NE-SW is not observed at none of these stations.

5.1.2. Roughness

Widespread mediterranean flora which is under effect of mediterranean climate is seen on the Cesme peninsula. Short trees and bushes cover the great deal of the Iztech campus area and the terrain of campus is very rocky and the soil depth is very low and not suitable for vegetation. Roughness of most of the campus area was taken $z=0.3\text{m}$ by considering the widespread flora and terrain. At the south regions, although some few meters high trees can be seen, they could not form a block effect to wind as much as a forest. Due to this low porosity, the roughness of these regions were taken $z=0.4\text{m}$. At

the west side of the campus area, there is Barbaros village, and due to this residential area, the roughness of this region was taken $z=0.5\text{m}$. At the east side of campus, there are residential areas of Iztech campus and Gulbahce village. Again the roughness of these areas were taken $z=0.5\text{m}$. Roughness of the sea was taken $z=0.001$ and this condition is an advantage due to the wind blowing from prevailing north direction for the wind energy production. Wind is less influenced from the sea surface than land surface, and this provides less effect for the site due to wind shear.

5.1.3. Obstacles

Shelter effect of the residential areas to the first and second measurement station is assumed negligible. Because, there is not any residential area or any structure which can be assumed as an obstacle, at the N-NE which prevailing direction of wind. At the south which is the secondary prevailing direction, there are two dwellings which are far away than forty times of their heights to the measurement stations. For other directions, any dwelling that is closest to measurement towers is far away than 2,000 meters and because of this reason, they are not taken into account.

Shelter effect is only calculated for the third station (Benzinlik, 30m) due to two obstacles which are closer than 1000m to the mast on the directions of NW. It is observed that speed of wind which is blowing from NW direction is decreased by 0.07% because of shelter effect due to these obstacles.

5.2. Measurement Devices & Masts

“IZTECH new mast” is 70 m tall lattice tower, which was erected in September 2008 at the coordinates of 4241273N and 465440E (in UTM- WGS84 coordinate system). It has two Ornytion 107A series anemometers which are 30 m, 50 m and at 70 m and an Ornytion 207 series wind vane at 70 m. Temperature data are obtained from EOL 307 series temperature probe which is mounted at 11 m on the mast. First data were measured at the end of September 2008. Data collected from September to end of November 2008, but data could not collect between November and February because of

fell down of tower and then from the beginning of the February 2009, it is re-erected and collected data in 10-min interval again.



Figure 5.3. 70 meters of height lattice tower on the campus area of Iztech

“IZTECH old mast” was 30 m tall tubular tower, which has been erected in March 2000 at the same coordinates of the “IZTECH new mast”. It had two NRG brand anemometers which are 10 m at 30 m and a NRG series wind vane at 30 m. Temperature data were obtained from NRG temperature probe which was mounted on the mast. First data were measured at the beginning of March 2000. Data were collected from March to end of December 2001 in 10-min interval.

“Barbaros mast” was 30 m tall tubular tower, which was erected in July 2000 at the coordinates of 4243843 N and 465684 E (in UTM- WGS84 coordinate system). It had two Ammonit “Classic” series anemometers which were 10 m and at 30 m and a Ammonit “Classic” series wind vane at 30 m. Temperature, humidity and atmospheric pressure data are obtained from Ammonit “xPC” series temperature & humidity probe

and Ammonit pressure gauge, which are all mounted on the mast. First data were measured at the end of July 2000. Data collected from July to end of year 2000 were collected in 1-hour interval. From the beginning of the year 2001 wind computer was reconfigured to collect data in 10-min interval. Last data were measured at the end of April 2003 due to fell down of mast, and it was not erected again.

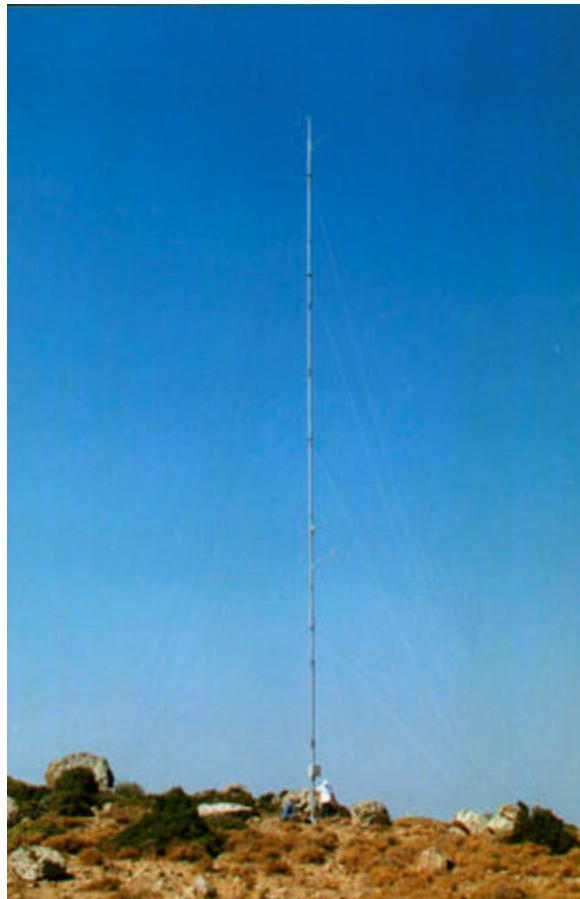


Figure 5.4. 30 meters of height tubular mast on the campus area of Iztech

“Benzinlik mast” is 30 m tall tubular tower which is at the coordinates of 4240733 N and 469661 E (in UTM-ED50 coordinate system), and it has one NRG brand anemometers which is at 30 m and a NRG brand wind vane at 30 m. Temperature, humidity and atmospheric pressure data are obtained from NRG type temperature, humidity probe and NRG pressure gauge, which are all mounted at 10 m on the mast. First data were measured at the end of October 2003. Data collected from October to end of year 2004.

5.2.1. Measurement Devices

Different brand sensors were used on each mast. Brands and specifications of each sensor are stated below.

5.2.1.1. Anemometers

Three different brands of anemometers were used on these masts. Specifications of each anemometer are defined below as tables.

Table 5.1. Specifications of Ornytion 107A type anemometer

Wind speed	< 60 m/s
Temperature	-25 ... +60 °C
Starting threshold	< 0,3 m/s
Output signal	Sine wave without dc component
Weight	0,173 kg

Table 5.2. Specifications of Ammonit Classic type anemometer

Measurement range	0.3 ... 50 m/s
Accuracy	± 2 % of measurement value or ± 0.3 m/s
Resolution	0.05 m/s
Max. wind load	60 m/s
Ambient temperature	-35 °C ... + 80 °C
Power supply	4 - 18 V DC - approx. 0.35 mA
Heating	24 V AC / DC max. 20 W
Weight without cable	1 kg

Table 5.3. Specifications of NRG type anemometer

Wind speed	1 m/s to 96 m/s
Temperature	-55 °C to 60 °C
Starting threshold	0.78 m/s
Humidity	0 to 100% RH
Weight	0.14 kg

5.2.1.2. Wind Vanes

Three different brands of wind vanes were used on those masts. Specifications of each vane are defined below as tables.

Table 5.4. Specifications of Ornytion 207 type wind vane

Sensor range	0 ... 360°
Temperature range	-25 ... +60 °C
Resolution	infinite
Wind speed	< 60 m/s
Linearity	< 1°
Weight	0,225 kg

Table 5.5. Specifications of Ammonit Classic type wind vane

Sensor range	0 ... 360° without north gap
Temperature range	-35 °C ... + 80 °C
Resolution	1°
Max. wind load	60 m/s
Accuracy	± 2°
Weight without cable	1.5 kg

Table 5.6. Specifications of NRG type wind vane

Sensor range	360° mechanical, continuous rotation
Temperature range	-55 °C to 60 °C
Resolution	potentiometer linearity within 1%
Threshold	1 m/s
Weight	0.14 kg

5.2.1.3. Thermometers & Humidity Sensors

Three different brands of temperature and two different brands humidity sensors were used on those masts. Specifications of each sensor are defined below as tables.

Table 5.7. Specifications of EOL 307 series temperature sensor

Temperature range	-30 °C to +65 °C
Accuracy	+/-2.22 °C
Resolution	+/-0.5 °C
Response time	5 min
Ambient temperature	-40 °C to 52.5 °C
Weight Sensor without cable	0.2 kg

Table 5.8. Specifications of Ammonit “xPC” series temperature sensor

Temperature range	-30... +70 °C
Accuracy	± 0.2 K
Additional error	± 0.004 %/K (<10 °C, >40 °C)
Resolution	0.1 °C
Response time	5 min

(cont. on next page)

Table 5.8. (Cont.).

Measurement principle	Pt100 - 1/3 DIN
Ambient temperature	-40 °C ... + 80 °C
Weight Sensor without cable	0.350 kg

Table 5.9. Specifications of Ammonit “xPC” series humidity sensor

Humidity range	0... 100 % r.H.
Accuracy	±2 % r.H
Additional error	± < 0.1 %/K (<10 °C, >40 °C)
Resolution	1 % r.H
Response time	5 min.
Measurement principle	capacitive

Table 5.10. Specifications of NRG brand temperature sensor

Temperature range	-40 °C to 52.5 °C
Accuracy	+/- 1.1 °C
Resolution	0.8 °C
Response time	10 min
Ambient temperature	-40 °C to 52.5 °C
Weight Sensor without cable	0.47 kg

Table 5.11. Specifications of NRG brand humidity sensor

Humidity range	0... 100 % r.H.
Accuracy	±2 % r.H
Response time	5 min.

(cont. on next page)

Table 5.11. (Cont.).

Resolution	0.1 °C
Measurement principle	capacitive
Weight Sensor without cable	0.62 kg

5.2.1.4. Barometers

Two different brands barometers were used on those masts. Specifications of each sensor are defined below as tables.

Table 5.12. Specifications of Ammonit PTB 100A model air pressure transducer sensor

Range	800 ... 1600 hPa
Resolution	1hPa
Reproducibility	±0.03hPa
Response time	1s

Table 5.13. Specifications of NRG brand barometric pressure sensor

Range	15 kPa to 115 kPa
Accuracy	+/- 1.5 kPa
Response time	1s
Weight	0.1 kg

5.3. Assessment of Wind Potential

Wind data is collected from three different locations for wind potential evaluation of the Iztech campus area.

Data ranges of each measurement mast are:

- IZTECH old 30m 2000-2001
- Barbaros 30m 2000-2003
- Benzinlik 30m 2003-2004
- IZTECH new 70m 2008-2010

All data belonging to each mast is examined, cleaned and get ready for the potential assessment.

5.3.1. Digital Maps

After inspection of site and data collection and cleaning process, next step for the potential assessment is preparation of the digital maps.

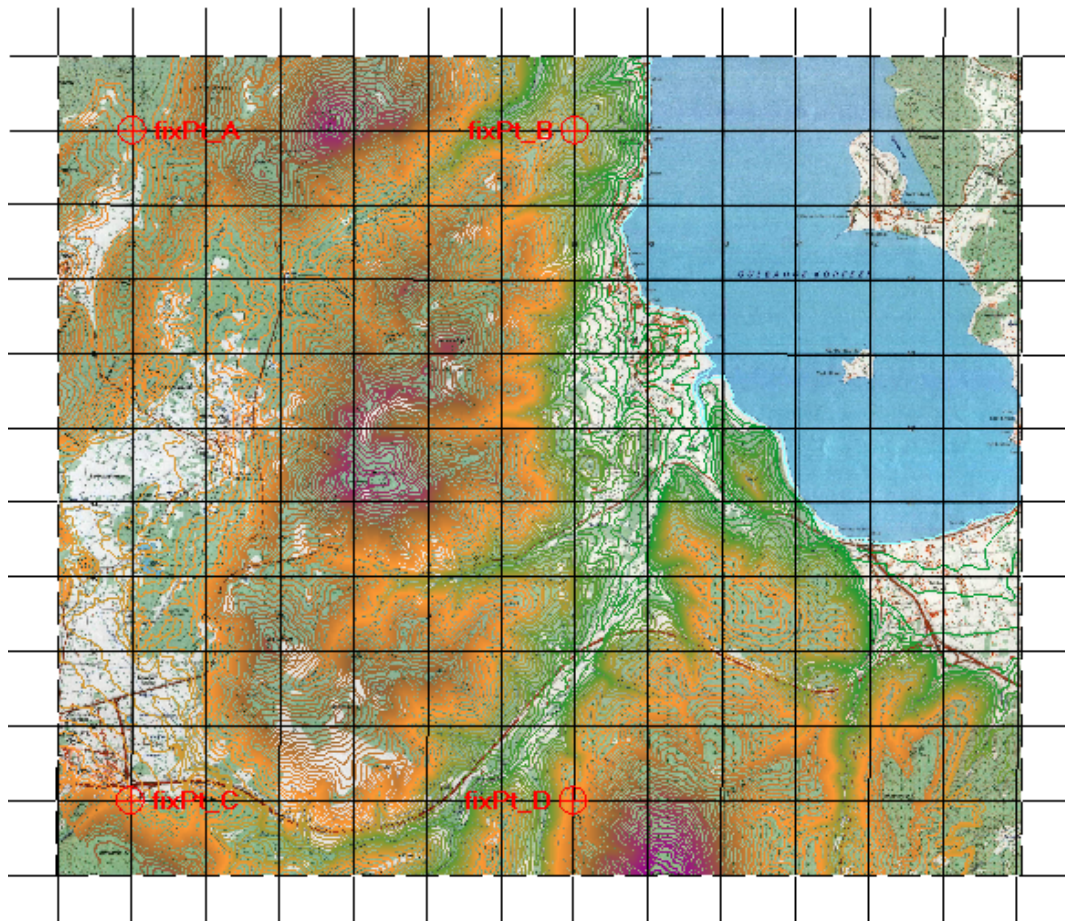


Figure 5.5. Digital topographical map overlaid on background map

Three types of digital maps should be prepared:

- 1/25000 digital topographic map
- Roughness map
- Obstacle map

5.3.1.1. Topographical Map

For preparation of digital topographical map, the methodology below is followed:

1. SRTM (Shuttle Radar Topography Mission) digital maps which cover the IZTECH campus area with resolution of 10 meters are downloaded.
2. Downloaded digital maps are edited near the measurement masts for more accurate result by using 1/25000 terrain maps that are prepared by General Command of Mapping (GCM) as background images.

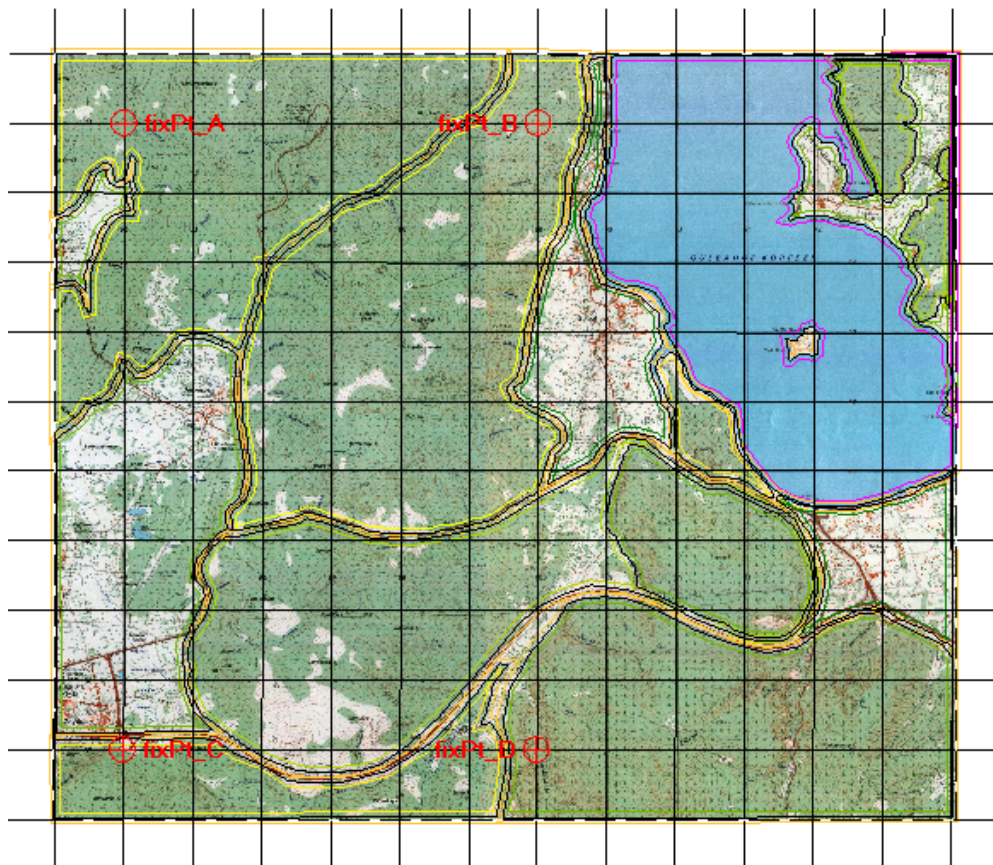


Figure 5.6. Digital roughness map overlaid on background map

5.3.1.2. Roughness Map

For preparation of roughness map, the methodology below is followed:

1. Iztech campus area is inspected personally,
2. Roughness of surrounding terrain is prepared by using the 1/25000 terrain map of GCM and photographs that belongs to these areas.

5.3.1.3. Obstacle Map

Obstacle map which is prepared by WASP obstacle list for the third station (Benzinlik, 30m) only, consists of two obstacles that are closer to measurement mast than 1000m on the direction of prevailing wind.

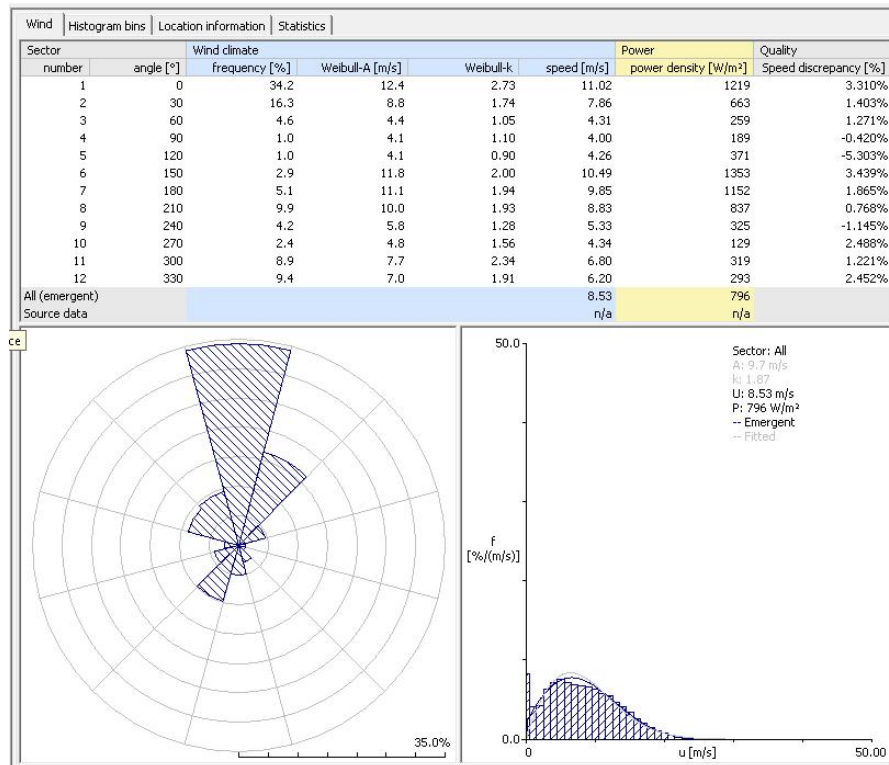


Figure 5.7. Observed frequency distribution and wind rose of 70 m tower

5.3.2. Wind Climate

Same vector map is used for each wind climate which is calculated for each one of stations.

It includes three analyses;

1. Frequency Distribution
2. Wind Rose
3. Turbulence Intensity

5.3.2.1. Frequency Distribution

Although every measurement station has same wind climate, they are varies according to their specific location. Prevailing wind direction and mean wind speed distribution of the first and second station are close to each other because of the closeness of measurement stations. For the third station, prevailing wind direction and mean wind speed distribution differs from the other two stations because of the low altitude and the “Carpan Hill” with 122 meter of height which is located at the north.

5.3.2.2. Wind Rose

Effect of the prevailing wind direction is observed at the each measurement station. The prevailing wind directions are North and North-East with 40% of frequency. Strong winds with 20% of frequency are also measured from the South and South-West directions. Some direction deviations are occurred depending on the orographic conditions of the region, but winds that are blowing from the North-South axis dominate the Cesme peninsula and also Iztech campus area.

5.3.2.3. Turbulence Intensity

Turbulence intensity of the first and second measurement station is lower than the third station. The reason for this, the third station is located on lower altitude than others and affected from obstacles and residential areas near to it. The region and three stations have an advantage of low turbulence intensity due the prevailing wind blows above the sea from that direction. Wind that blowing with low turbulence intensity level depending on the low values of roughness value of sea, is affected from the medium level of roughness of residential areas and decelerated because of the surface friction.

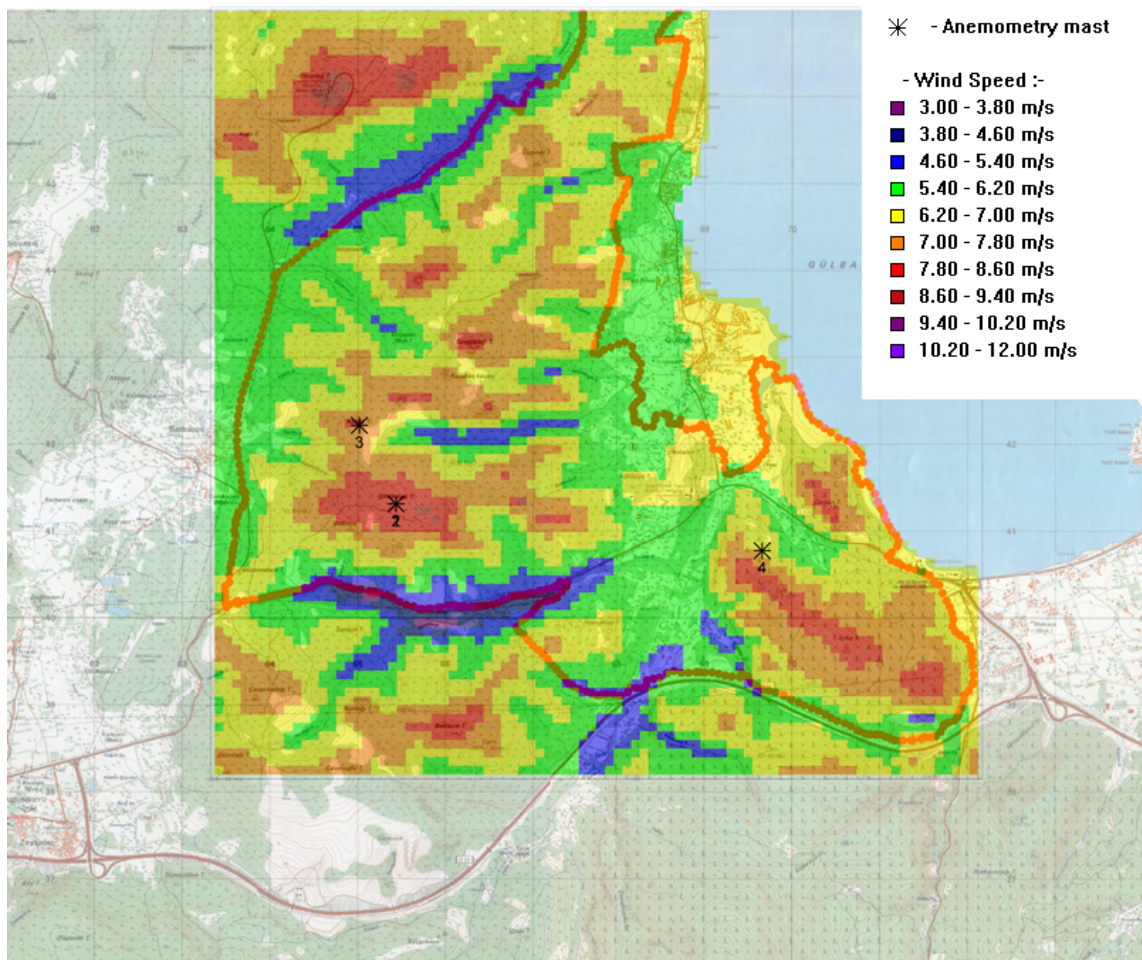


Figure 5.8. Mean wind speed map of Iztech campus area

5.3.3. Wind Resource Map

Grid size of resolution of wind atlas is that calculated for every station according to hub height of 80 meters, 25 meters. Same vector map is used for each calculation of three stations. All three wind atlas of different locations are calculated and generated by WASP program, then combined by WindFarmer in order to provide better estimation of wind potential of campus area which has complex terrain that makes the works and calculations harder. The better wind potential estimation provides us to better planning of the future investments and lowers the risks.

Nordex wind turbines that have rotor with 90 meters of diameter and hub height with 80 meters of height with 2,500 kW nominal powers are used for possible locations of wind turbines on the campus area and micrositing process for best locations is calculated by using WindFarmer software.

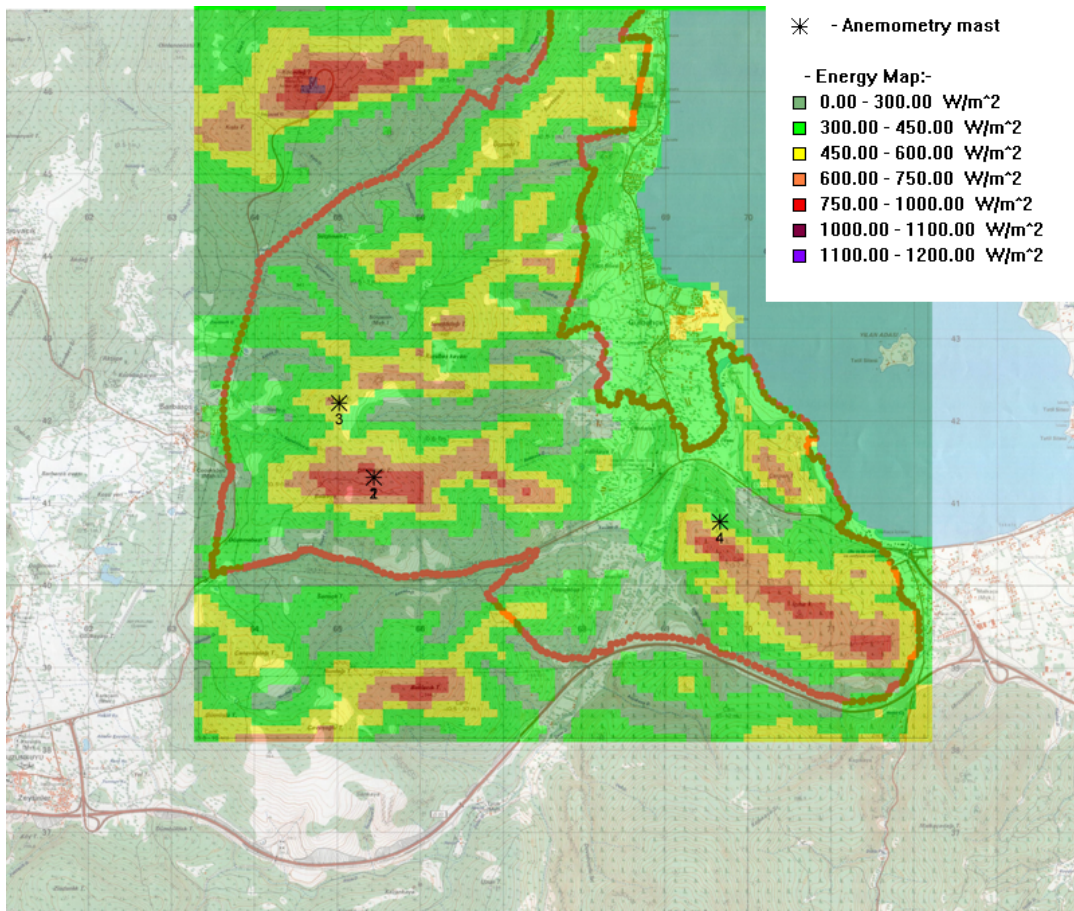


Figure 5.9. Wind power density map of Iztech campus area

5.4. Environmental Effect of Potential Site

Environmental effects due to noise levels and shadow flicker are calculated for possible wind park on the campus area by using WindFarmer software. For another issue of environmental effects, it was seen that possible wind park on the campus area is not on the way of migrating birds. Thus, possible wind turbines on the campus area will not cause to death of migrating birds. Also, the effect of electromagnetic interaction was examined and observed that the blades of possible wind turbines on the campus area might cause to disturb electromagnetic waves that emitted from the Telekom Radio Link Transmitter Station with height of 40 meters on the “Kocadag Hill” which is located at the north of campus area with height of 494 meters.

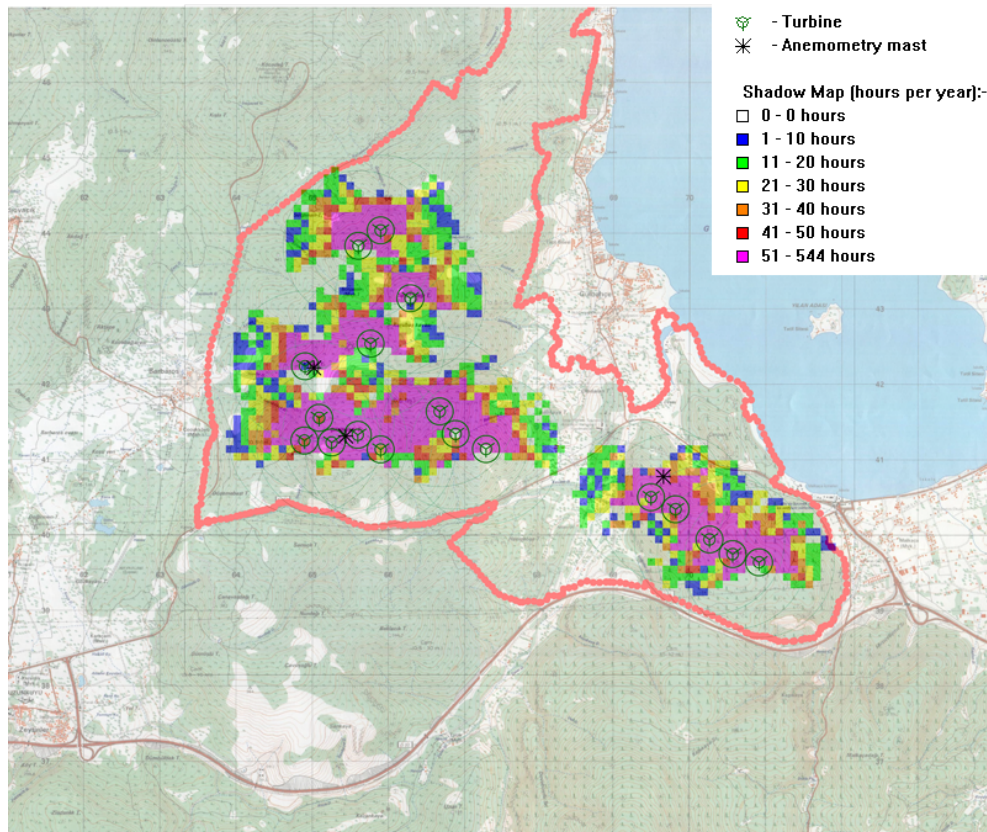


Figure 5.10. Shadow flicker effect of potential wind farm

5.4.1. Shadow Flicker Effect

It was examined and observed that the effect of shadow flicker is under the standard limit of two hours in year and the possible wind turbines have enough distance from the residential areas (Figure 5.10.). All calculations for shadow flicker effect are done by using WindFarmer software by assuming the iteration for every 30 minutes.

5.4.2. Noise Levels

Possible effects of wind turbines on the campus area caused by mechanical and aerodynamic noise of wind turbines are also examined and it was observed that the noise levels are nearly 40dB at the closest buildings of the Architecture and Technology Development Zone (Figure 5.11.). This level of noise is under the level of noise of common office and probably it will not disturb the people that are working or studying in these buildings.

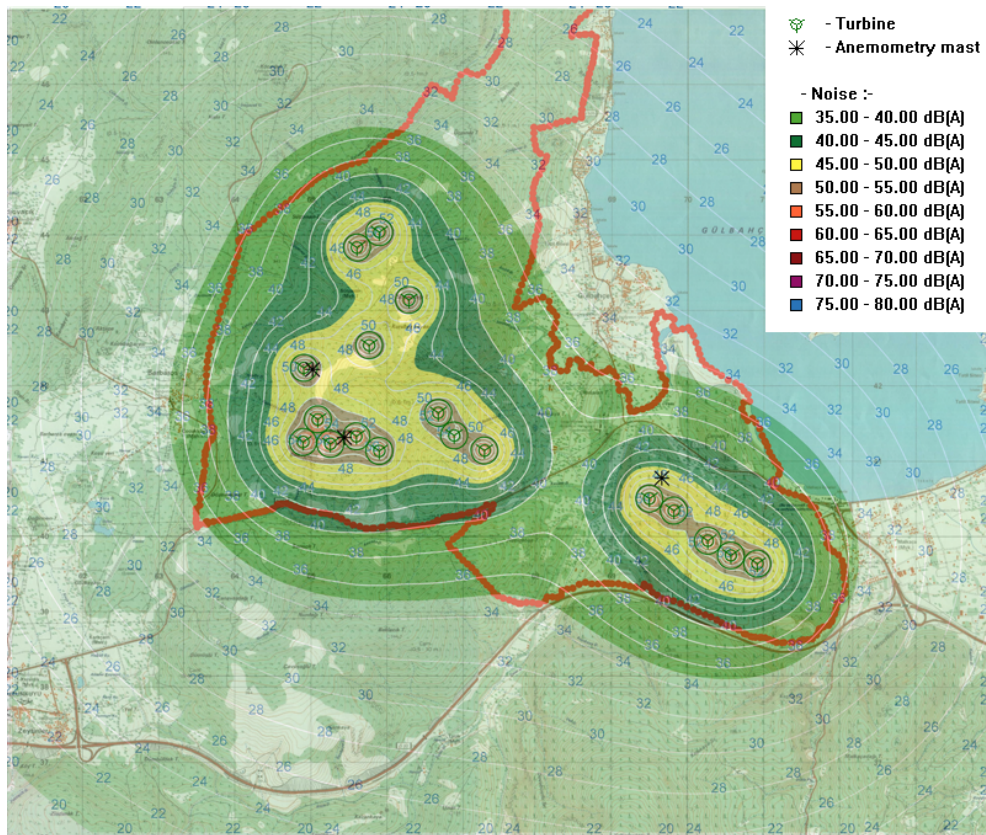


Figure 5.11. Noise levels of potential wind farm

CHAPTER 6

CONCLUSIONS

In this study, for the purpose of using wind power in ideal way on the campus area, wind data which were measured at the three different points on the campus area is used and wind speed and energy density maps were created by combining the wind resource maps that belong to each measurement mast.

GH WindFarmer software was used in processing raw data, combining wind resource maps that created in WAsP software and calculations of environmental effects that contain noise levels and shadow flicker of potential wind farm on the area. For obtaining wind climate and wind rose that belongs to each mast and creating wind resource maps that have resolution of 25 meters, the WAsP software is used.

Measured wind data was inspected, cleaned from malfunction data and processed by WAsP and GH WindFarmer and maps that contain mean speed and wind energy density were created for the campus area. According to information that obtained from these maps; averages of the wind speed maps were 5.81 m/s (8.17 m/s max.) at 50 m and 6.59 m/s (8.63 m/s max.) at 80 m. The prevailing wind direction of the site is direction of North (N)-Northeast (NE) and the second most frequent direction of the site is direction of South (S)-Southwest (SW).

According to wind energy density map, 18 wind turbines which have 2500 kW nominal power were located on most suitable points on the campus area. This potential wind farm has capacity factor over 42% and total capacity of 45 MW and the estimated annual net energy productions of the wind turbines have been calculated as 167 GWh/year for the probability of 50%.

This study shows that, mean wind speed which was calculated by using measurements at different points on the campus area and capacity factor are higher than the values that shown in Wind Energy Potential Atlas of Turkey. High potential of wind energy on the Iztech campus area was shown one more time by this study and it is aimed to contribute that obtaining the wind energy potential of the peninsula more accurately with the aid of other studies on peninsula.

REFERENCES

- [1] S. Mathew, "Wind energy: fundamentals, resource analysis and economics," *TIDEE (TERI Information Digest on Energy & Environment)*, vol. 6, p. 410, 20070901 2007.
- [2] M. Stiebler, *Wind energy systems for electric power generation*, 1st ed. New York: Springer, 2008.
- [3] T. Burton, *Wind energy : handbook*. Chichester ; New York: J. Wiley, 2001.
- [4] D. Pimentel, *Biofuels, solar and wind as renewable energy systems : benefits and risks*. [Dordrecht, Netherlands]: Springer, 2008.
- [5] P. C. Fusaro and M. Yuen, *Green Trading markets : developing the second wave*, 1st ed. Amsterdam ; Boston: Elsevier, 2005.
- [6] WWEA, "World Wind Energy Report 2009," ed. Bonn, Germany: WWEA, 2009.
- [7] J. Wilkes, "Wind In Power 2009 European Statistics," 2009.
- [8] 3TIER, "5km Resolution Wind Map at 80m," k. R. W. M. a. 80m, Ed., ed: 3TIER, 2010.
- [9] C. L. Archer and M. Z. Jacobson, "Evaluation of global wind power," *J. Geophys. Res.*, vol. 110, p. 45, 2005.
- [10] I. Fyrippis, *et al.*, "Wind energy potential assessment in Naxos Island, Greece," *Applied Energy*, vol. 87, pp. 577-586, Feb 10 2010.
- [11] N. Vogiatzis, *et al.*, "Analysis of wind potential and characteristics in North Aegean, Greece," *Renewable Energy*, vol. 29, pp. 1193-1208, Jun 2004.
- [12] A. Keyhani, *et al.*, "An assessment of wind energy potential as a power generation source in the capital of Iran, Tehran," *Energy*, vol. 35, pp. 188-201, 20100101 2010.
- [13] A. Al-Mohamad and H. Karmeh, "Wind energy potential in Syria," *Renewable Energy: An International Journal*, vol. 28, p. 1039, 20030601 2003.
- [14] A. Ouammi, *et al.*, "Monthly and seasonal assessment of wind energy characteristics at four monitored locations in Liguria region (Italy)," *Renewable & Sustainable Energy Reviews*, vol. 14, pp. 1959-1968, 20100901 2010.
- [15] E. Migoya, *et al.*, "Wind energy resource assessment in Madrid region," *Renewable Energy: An International Journal*, vol. 32, pp. 1467-1483, 20070715 2007.

- [16] L. de Araujo Lima and C. R. Bezerra Filho, "Wind energy assessment and wind farm simulation in Triunfo - Pernambuco, Brazil," *Renewable Energy*, vol. 35, pp. 2705-2713, 2010.
- [17] A. Ucar and F. Balo, "Investigation of wind characteristics and assessment of wind-generation potentiality in Uludag-Bursa, Turkey," *Applied Energy*, vol. 86, pp. 333-339, 2009.
- [18] B. Sahin and M. Bilgili, "Wind Characteristics and Energy Potential in Belen-Hatay, Turkey," *International Journal of Green Energy*, vol. 6, pp. 157-172, 2009.
- [19] M. A. Ozgur, *et al.*, "Statistical evaluation of wind characteristics in Kutahya, Turkey," *Energy Sources, Part A: Recovery, Utilization and Environmental Effects*, vol. 31, pp. 1450-1463, 2009.
- [20] Y. Oner, *et al.*, "Prediction wind energy potential using by wind data analysis in Bababurnu-Turkey," in *Clean Electrical Power, 2009 International Conference on*, 2009, pp. 232-235.
- [21] M. S. Genc and M. Gokcek, "Evaluation of Wind Characteristics and Energy Potential in Kayseri, Turkey," *Journal of Energy Engineering-Asce*, vol. 135, pp. 33-43, Jun 2009.
- [22] M. Bilgili and B. Sahin, "Investigation of wind energy density in the southern and southwestern region of Turkey," *Journal of Energy Engineering*, vol. 135, pp. 12-20, 2009.
- [23] N. Eskin, *et al.*, "Wind energy potential of Gokceada Island in Turkey," *Renewable & Sustainable Energy Reviews*, vol. 12, pp. 839-851, 20080401 2008.
- [24] B. Ozerdem and H. M. Turkeli, "Wind energy potential estimation and micrositting on Izmir Institute of Technology Campus, Turkey," *Renewable Energy: An International Journal*, vol. 30, pp. 1623-1633, 20050815 2005.
- [25] F. Turksoy, "Investigation of wind power potential at Bozcaada, Turkey," *Renewable Energy: An International Journal*, vol. 6, p. 917, 19951101 1995.
- [26] "Earth Global Circulation," ed: <http://en.wikipedia.org/>, 2009.
- [27] N. G. M. Erik L. Petersen, Lars Landberg, Jrgen Hjstrup and Helmut P. Frank. (1997). *Wind Power Meteorology*.
- [28] V. Weather, "Lake - Sea breeze chart," 2006.
- [29] J. C. Kaimal and J. J. Finnigan, *Atmospheric boundary layer flows : their structure and measurement*. New York: Oxford University Press, 1994.
- [30] G. Baumbach, "Luftreinhaltung," ed. Berlin, Heidelberg, New York: Springer Verlag, 1991.

- [31] R. H. Thuillier and U. O. Lappe, "Wind and Temperature Profile Characteristics from Observations on a 1400 ft Tower," *Journal of Applied Meteorology*, vol. 3, pp. 299-306, 1964.
- [32] E. Hau, *Wind turbines : fundamentals, technologies, application, economics*, 2nd [English] ed. Berlin ; New York: Springer, 2006.
- [33] A. Betz, *Introduction to the theory of flow machines*, [1st English ed. Oxford; New York,: Pergamon Press, 1966.
- [34] P. Gipe, "The Griggs-Putnam Index," ed.
- [35] W. E. K. Middleton, *Invention of the meteorological instruments*. Baltimore,: Johns Hopkins Press, 1969.
- [36] Ammonit, "Thies Cup Anemometer," ed: www.ammonit.com.
- [37] Young, "Propeller Anemometer," ed: www.youngusa.com.
- [38] "Hot-Wire Anemometer," ed: <http://www.efunda.com/>.
- [39] B. Nesbitt, *Handbook of pumps and pumping*, 1st ed. Oxford ; Burlington, MA: Elsevier in association with Roles & Associates Ltd., 2006.
- [40] MetOne, "2D Sonic Wind Sensor," ed: www.metone.com.
- [41] Y. B. Kumar, "Portable lidar system for atmospheric boundary layer measurements," *Optical Engineering*, vol. 45, p. 076201, 2006.
- [42] Iten, "Laser doppler anemometer " 3966324, 1976.
- [43] NaturalPower, "ZephIR laser anemometer," ed: <http://www.naturalpower.com/>.
- [44] KintechEngineering, "Ornytrion Wind Vane 207," ed: www.kintech-engineering.com.
- [45] KintechEngineering, "Temperature Sensor EOL 307," ed: www.kintech-engineering.com.
- [46] AWS Scientific Inc. and National Renewable Energy Laboratory (U.S.), *Wind resource assessment handbook : fundamentals for conducting a successful monitoring program*. Golden, CO: The Laboratory ; National Technical Information Service, distributor, 1997.
- [47] GL-GarradHassan, "Base Module of GH WindFarmer," ed: <http://www.gl-garradhassan.com>.
- [48] GL-GarradHassan, "MCP+ Module of WindFarmer," ed: <http://www.gl-garradhassan.com>.

- [49] GL-GarradHassan. (2009). *GH WindFarmer User Manual*.
- [50] D. N. H. Niels G. Mortensen, Lisbeth Myllerup, Lars Landberg and Ole Rathmann. (2007). *WAsP 9 help facility*.
- [51] IYTE, "IYTE Hava Fotoğrafları," ed: www.iyte.edu.tr, 2007.

APPENDIX A

WIND SPEED AND WIND ENERGY DENSITY MAPS OF IZTECH CAMPUS AREA